UNIVERSITA' POLITECNICA DELLE MARCHE

FACOLTA' DI INGEGNERIA

Corso di Laurea magistrale in Environmental Engineering

GROUNDWATER FLOW MODEL OF THE UNCONFINED COASTAL AQUIFERS OF THE CAMPANIA REGION (IT)

Relatore: Tesi di Laurea di:

Dott. **Nicolò Colombani**   **Simone Tavoni**

Correlatore:

Dott. Gianluigi Busico

A.A. 2020 /2021

INDEX

1. INTRODUCTION

Water is a fundamental natural resource for human need, indispensable for any socio-economic activity, which will be interested by an increasing pressure in the next years due to population growth and industrial and agricultural development (Arnell,1999).

In order to meet the ever-increasing water demand in the world, groundwater has been extensively overexploited to supplement the available surface water (Ranjan et al.,2006). This has progressively put more pressure onto groundwater resources, producing depletion of groundwater table, reduction of springs discharge and groundwater quality deterioration.

To make things worse, additional pressure on groundwater resources has been exercised by the phenomenon of global warming that, due to enhanced greenhouse effect, could have significative effects on the hydrological cycle (Arnell, 1999; Famiglietti, 2014; Wada et al. 2010). Specifically, in the Mediterranean Region, recent studies predict: i) a significative sea level raise (SLR), ii) an increase in temperature, especially in summer, iii) a decrease in yearly precipitation and iv) a change in the in-year recharge and evapotranspiration patterns (Cramer et al.,2018).

Therefore, water resource managers must consider the potential impacts of climate change that could further stress water availability for human use and natural ecosystem and plan appropriate measures accordingly (Erturk et al., 2014).

The majority of the studies that have been published so far are mainly focused on the evaluation of Climate Change's impacts on the above ground components of the hydrological cycle, analysing both historical and projected changes, while the scientific knowledge is still limited and only few applications are focused on the impacts on the subsurface components, like recharge, groundwater levels, aquifer fluxes and groundwater quality (Mastrocicco et al., 2021).

Anyway, several studies have been published aiming to understand Climate Change effects on groundwater system, using different approaches and techniques; for example, Ducci et al. (2008) tried to estimate the influence of Climate Change upon the hydrological regime and variations in the water budget, starting from an empirical evaluation of precipitations and temperatures recorded by several rain gauges in the Campania region. Busico et al. (2021) and Ertuck et al. (2014) managed to estimate future impacts of Climate Change on the water budget components (recharge and runoff) for a small watershed in the Western Mediterranean Region of Greece and Turkey, respectively, using the Soil and Water Assessment Tool (SWAT) model forced with forecasted meteorological time series from future climate simulations in different scenarios.

Similarly, other studies have also used hydrogeological models to evaluate and quantify the effects of Climate Change and Sea Leave Raise on salinization of coastal aquifer, like Oude Essink (2010) for low-lying coastal area of Netherlands or Colombani et al. (2016) and Mastrocicco et al. (2020) for the Po delta region and Variconi region in North and South Italy, respectively.

In this context, the work of this master thesis, aimed to the reconstruction of the groundwater flow model of the unconfined aquifers of the Campania region (Italy), simulate groundwater levels variation and groundwater circulation at regional scale.

The simulation was performed considering different stress periods, characterized by spatially interpolated values of evapotranspiration and recharge. The evapotranspiration trends were obtained from elaboration of MODIS raw satellite data via a published algorithm by Mu et al. (2011), covering the period 2000-2015. The recharge rate spatial variations were retrieved by the global numerical model available from de Graaf et al. (2017). The implementation of a complete groundwater model using the available data would make possible: i) to investigate how the groundwater flow system is changed during the last two decades as consequence of

changes in evapotranspiration and recharge patterns and ii) to evaluate which have been the impacts of Climate Change on the regional aquifer.

For the purpose of simulation of groundwater flow system, a numerical groundwater flow code is required. Between those available, the one selected in this study is MODFLOW simulation code, that is a modular three-dimensional finite-difference groundwater flow model of U.S. Geological Survey, able to describe and predict the behaviour of groundwater flow system (McDonald and Harbaugh, 1988).

The chosen modelling environment to support the numerical code of MODFLOW is instead Processing Modflow 11 (PM11).

Starting from detailed topography, stratigraphic information taken from existing well drilling reports and pumping tests, a conceptual model of the unconfined aquifers of Campania region was developed, and, based on such conceptual model, a groundwater flow model of the region was built up and calibrated using a recorded piezometry of the year 2000 and exploiting the functionality of PEST, for inverse parameter estimation. The calibrated groundwater flow model was finally used to investigate changes on the groundwater flow system related to variation of real values of evapotranspiration and recharge for the period 2000-2015.

2. THE STUDY AREA

The Campania region (Figure 1) is located in the southern part of the Italian peninsula and covers approximatively an area of 13 500 km^2. Its extension is delimited by the Garigliano river at North, by the Tyrrhenian Sea at West, while at South and East it is surrounded by the southern Apennine Mountain. Morphologically, the regional territory consists mainly in low altitude hills (50%) with important coastal plains (15%) and mountains area (35%).

Figure 1- View of Campania region from Google Earth

For this study only the unconfined aquifers of the region were considered. Specifically, the considered area extends from the Tyrrhenian Sea up to 50 km inland, while southward it is delimited by the foot of the Cilento mountain region, where the Sele alluvial plain ends (Figure 2).
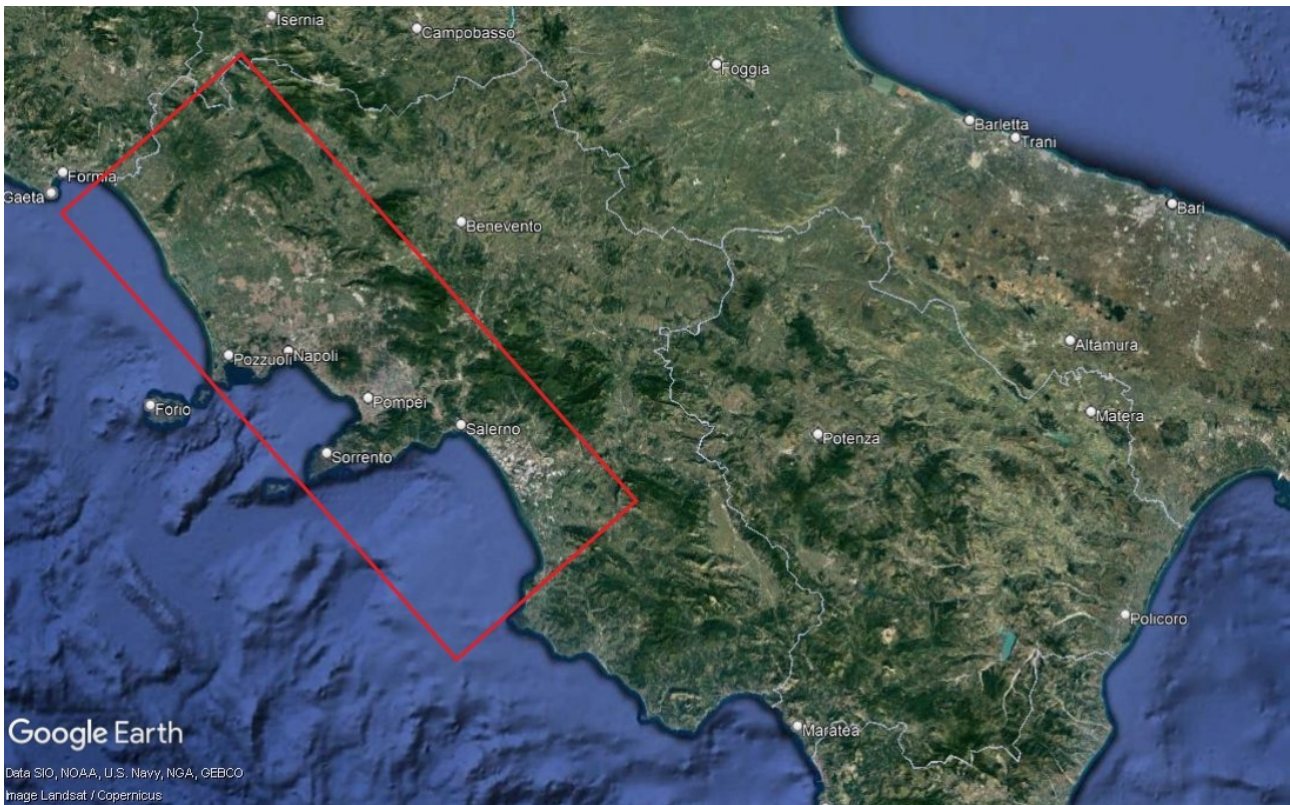
Figure 2-View of Campania region from Google Earth highlighting the study area inside the red box

The territory of the study area includes the alluvial plains of Garigliano, Volturno, Regi Lagni, Sarno and Sele rivers. The alluvial plains are interrupted by the presence of some topographic highs, that correspond, going from North to South, to the Monte Massico, Phlegraean Fields, Vesuvio volcano and Monti Lattari in the Sorrento peninsula.

Part of the Volturno coastal plain is also characterized by a wide lowland area that was subjected to huge land reclamation since the end of the seventeenth century, promoting the development of agriculture and farming, as well as a strong coastal urbanization (Ruberti and Vagliotti,2017).

The hydrographic system is instead composed mainly by the Garigliano, Volurno, Regi Lagni, Sarno and Sele rivers that, together with their tributaries and also some artificial channels constructed in the Voltuno plain, carry water from the Apennines towards the sea.

2.1. GEOLOGICAL AND GEOMORPHOLOGICAL SETTINGS

The Campania region include composite geological and geomorphological frameworks. It embraces a wide sector of the southern Apennines chain, whose structure was originated during the Miocene by compressive tectonic phases involving the subduction of oceanic crust of the African plate. During this crustal shortening, series of paleo-geographical units varying from shallow water carbonate platform to terrigenous ocean basin environments were detached, tectonically deformed in fold-and-thrust sheets, carried north-eastwardly and overthrust the Apulian carbonate platform foreland. Subsequently, during the Quaternary extensional tectonic phases, the western side of the Apennine chain was faulted forming semigraben structures in which volcanic activity began with the Roccamorfina volcano, Ischia Island, Phlegraean Fields and Somma-Vesuvio volcanos (Tufano et al.,2020).

As result of extensional tectonics, the western slope of the Campanian Apennines is characterized by graben-like coastal depressions (Brancaccio et al.,1991) and the plains along the coastal strip of the Campania result from the aggradation of such structural depressions, whose bed is as much as several thousand metres lower than the Apennine massifs and other hills between (Pappone et al., 2011).

In particular, the Campania Plain, composed by Volturno and Sarno plains, comes from volcano-sedimentary aggradation of the peri-Tyrrhenian graben, identifiable from the Lower Pliocene, when most of the plain was occupied by transitional and shallow marine environment (Mastrocicco et al., 2020). Large contribution to the formation of the plain was brought by the Phlegrean and Vesuvio eruptions and consequent formation of the thick ignimbrite layer of Tufo Campano, which produces rapid volcanoclastic aggradation.

The Sele Plain instead derives from aggradation of a Plio-Quaternary depression along the western margin of the southern Apennine chain. This extends for about 400 km^2 and it is encircled landward by a range of calcareous mountains as well as by arenaceous mountains in the Cilento.

In the last six millennia the plains of the Campania region have experienced coastal progradation amply documented by several dune system, but since the 20th century this trend has been interrupted and many stretches of the coastline are now affected by erosion, at time severe. The causes of this interruption are essentially related to the decrease of sedimentary discharge due to forest hydraulic engineering works and to the construction of many artificial dams along the main water courses. A further contribution was given by the intense urbanization that took place after World War II and this trend can be further amplified by the raise in sea level due to climate change. This transformation could increase the possibility of storms producing coastal erosion and temporary or episodic inundation. (Pappone et al., 2011).

The study area is also characterized by the presence of the phenomena of natural and human-induced subsidence. In particular the Volturno Plain is subjected to significant subsidence in the central axial sector and in the river mouth area, while other sectors of the plain are subjected to moderate subsidence (Figure 3). The phenomenon of subsidence here is related to natural processes, mainly compaction of the fluvial and palustrine deposits of the alluvial plain, while anthropic influences are considered only as addition factors that enhance subsidence locally. The eastern part of the plain instead is subjected to moderate uplift due to tectonic activity of the Apennine chain (Matano et al,2018). Even in the Sarno Plain, subsidence appears to have continued until historical period, reaching mean value of 2mm/year in the Late Quaternary. (Pappone et al., 2011).
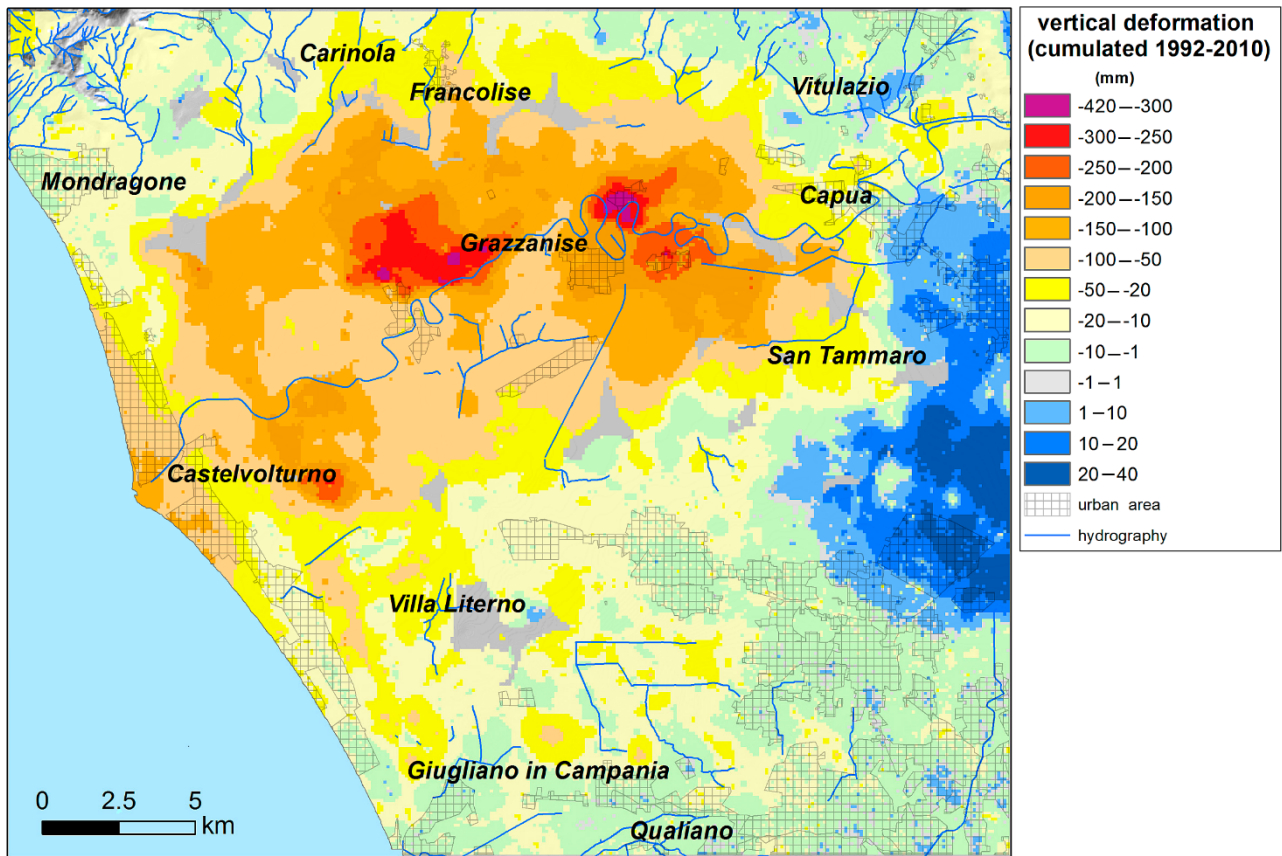
Figure 3- Cumulative vertical ground displacement estimated during 1992-2010 in the Volturno river plain (Matano et al.,2018)

2.2. HYDROGEOLOGICAL SETTING

The lithological and structural complexity of the Campania region controls the variability of hydrogeological settings that can be found in the region, comprising several hydrogeological complexes (Figure 4). They can be classified in four principal genetic groups:

- Meso-Cenozoic carbonate platform complexes;
- Plio-Quaternary alluvial and epiclastic complexes;
- Plio-Quaternary volcanic complexes;
- Meso-Cenozoic terrigenous complexes;

2.2.1. MESO-CENOZOIC CARBONATE PLATFORM COMPLEXES

The Meso-Cenozoic carbonate platform complexes constitute mountain ranges that are among highest of southern Italy and host the most important regional aquifers since they supply the main drinkable water resources of southern Italy.

According to their hydrogeological features, the carbonate aquifers can be arranged into three subgroups:

a) Limestone aquifers, generally characterized by high permeability grade due to fracturing and karst;

b) Dolomite aquifers, characterized in general by medium permeability grade due to fracturing and negligibly to karst;

c) Carbonate aquifers, constituted by alternating limestone, limestone with chert, marl limestone and subordinately marls, and characterized by a permeability mainly due to fracturing, and whose grade varies from medium to low, accordingly to relevant abundance of low-permeability lithotypes.

In fact, the Miocene and Pliocene- Quaternary tectonic phases were accomplished by brittle mechanical behaviour and stresses which resulted in pervasive fracturing of the carbonate aquifers which enhances karst processes, particularly in limestone aquifers where permeability grade is generally high.

Groundwater flow direction are controlled by geometric relationship of the permeability boundaries with the adjoining low-permeability Meso-Cenozoic terrigenous complexes. Moreover, faults with low permeability, damage and core zones, or stratigraphic intervals in the carbonate series, with marly or argillaceous composition, can divide the groundwater circulation allowing the compartmentalization of the aquifers in groundwater sub-basins, that can be reciprocally interconnected forming a basin-in-series systems.

2.2.2.   PLIO-QUATERNARY ALLUVIAL AND EPICLASTC COMPLEXES

The second group comprises alluvial and epiclastic aquifers of high interest due to intensive groundwater exploitation by wells, which is encouraged by the limited depth of the groundwater table and numerous settlements with water-demanding activities, mainly for agricultural and industrial uses.

These aquifers are homogenous and anisotropic due to spatial variable depositional mechanisms that controls the grain sizes and the related permeability. These deposits only rarely present low cementation grade, and their permeability is due to primary porosity. Depending on the occurrence of low-permeability levels interbedded within the aquifer deposits, at local scale, the groundwater flow occurs in multi-layered aquifer system in which confined and unconfined aquifers can coexist. Besides the recharge from the effective rainfall, alluvial aquifers are fed directly by groundwater from the adjoining hydrogeological units, especially in the cases of carbonate and volcanic aquifers.

2.2.3. PLIO-QUATERNARY VOLCNAIC COMPLEXES

The volcanic hydrogeological complexes of southern Italy are deposits of the eruptive centres that developed along the Tyrrhenian side beginning at the end of Pliocene (Roccamorfina, Phlegrean Fields and Somma-Vesuvius volcanos).

Aquifers formed by these complexes are relevant due to high economic value of their groundwater, often characterized by valuable organoleptic properties like CO_2 concentration among the others.

Th hydrogeological features of these complexes depend on the variable hydraulic properties of volcanic soils, rocks and the complex stratigraphic architecture.

They can form aquifers characterized by fracture permeability, as in hard volcanic rock masses or welded tuff, or aquifers characterized by porous permeability as in ash-fall pyroclastic deposits.

Due to the alkali-potassic volcanism of southern Italy, with explosive and subordinately effusive styles of activity, pyroclastic deposits are predominant on the lava hydrogeological complex. Pyroclastic deposits can be differentiated as ash-fall or ash-flow deposits, forming aquifers with different hydrogeological properties. In fact, ash-fall deposits are transported by ballistic mechanism and prevailing winds, inducing a grain size sorting over different grain size classes. Thick pyroclastic ash-fall deposits are present in the surrounding of the Phlegrean Fields and Somma-Vesuvio volcanos.

In case the column of pyroclasts and ash collapses, a *nuée ardente* phenomenon occurs leading to the formation of ash-flow deposits. Lithification of the ash-flow deposits occurs by welding and recrystallization may occurs in different grades and affects the hydrogeological properties of tuffs. Their primary porosity is inversely related to the lithification, which occurs by the partial occlusion of the inter-clast pore

spaces. The cooling fracturing represents an important part of secondary porosity that could exist in the lithified and brittle parts only.

Volcanic rocks, derived by the cooling of lava flows, form aquifers whose hydraulic characteristics depend on the content of dissolved gases and thickness of the deposit. The shallower part of the lava flows is characterized by very high permeability due to the diffuse occurrence of breccias, open cooling cracks and outgassing pores. Instead, the central part is generally characterized by a relatively lower permeability, mainly related to cooling joint sets.

Groundwater flow of principal volcanic structures is unique at global scale, being not divided in autonomous aquifers, with radial pattern and recharge independent of adjoining aquifers.

2.2.4. MESO-CENOZOIC TERRIGENOUS COMPLEXES

Meso-Cenozoic terrigenous aquifers are formed by terrigenous sediments deposited in inner and outer marine basins. Such lithostratigraphic units comprise mainly turbidite rocks from sandstone to calcarenite interbedded with mudrocks from shales to marls and constitute the minor mountains and hills of the southern Apennine. They form hydrogeological complexes with double permeability, mainly due to fracturing and secondary porosity and their permeability varies between medium to impervious depending on if the relative abundance of shale component is negligible or dominant.

In general, the permeability of the rock mass is relatively higher in the superficial zone due to existence of a regolith mantle that allows the formation of a groundwater flow in the superficial zone. Such groundwater circulation occurs with an approximate correspondence between watershed and groundwater divides, with piezometric profiles roughly parallel to the topographic morphology (De Vita et al.,2018).
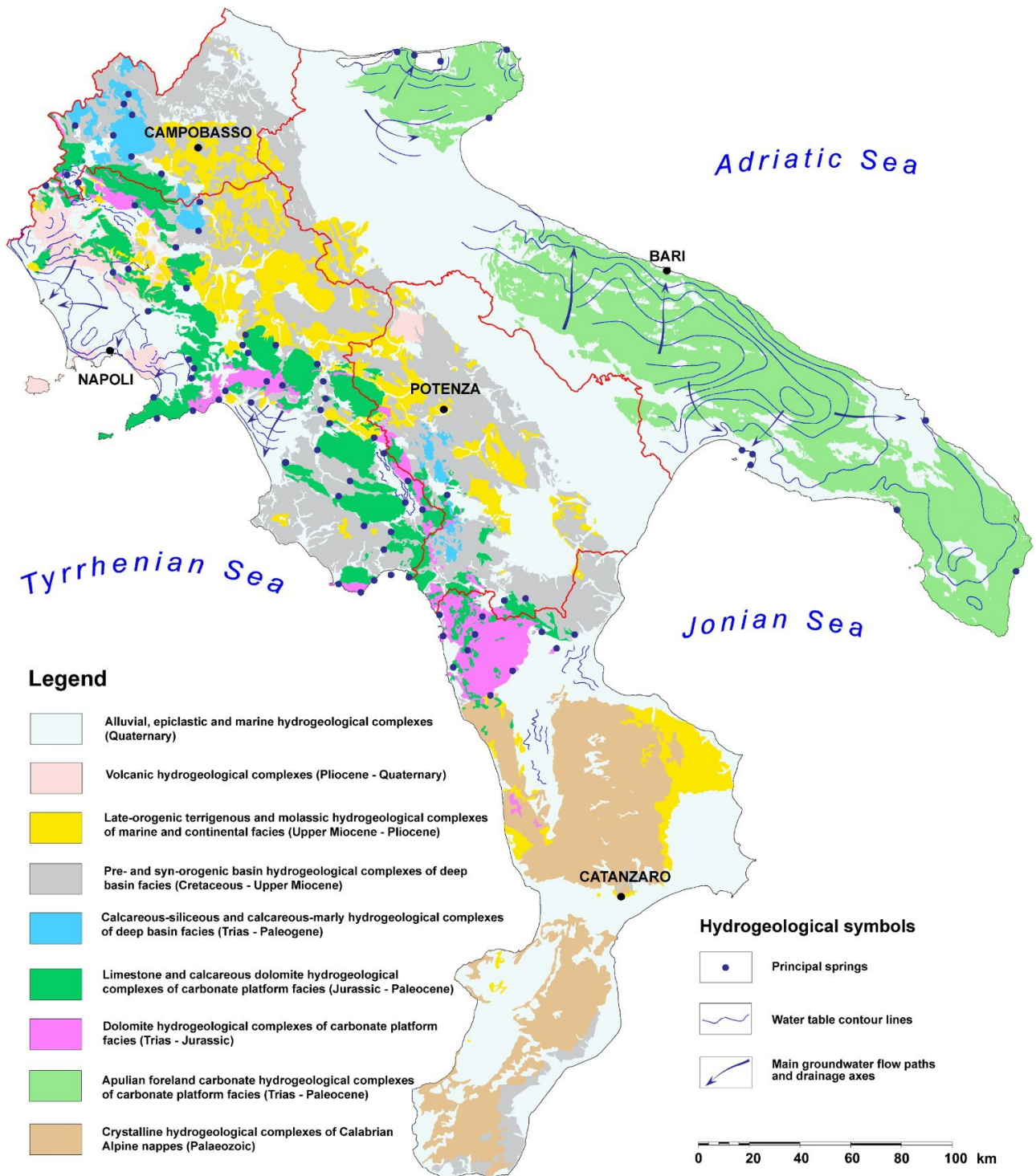
Figure 4- Hydrogeological scheme of southern Italy showing groups of hydrogeological complexes (De Vita et al.,2018)

2.2.5.   HYDROGEOLOGY OF THE STUDY AREA

The hydrogeological heterogeneity that characterizes the whole Campania region is respected also in the study area, where, analysing a hydrogeological map, is possible to notice the simultaneous presence of different outcropping formations with different origin and characteristics.

In the present study, such formations are subdivided in 9 lithology types characterized by different values of hydraulic conductivity, estimated empirically from the results of permeability tests. Their distribution is highlighted by the hydrogeological map of Figure 5.

Large part of the study area is occupied by debris and alluvial deposits (yellow and red in the map), especially in the Garigliano, Volturno, Sarno and Sele river plains. An important part is also occupied by volcanic units, originated from aggregation of volcanic material released during historical eruption of Phlaegrean Fields volcano (light blue) and Vesuvio and Roccamorfina volcanos (blue).

With smaller extension also clayey units are recorded (brown) as well as limestone and dolomite formations (orange and violet) mainly present in the monte Massico horst and along the Monti Lattari in the Sorrento peninsula. Finally, aeolian deposits characterize the coastal zone (green).
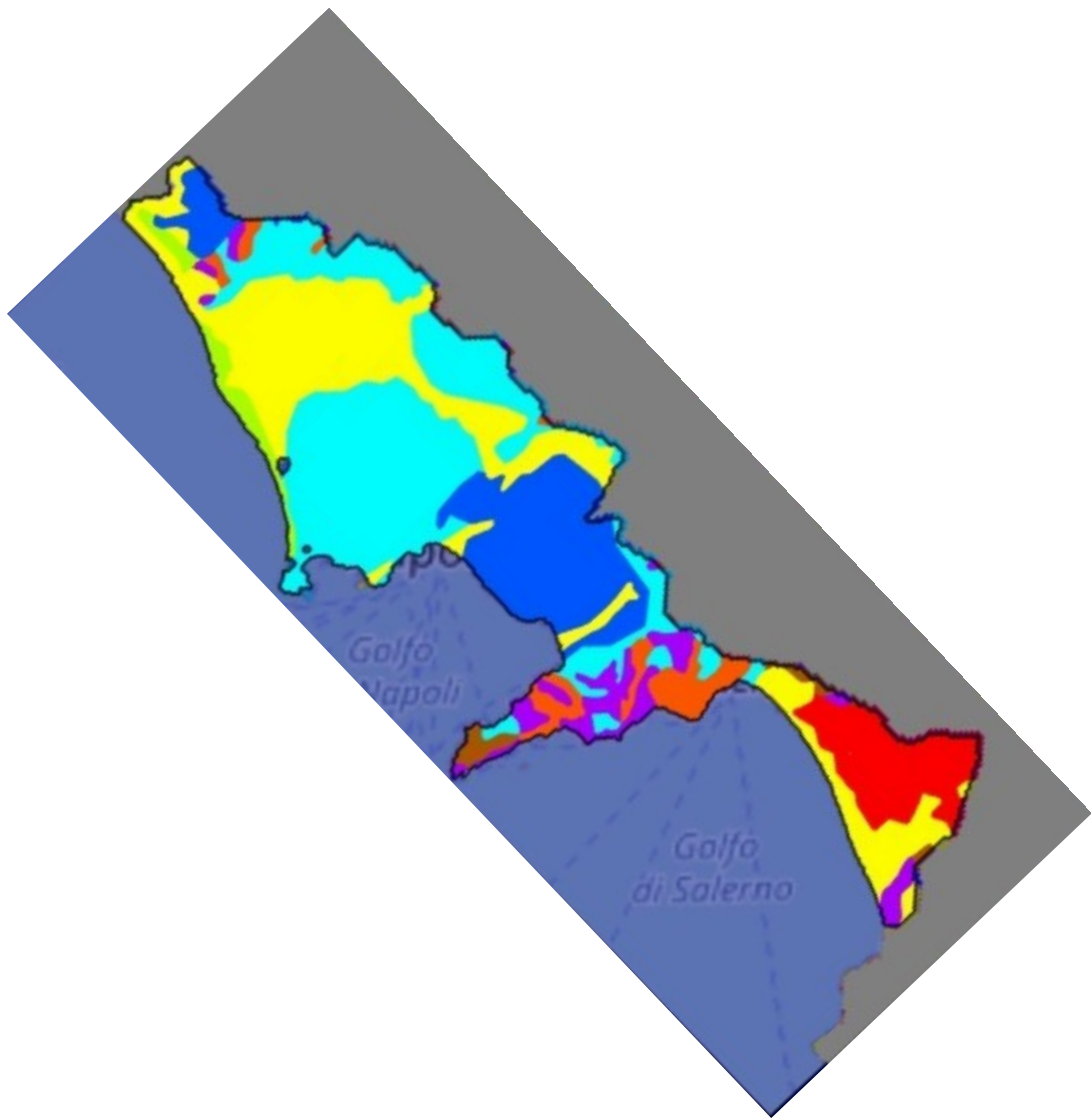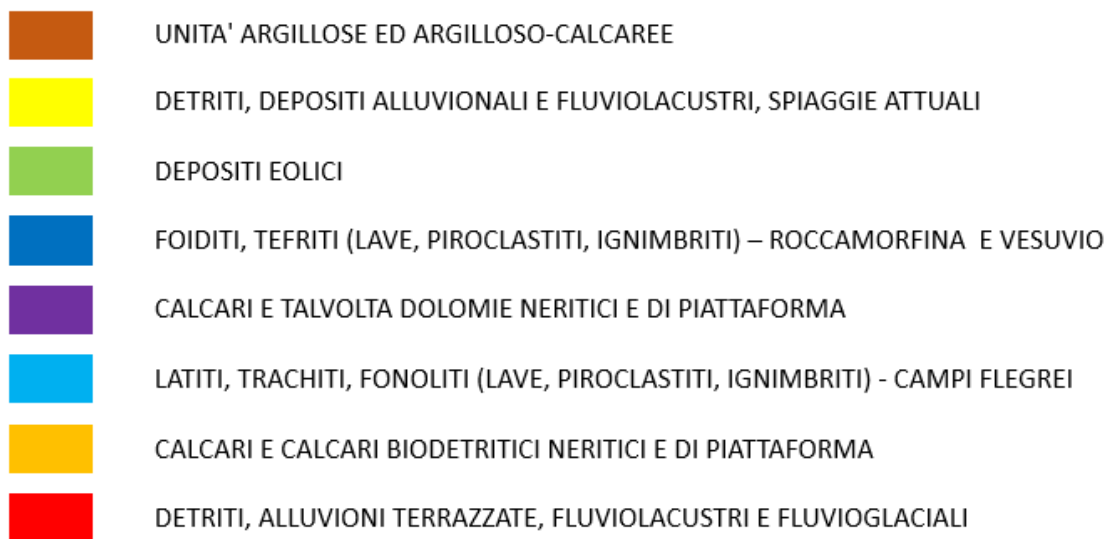
Figure 5- Hydrogeological map of the study area

⬤ (brown)	UNITA' ARGILLOSE ED ARGILLOSO-CALCAREE
⬤ (yellow)	DETRITI, DEPOSITI ALLUVIONALI E FLUVIOLACUSTRI, SPIAGGIE ATTUALI
⬤ (green)	DEPOSITI EOLICI
⬤ (blue)	FOIDITI, TEFRITI (LAVE, PIROCLASTITI, IGNIMBRITI) – ROCCAMORFINA E VESUVIO
⬤ (purple)	CALCARI E TALVOLTA DOLOMIE NERITICI E DI PIATTAFORMA
⬤ (light blue)	LATITI, TRACHITI, FONOLITI (LAVE, PIROCLASTITI, IGNIMBRITI) - CAMPI FLEGREI
⬤ (orange)	CALCARI E CALCARI BIODETRITICI NERITICI E DI PIATTAFORMA
⬤ (red)	DETRITI, ALLUVIONI TERRAZZATE, FLUVIOLACUSTRI E FLUVIOGLACIALI

Figure 6- Legend of hydrogeological map of the study area

3. PRELIMINARY ACTIVITIES

Before to build up the groundwater flow model of the study area, preliminary activities have been carried out to collect all the available information that can be useful for the subsequent modelling phase.

3.1. TOPOGRAPHIC RECONSTRUCTION

In order to retrieve topographic information on the study area, a regional SRTM Digital Terrain Model (DTM) with spatial resolution of 20x20 meter cells has been used.

Digital Terrain Model (DTM), also called Digital Elevation Model (DEM), is a topographic model of the bare Earth that can be manipulated by computer programs. The data files contain the elevation data of the terrain in a digital format which relates to a rectangular grid. Vegetation, buildings and other cultural features are removed digitally, leaving just the underlying terrain (European Environment Agency Glossary).

DTMs can be retrieve from different sources, the most common ones are satellite or LIDAR. About satellite sources, when a radar signal is transmitted from the shuttle and hits a target on the Earth, part of the signal is reflected back toward the shuttle. A receiver on the shuttle measures the strength of the reflected wave, and that strength, when plotted versus distance from the target, produce a typical oscillating trend (Figure 7).
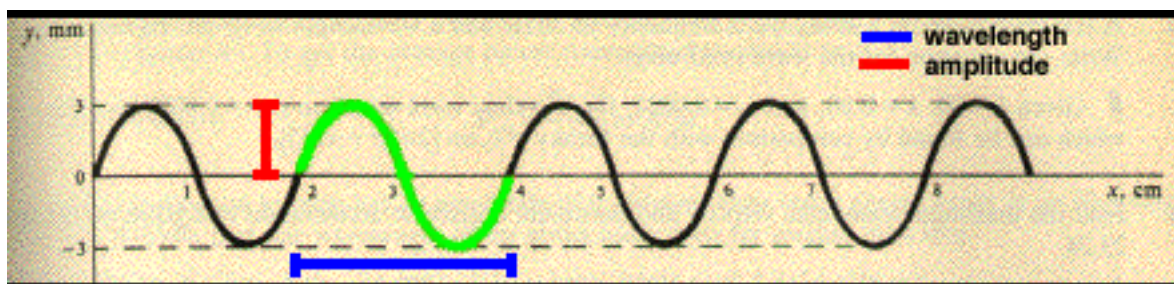

Figure 7- Typical oscillating trend of reflected radar signal

If the shuttle had two receivers separated by a fairly big distance, it would have the components of an interferometer and the two receivers are said to be at the ends of the interferometric baseline.

An interferometer measures the difference in phase between two signals received at the ends of a baseline using a signal-processing technique called complex cross correlation. This phase difference is called the interferometric phase and it is determined by effectively subtracting the measured phase at each end of the baseline. Because each received phase depends on the distance between the receiver and the target, the interferometric phase is a measurement of the difference between the distances from each receiver to the target.

Having two different targets at two different heights (Figure 8), it can be seen that the differential distance of each of these targets between the ends of the baseline depends on the height of the target. For the higher target (target 2), the differential distance is greater than for the lower one (target 1) and the interferometric phase for target 2 is therefore larger than that for target 1. In addition, the differential distance gets larger as the incidence angle (theta 1 < theta 2) to the target gets larger.
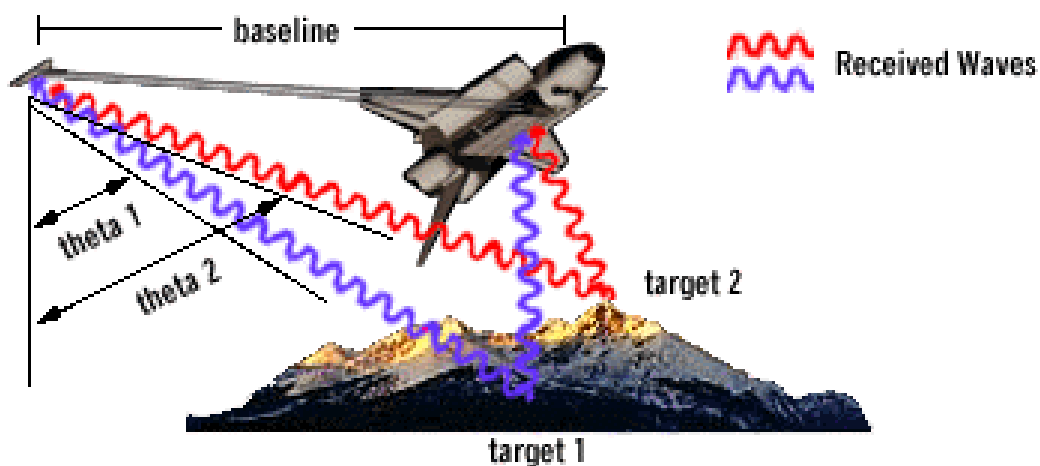

Figure 8- Functioning scheme of interferometers

The interferometric phase can be related to the incidence angle by the very-nearly-exact formula:

$$\text{interferometric phase} = B \cdot \sin(\text{theta}) / \text{wavelength}$$

where B is the baseline length.

For a given target height, theta can be calculated and the interferometric phase can be calculated with the above equation. It's possible also to start from the measured interferometric phase and solved the equation to find theta and then find the topographic height of the target. (Robert Treuhaft, JPL, NASA)

LIDAR (Light Detection and Ranging) is another environmental remote sensing system that can be used to retrieve digital terrain models, this time based on the use of laser. It is aimed to measure the distance of an object by the emission of electromagnetic beams reflected by the irradiated object. The logic of LIDAR instrument is similar to radars, but with a significant difference in the type of emitted radiations: in the case of LIDAR the laser transmitter can generate a luminous beam, collimated by an adequate lens and mirror system, in an interval of the electromagnetic spectrum typical of the optical frequencies (0,3-15 μm).

The method is based on the measure of distances between an airplane, or a helicopter, and the terrestrial surface measuring with precision the time taken by the laser signal's pulse to reach the ground and, reflected, to go back to the emitting platform.

The reflected laser signal is received by a small telescope collecting the light in a detector. The time taken by the signal is converted in distance from the platform considering the laser beam speed equal to the light speed in the vacuum ($2,99 \times 10^{10}$ cm $\cdot$ s^{-1}).

The measured distances are converted in planimetric coordinates and altimetric values for each laser pulse combining the measures of the distance with the exact position of the instrument on the acquisition platform, retrieved by a satellite positioning system and applying the technique known as kinematics differential solution (Gomarasca, 2009).
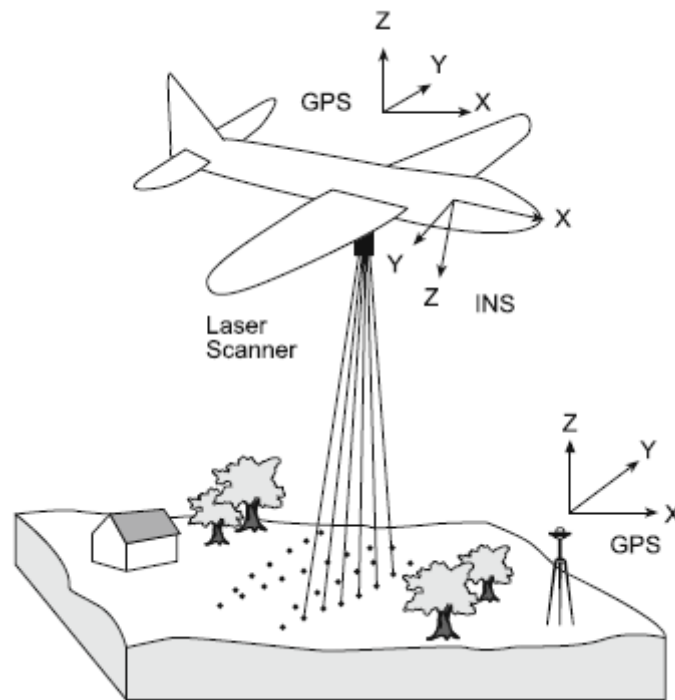

Figure 9- Functioning of a LIDAR acquisition system taken from Gomarasca,2009)

3.2. STRATIGRAPHIC RECONSTRUCTION

A stratigraphic analysis has been performed in this stage in order to retrieve information about the depth of the unconfined aquifers in the study area. To achieve this goal, already existing data have been used. Specifically, the online database of Istituto Superiore per la Protezione e Ricerca Ambientale (ISPRA) proved to be a valuable source of information, since it contains the national archive of subsurface investigations, including several reports of boreholes analysis (Figure 12), conducted all over the Italian peninsula.

Ninety one boreholes reports, which locations are distributed all over the entire study area (Figure 10), have been analysed. The depth of the unconfined aquifer for each borehole has been investigated and collected along with spatial information (latitude, longitude and UTM coordinates).
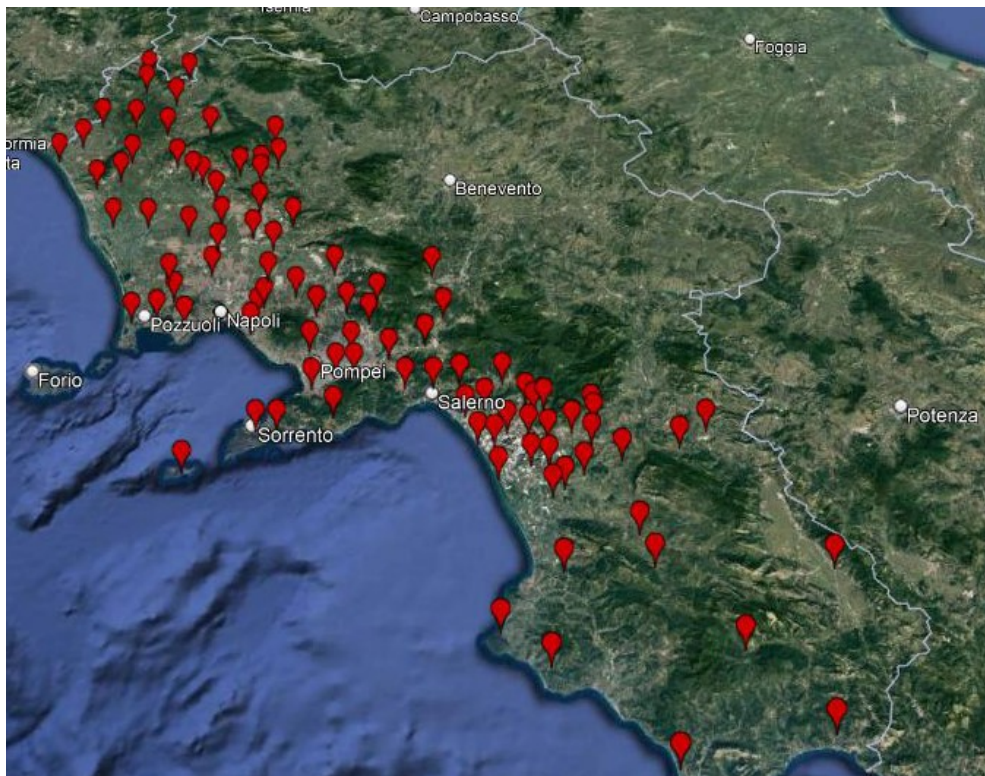

Figure 10- Distribution of boreholes reports over the study area

In addition, other information on the aquifer's depth have been taken from previous studies conducted in the Campania region, such as logs on the Volturno river plain (Figure 11) (Busico et al. 2021; Corniello & Ducci, 2014) or aquifer information in Cuma (Allocca et al., 2018; Stellato et al., 2020), Bagnoli, Giuliano and San Valentino Torio.
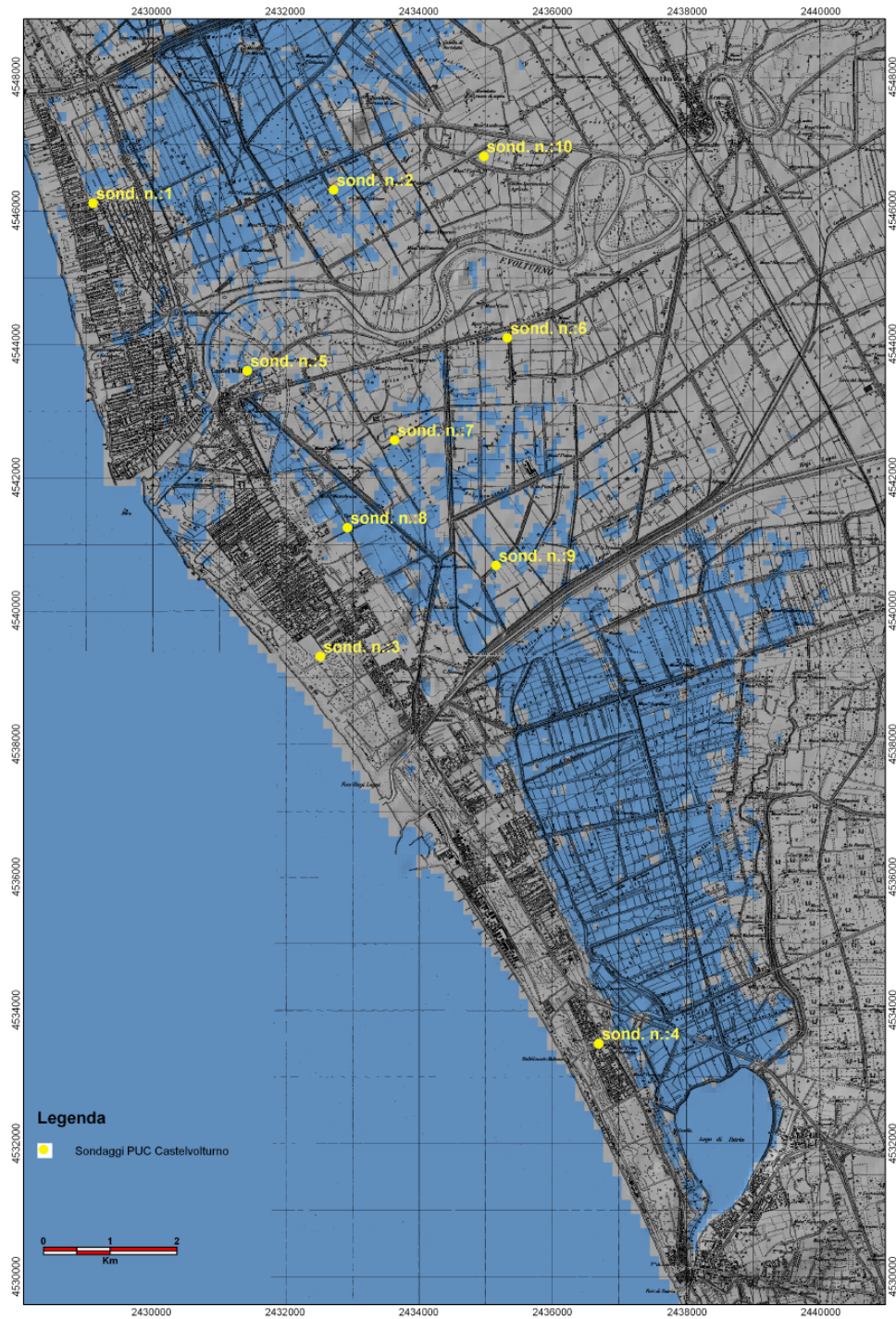

Figure 11- Location of analysed logs in the Volturno plain

Dati generali	Ubicazione indicativa dell'area d'indagine

Codice: 157429
Regione: CAMPANIA
Provincia: CASERTA
Comune: MONDRAGONE
Tipologia: PERFORAZIONE
Opera: POZZO PER ACQUA
Profondità (m): 62,00
Quota pc slm (m): 45,00
Anno realizzazione: 1993
Numero diametri: 1
Presenza acqua: SI
Portata massima (l/s): 6,000
Portata esercizio (l/s): 5,000
Numero falde: 2
Numero filtri: 0
Numero piezometrie: 1
Stratigrafia: SI
Certificazione(*): SI
Numero strati: 6
Longitudine WGS84 (dd): 13,915800
Latitudine WGS84 (dd): 41,130069
Longitudine WGS84 (dms): 13° 54' 56.89" E
Latitudine WGS84 (dms): 41° 07' 48.26" N

(*)Indica la presenza di un professionista nella compilazione della stratigrafia

Maxar, Microsoft

DIAMETRI PERFORAZIONE

Progr	Da profondità (m)	A profondità (m)	Lunghezza (m)	Diametro (mm)
1	0,00	62,00	62,00	300

FALDE ACQUIFERE

Progr	Da profondità (m)	A profondità (m)	Lunghezza (m)
2	40,00	44,00	4,00
1	13,00	14,00	1,00

MISURE PIEZOMETRICHE

Data rilevamento	Livello statico (m)	Livello dinamico (m)	Abbassamento (m)	Portata (l/s)
lug/1993	13,00	42,00	29,00	6,000

STRATIGRAFIA

Progr	Da profondità (m)	A profondità (m)	Spessore (m)	Età geologica	Descrizione litologica
1	0,00	1,00	1,00		TERRENO VEGETALE
2	1,00	34,00	33,00		TUFO GRIGIO
3	34,00	40,00	6,00		ARGILLE CON GHIAIA
4	40,00	44,00	4,00		GHIAIA SCIOLTA
5	44,00	61,00	17,00		ARGILLE
6	61,00	62,00	1,00		CALACARI COMPATTI

Figure 12- Example of borehole report taken from ISPRA database

3.3. ESTIMATION OF HORIZONTAL HYDRAULIC CONDUCTIVITY

There are numerous ways to determine or estimate permeabilities.

In our study, the horizontal hydraulic conductivity estimation is based on the results of gravity permeability tests.

The parameter required for the estimation of hydraulic conductivity through gravity permeability tests are shown in the figure 13, together with the suitable equations, differentiated depending on the investigated zone of subsoil.
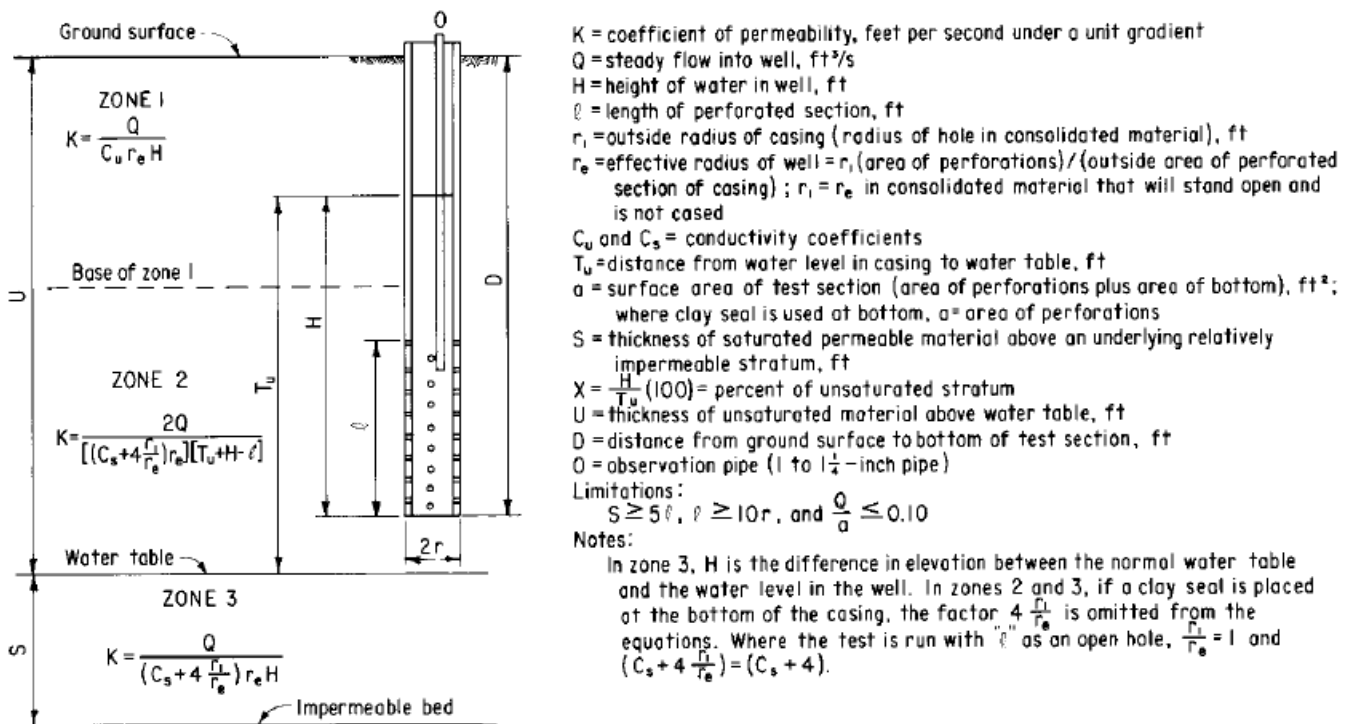

Figure 13- Required parameters and equations for the estimation of hydraulic conductivity with gravity permeability tests

In the zone 3, below the groundwater table, the parameters required for the estimation of hydraulic conductivity are:

- Q = Well flowrate
- H = Difference in elevation between the normal water table and the water level in the well
- r_e = Effective radius
- C_s = Saturated conductivity coefficient

The saturated conductivity coefficient C_s can be determined using the graph in figure 14, starting from the ratio between the length of the perforated section and the radius of the well.
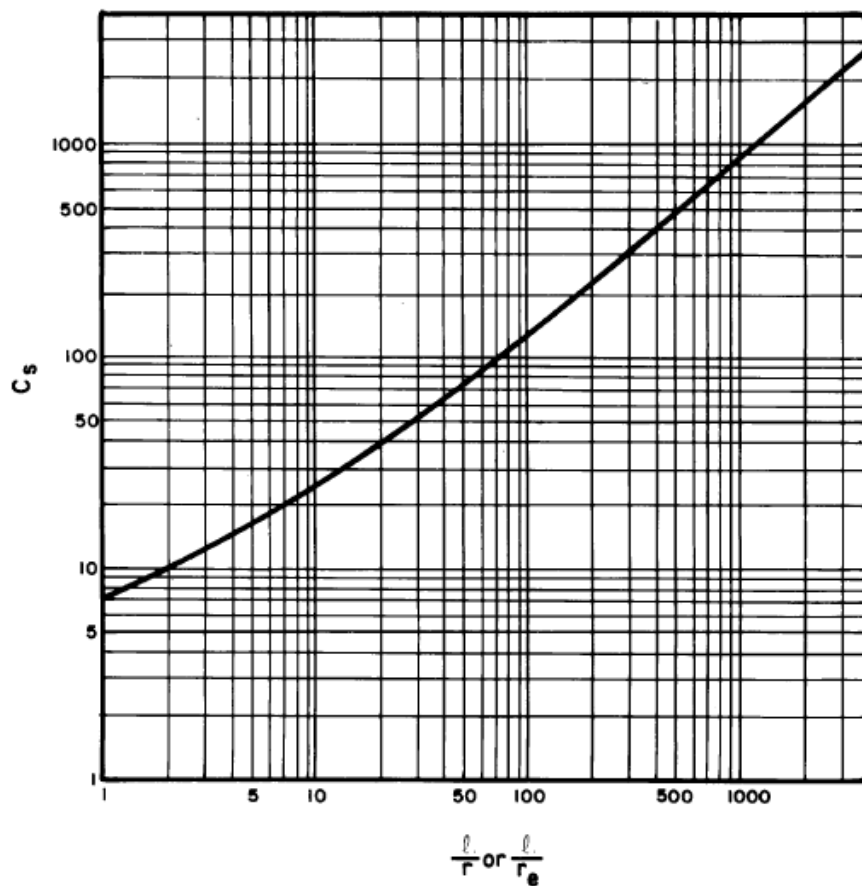

Figure 14- Graph for the determination of saturated conductivity coefficient C_s

Once all the parameters have been determined, the hydraulic conductivity values can be estimated through the equation:

$$K = \frac{Q}{\left(C_s + 4\frac{r_i}{r_e}\right)r_e H}$$

It has been possible to retrieve all the required data about well rates, effective radius, screen length and drops of groundwater level from the same 91 boreholes reports used for the stratigraphic reconstruction and contained in the ISPRA database. Therefore, fitting the above equation with such data, values of hydraulic conductivity has been retrieved for each borehole location.
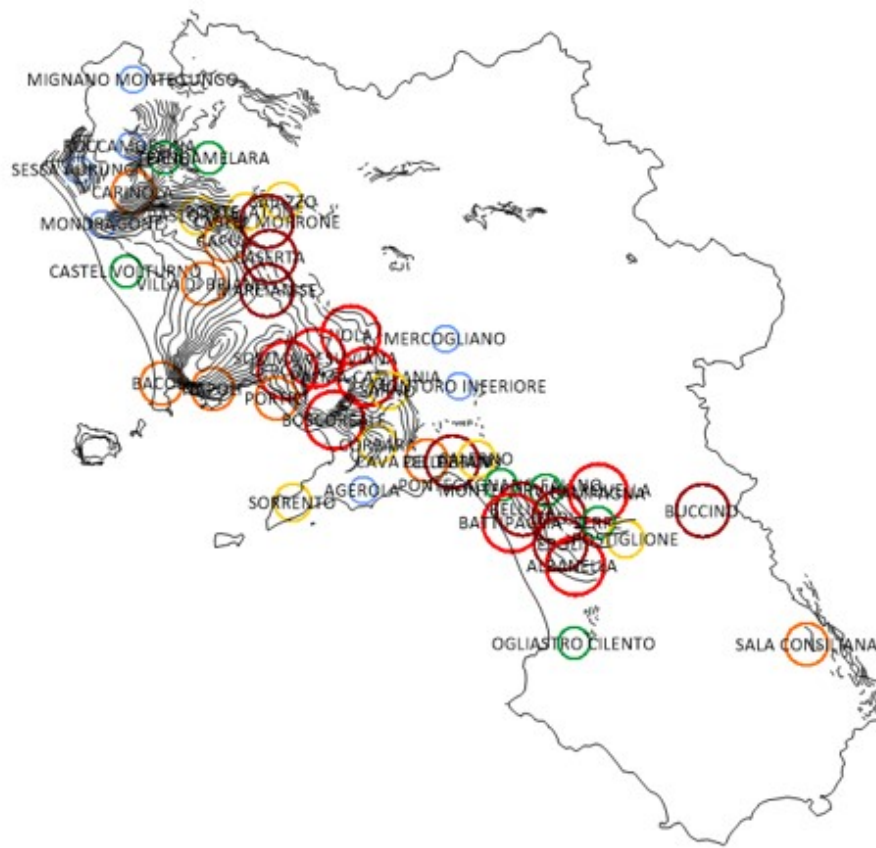

Figure 15- Surfer post map showing part of the estimated values of hydraulic conductivity. Larger circles correspond to higher hydraulic conductivity values

3.4. EVALUATION OF THE MARINE LEVEL TREND

For the evaluation of the sea level trend in Campania region, open data from the Servizio Mareografico Nazionale (SMN) has been utilized.

Task of the SMN is to provide take-over, processing and publication of quantities relative to the marine climate, to the state of the shorelines and to the marine levels, and to predispose criteria, methods and standard of collection, analysis and consultation of the data relative to the cognitive activities performed.

In order to accomplish the task, the SMN exploit the Rete Mareografica Nazionale (RMN). This is a network composed by 36 measuring stations uniformly distributed all over the national territory and located mainly inside the port facilities.

For all the stations, the published hydrometric level is monitored using a new microwave (radar) level meter with millimetric precision, coupled with a second level meter with a floater and also is still maintained active the ultrasonic hydrometric sensor presents in the RMN from 1998. Each level meter is reported to a basis, which quote has been determined referring to the I.G.M. altimetric network. The measuring stations are also equipped with an anemometric sensor to measure wind direction and velocity at 10 m above the ground level, with a barometric sensor, with sensors for air and water temperature measurements and also with a sensor for relative humidity measurements.

The measuring stations of the RMN that fall in the study area are those of Napoli and Salerno and so data recorded by such stations has been analysed. In addition to them, also the data from the stations of Gaeta and Palinuro have been taken into account in order to have a better understanding of the sea level situation over the entire region.

3.4.1. NAPOLI

The station of Napoli is located in the Molo del Carmine, inside the city port, and it records measurements of hydrometric level every 10 min. The available dataset, from the ISPRA website, covers the period from January 2010 to November 2015.

In the present study raw data have been processed to obtain an average value of hydrometric level per day, which was plotted vs time and the trendline is finally extrapolated from the observed trend.
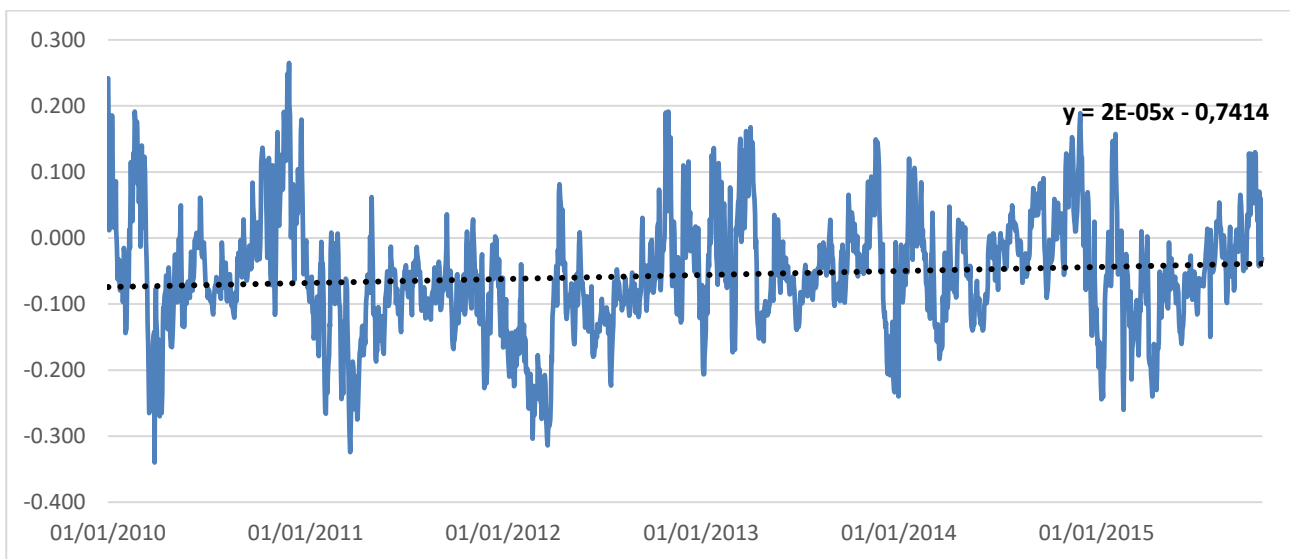

Figure 16- Trend of marine level recorded in Napoli for the period 2010-2015

The recorded trend shows many fluctuations typical of tidal movement but from the graph is possible to see that the sea level is lower than 0 m a.s.l. with an average level, for the period considered, equal to – 0,057 m.

The trendline shows a slightly increasing trend that highlights the issue of sea level raise.

3.4.2. SALERNO

The measuring station of the RMN in Salerno is located in the dock Manfredi and it records measurements of hydrometric level every 10 min. The available dataset, from the ISPRA website, covers the periods from January 2010 to December 2014 and from April 2017 to December 2020.
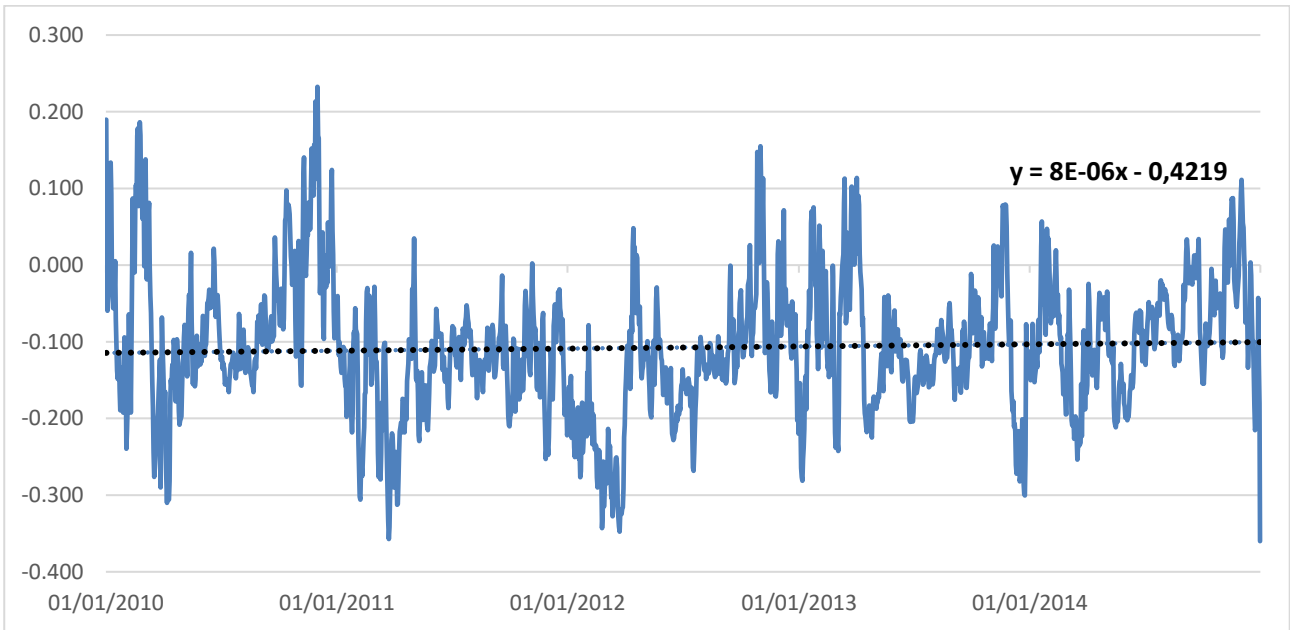

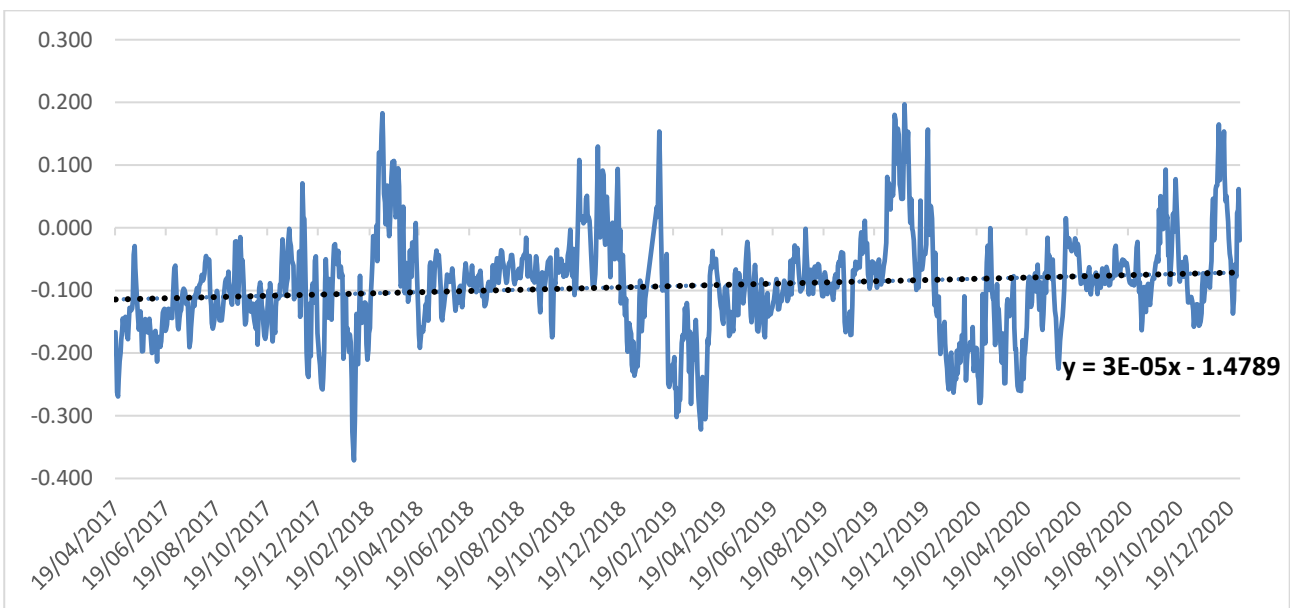*Figure 17- Trend of marine level recorded in Salerno for the period 2010-2014*

Figure 18- Trend of marine level recorded in Salerno for the period 2017-2020

Similar to the case of Napoli, the sea level in Salerno is lower than 0 meters a.s.l with average level of -0,107 m for the period 2010-1014 and an average level of – 0,093 m for the period 2017-2020.

From the trendlines is possible to see that there is an increasing trend of sea level in both periods considered, more pronounced in 2017-2020 than in the period 2010-2014.

3.4.3. GAETA

The analysis of data from the measuring station of Gaeta has been investigated despite Gaeta is located northern than the study area because it can be useful for a comprehensive understanding of the marine level at regional scale.

In that case, the available dataset, from the ISPRA website, is more fragmented. Continuous measurements have been recorded only from June 2010 to January 2015 and from April 2019 to December 2020.
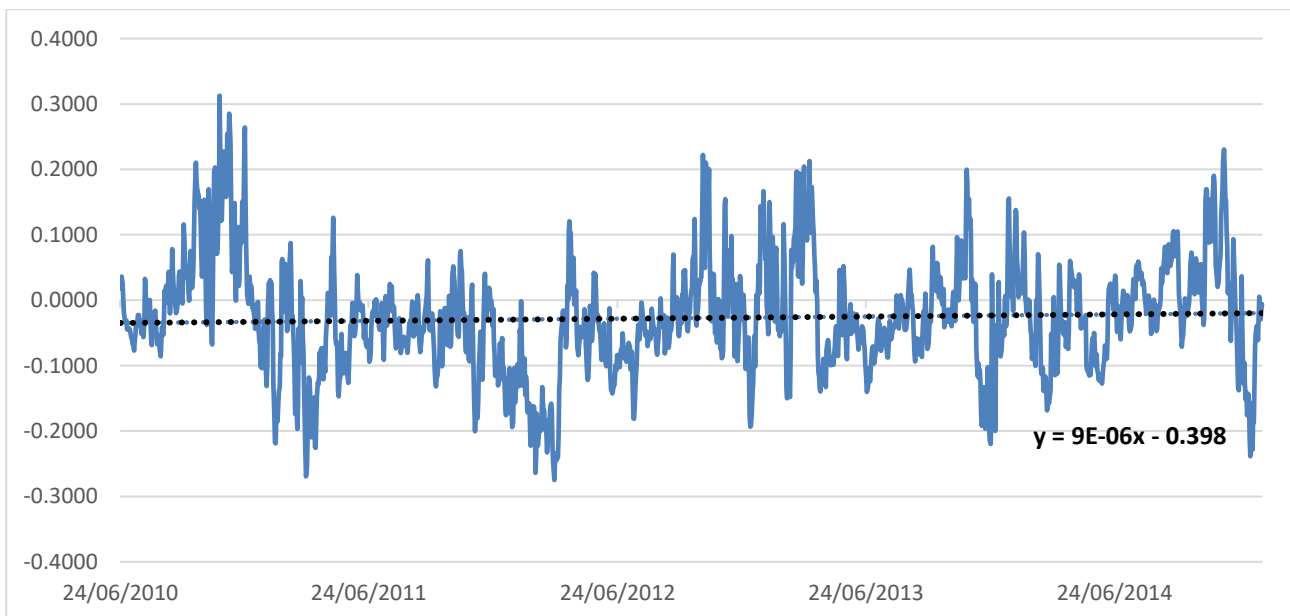

$$y = 9E-06x - 0.398$$

Figure 19- Trend of marine level recorded in Gaeta for the period 2010-2014
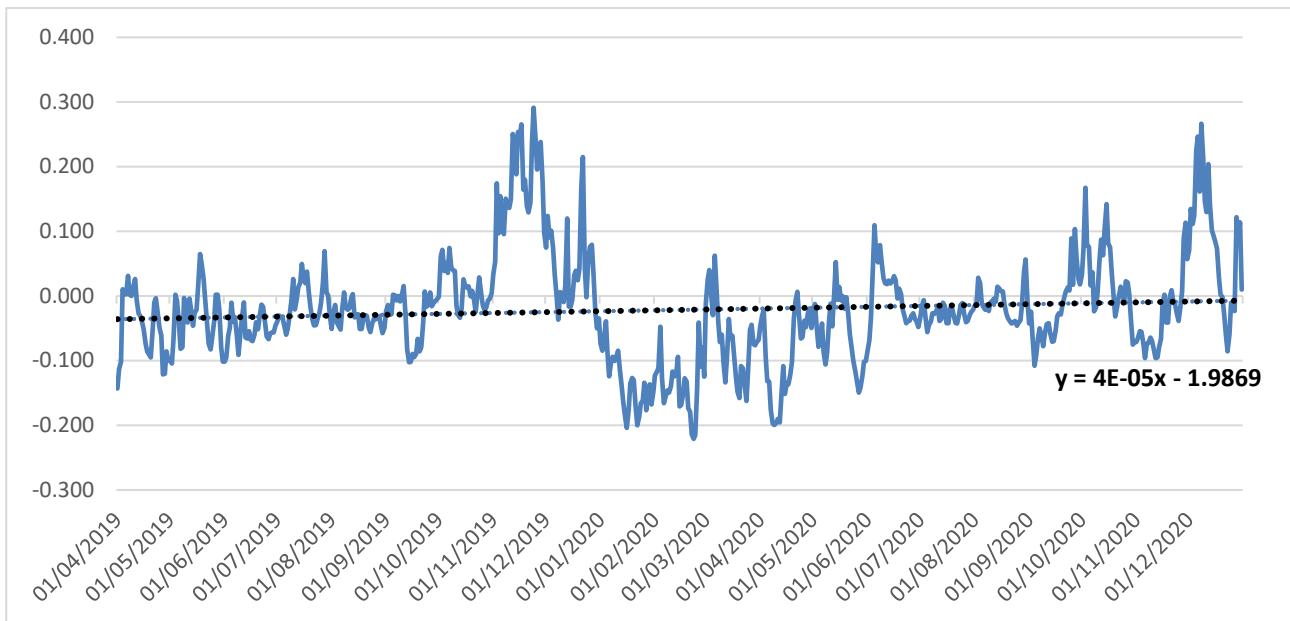
Figure 20- Trend of marine level recorded in Gaeta for the period 2019-2020

The same increasing trend of sea level is recorded even in Gaeta with a higher slope for the period 2019-2020 respect to the period 2010-2014, while there the average marine level is higher than Napoli and Salerno. In fact, it has been measured an average level of -0,027 m for 2010-2014 and an average level of - 0,022 m for 2019-2020.

3.4.4.   PALINURO

For the same reason of Gaeta, data from the Palinuro measurement station has been analysed despite it is located southern the study area. The available dataset from the INSPRA website, in this case, is continuous from January 2010 to December 2020.

Figure 21- Trend of marine water level recorded in Palinuro for the period 2010-2020

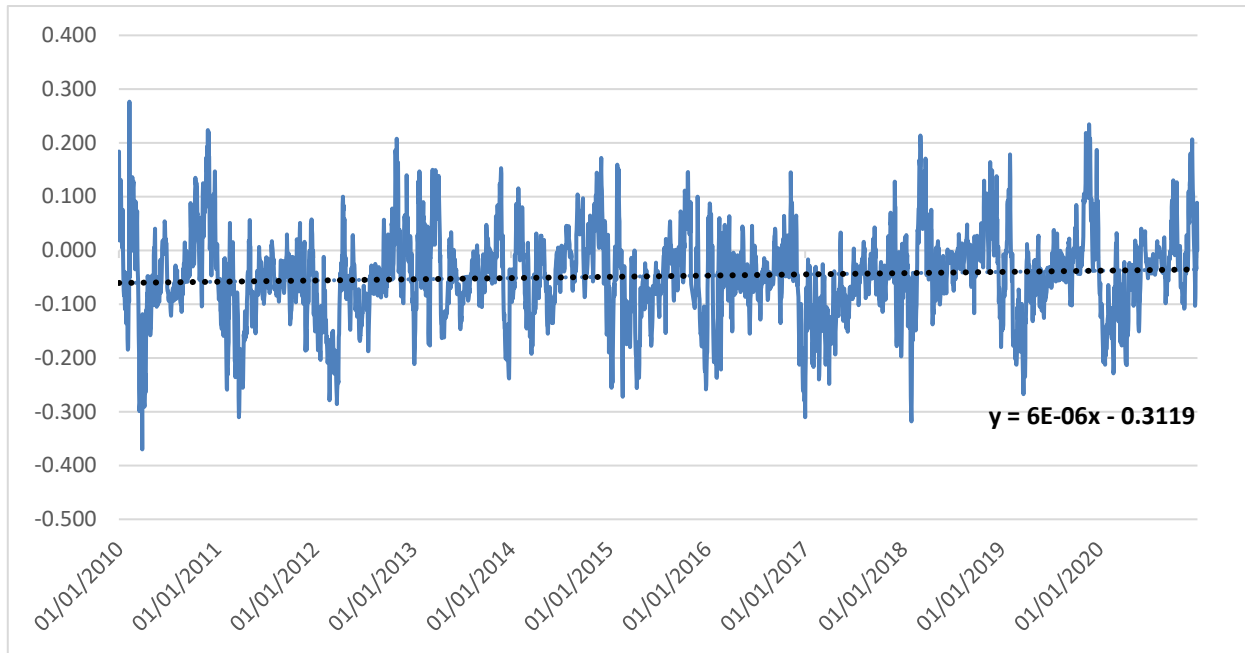The recorded behaviour in Palinuro has many analogies with the one of Napoli and Salerno. In fact, the average marine level for the entire period is below 0 m and in particular equal to -0,048 m above sea level. Even the increasing trendline has a slope similar to the one of the other analysed stations.

3.5. ELABORATION OF MODIS EVAPOTRANSPIRATION DATA

MODIS (or Moderate Resolution Imaging Spectroradiometer) is a key instrument aboard the Terra and Aqua satellites, lunched by the NASA Earth Observing System EOS. The MODIS instrument has been designed and developed since the Engineering Model (EM) was completed in mid-1995. Since then, two spaceflight units, the Protoflight Model (PFM), aboard the Terra Satellite, and the Flight Model 1 (FM1), aboard the Aqua Satellite, have been completed and launched. Terra was launched on December 1999, and Aqua was launched on May 2002. Terra's orbit around the Earth is timed so that it passes from North to South across the equator in the morning, while Aqua passes South to North over the equator in the afternoon. Terra MODIS and Aqua MODIS are viewing the entire Earth's surface every 1 to 2 days, acquiring data in 36 spectral bands between 0.405 and 14.385 µm, at three spatial resolutions (250 m, 500 m, and 1000 m). The many data products derived from MODIS observations describe features of the land, oceans and the atmosphere that can be used for studies of processes and trends on local to global scales.

In particular, MOD16 global evapotranspiration product can be used to calculate regional water and energy balance hence, it provides key information for water resource management. With long-term ET data, the effects of changes in climate, land use, and ecosystems disturbances on regional water resources and land surface energy change can be quantified.

The MOD16 global evapotranspiration datasets are regular 500x500 m land surface ET datasets for the 109, 03 million km^2 global vegetated land areas at 8-day, at monthly and annual intervals and they cover the time period 2000-2020 (MODIS Web (nasa.gov)).

The data was download using the AppEEARS (AppEEARS, 2020) interface and the MYD16A3GF model (Running et al. 2019) to obtain spatially interpolated values of

evapotranspiration in Campania region for the period 2000-2020 expressed with seasonal frequency (January, April, July and October). Specifically, the algorithm used in the MOD16 products is based on the Penman-Monteith equation, which includes inputs of daily meteorological data along with MODIS remotely sensed data products such as vegetation property dynamics, albedo and land cover (Mu et al. 2011).

The pixel values of ET have been averaged using seasonal intervals and then extracted inside monitoring points with spatial resolution of 500 m. The data obtained was then spatialized using kriging technique to obtain data also in no-data zones.

The graph of figure 22 shows the trend of the mean evapotranspiration recorded in the study area for the period 2000-2020. From the trendline it's possible to appreciate how the that the value of ET is increased in the period considered.
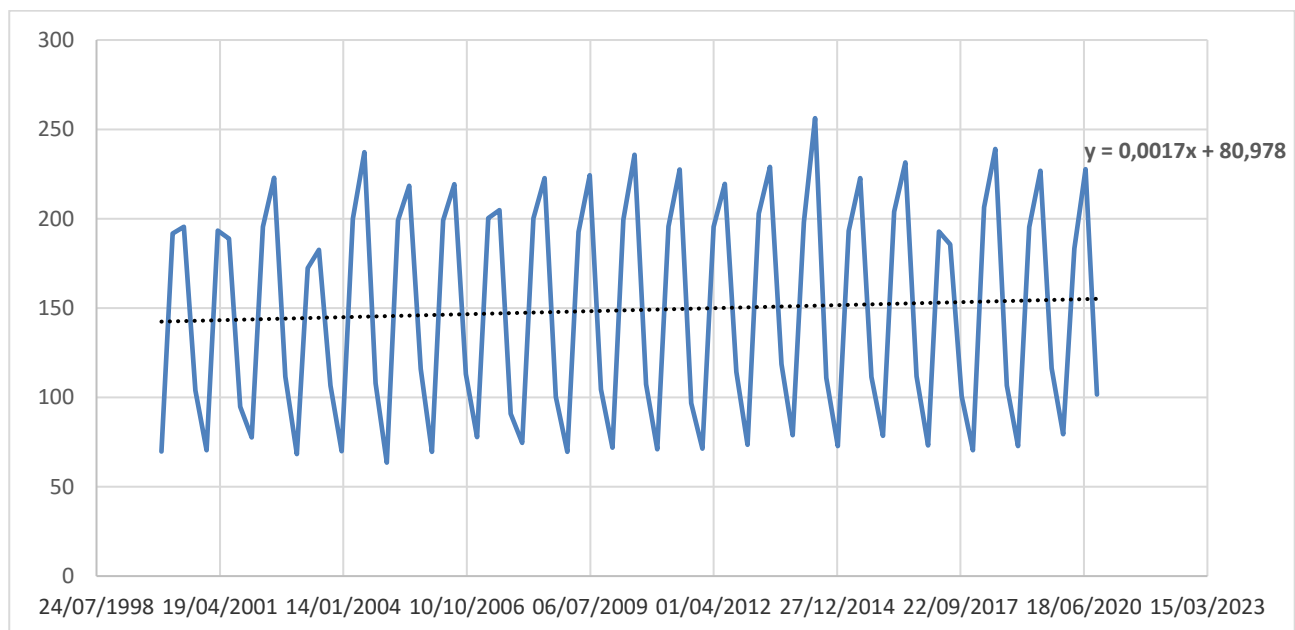
Figure 22-Trend of mean ET in Campania region for the period 2000-2020

Analysing separately the behaviour in the single seasons, it's possible to see that the largest increment of evapotranspiration is recorded in summer season (figure 23), when evapotranspiration is increased of about 70 mm in the twenty years considered, while in winter (figure 24) the increment is smaller (about 16 mm).

Figure 23-Trend of mean summer ET in Campania region for the period 2000-2020

Figure 24-Trend of mean winter ET in Campania region for the period 2000-2020

3.6. ELABORATION OF RECHARGE DATA

Time series of groundwater recharge have been retrieved by the PCR-GLOBWB 2, a global hydrology and water resources model described by Sutanudjaja et al. (2018).

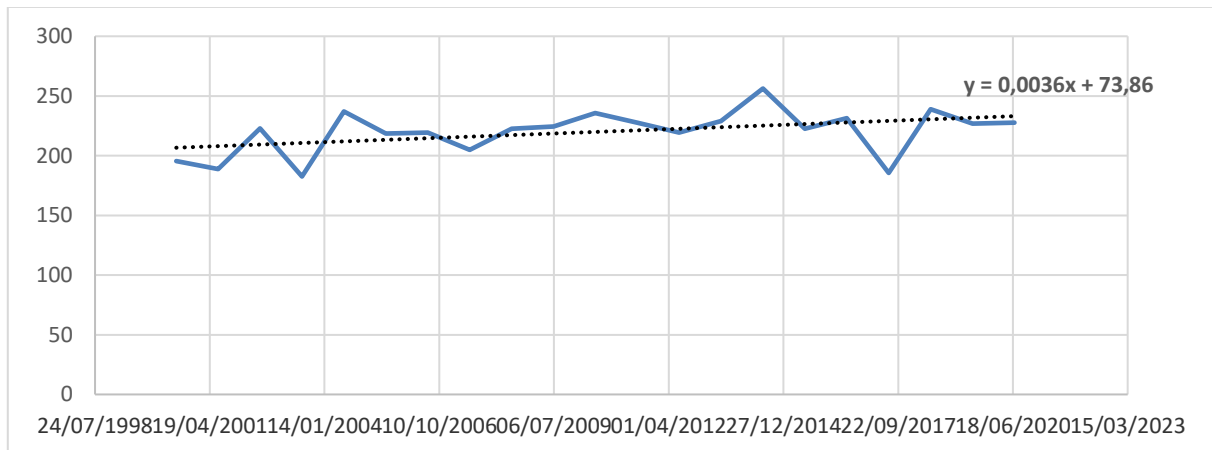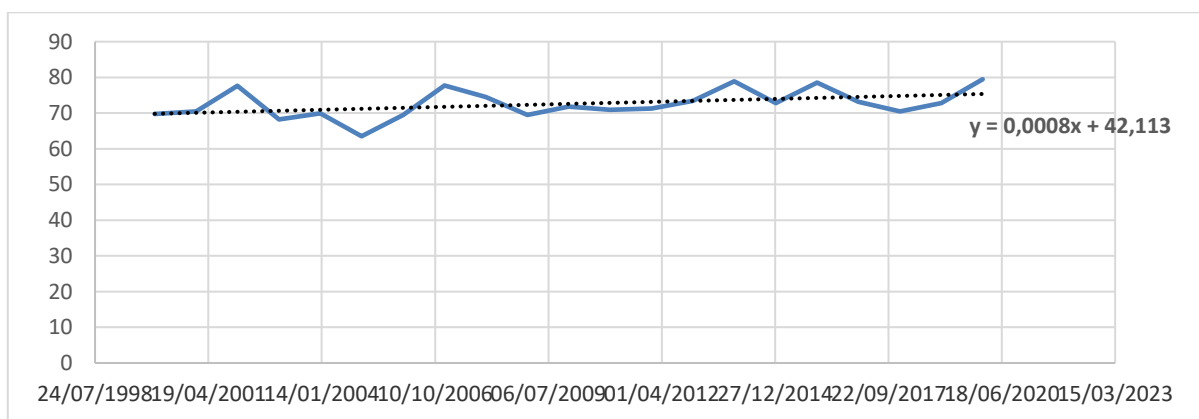Global hydrological models (GHMs) are invaluable tools to support of global change research and environmental assessments since they are able to quantify and understand the global terrestrial water cycle, simulating the distributed hydrological response to weather and climate variations at high resolution.

PCR-GLOBWB is a grid-based global hydrological model developed by the Utrecht University, Netherlands, that describes the terrestrial part of the hydrological cycle, covering all continents except Greenland and Antarctica. It was originally developed to solve the global daily surface water balance with a spatial resolution of 30 arcmin (about 50 km by 50 km at the Equator) and compare the resulting freshwater availability with monthly sectoral water demand in order to assess global-scale water scarcity. The new version of the model PCR-GLOBWB 2 is able to simulate the water balance at a finer spatial resolution of 5 arcmin, allowing a much better representation of the effects of spatial heterogeneity in topography, soil and vegetation on the terrestrial hydrological dynamics. For each grid cell and each time step, generally equal to 1 day, PCR-GLOBWB 2 simulates moisture storage in two vertically stacked upper soil layers, as well as the water exchange among soil, atmosphere and the underlying groundwater reservoir, in terms of precipitation, evaporation from soils, open water and snow, plant transpiration, infiltration, run-off, interflow, baseflow and groundwater recharge. In addition, human water use is fully integrated within the hydrological model, meaning that at each time step the water demands for irrigation, livestock, industry and households are estimated and then translated into actual withdrawals from groundwater and surface water.

In this present study, groundwater recharge data have been downloaded from the PCR-GLOBWB 2 model and elaborated in order to obtain spatially interpolated values of recharge in Campania region for the period 2000-2015 expressed with seasonal frequency (January, April, July and October).

In analogy to what has been done for evapotranspiration data, the trend of mean recharge recorded in the study area for the period 2000-2015 has been evaluated and shown in figure 25.
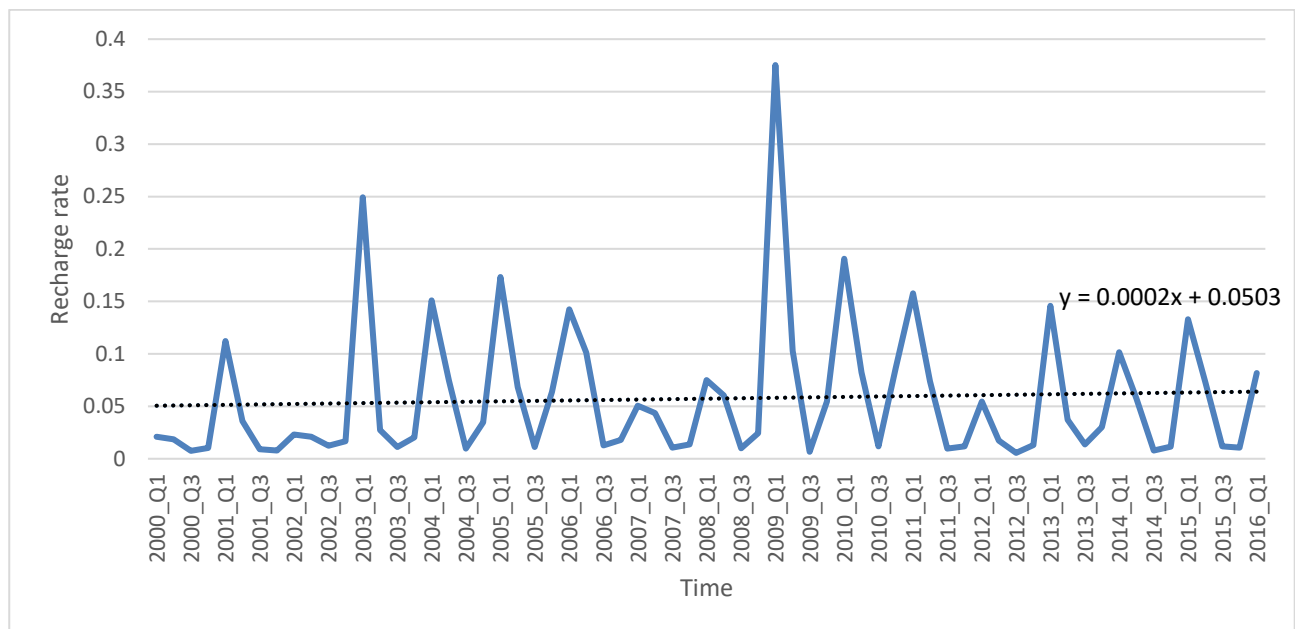
Figure 25-Trend of recharge rate recorder in the study area for the period 2000-2015

To check the reliability of the downloaded datasets, meteorologic statistics published by the agroclimatic observatory of the Italian Ministero delle politiche Agricole alimentari e forestali (MIPAAF) have been inspected. Figure 26 shows the available information about minimum and maximum temperature, precipitation and evapotranspiration that has been recorded in the Campania region for the period 2009-2018.

	2009	2010	2011	2012	2013	2014	2015	2016	2017	2018
Temp. minima (°C)	10.3	9.8	10	10.1	10.3	10.6	10.7	10.9	10.8	-
Media climatica (°C)	10.3	10.3	10.3	10.3	10.3	10.3	10.3	10.3	10.3	10.3
Scarto dal clima (°C)	0	-0.5	-0.3	-0.2	0	0.3	0.4	0.6	0.5	-
Temp. massima (°C)	19.6	19.1	20.3	20.5	20.2	20.2	20.2	19.6	19	-
Media climatica (°C)	18.9	18.9	18.9	18.9	18.9	18.9	18.9	18.9	18.9	18.9
Scarto dal clima (°C)	0.7	0.2	1.4	1.6	1.3	1.3	1.3	0.7	0.1	-
Precipitazione (mm)	1040.7	1084.7	734.5	827.8	1013.5	883.4	880.6	835.4	549.9	-
Media climatica (mm)	767.1	767.1	767.1	767.1	767.1	767.1	767.1	767.1	767.1	767.1
Scarto dal clima (%)	35.7	41.4	-4.2	7.9	32.1	15.2	14.8	8.9	-28.3	-
Evapotraspirazione (mm)	952.9	887.5	997.5	1082.8	1001.9	873.5	991.4	874.4	990.2	-
Media climatica (mm)	926.3	926.3	926.3	926.3	926.3	926.3	926.3	926.3	926.3	926.3
Scarto dal clima (%)	2.9	-4.2	7.7	16.9	8.2	-5.7	7	-5.6	6.9	-

Figure 26-Meteorologic statistics for the period 2009-2018

Specifically, the trends of recorded precipitation and evapotranspiration have been evaluated (figure 27) and after a qualitative comparison with the trends of evapotranspiration and recharge, obtained respectively from MODIS and PCR-GLOBWB 2 model, the downloaded datasets have been considered as reliable since they depict an increased precipitation and potential evapotranspiration respect to the historical dataset.
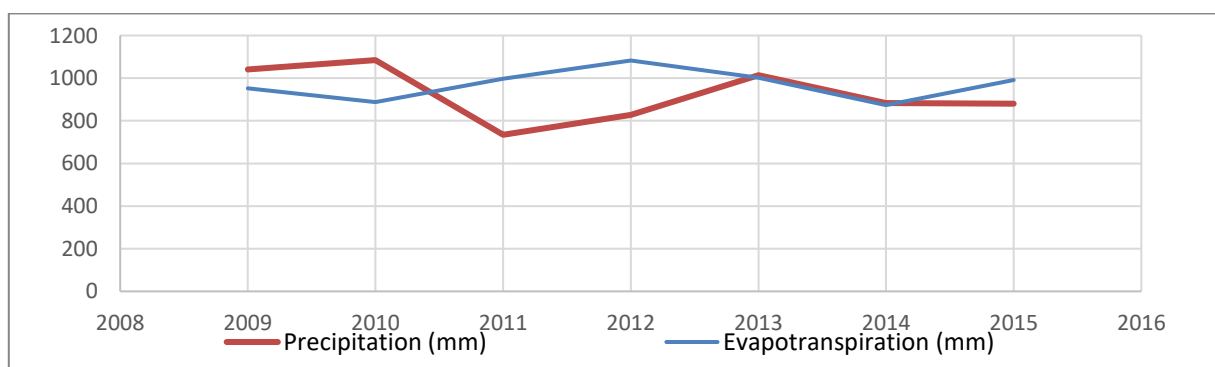

Figure 27-Trends of precipitation and evapotranspiration recorded in the Campania region for the period 2009-2018

4. MODELLING PHASE

The modelling phase in the present study is conducted through the use of Processing Modflow 11, published by Simcore Software.

Processing Modflow (PM) is a graphical user interface for preparing input data files to the supported numerical models. It was originally developed to support the first official release of MODFLOW (McDonald and Harbaugh, 1988) but, in the following years, the list of model codes supported by PM has grown due to the subsequent release of several versions of MODFLOW and to the development of many model codes to add functionalities to MODFLOW.

The supported model codes in the PM 11 version are several, including MODFLOW for groundwater flow modelling, SEAWAT for density dependent flow and transport models, MODPATH for particle tracking, MT3D-USGS for groundwater solute transport models, PEST for model calibration and other codes with different functionalities.

The theoretical part of MODFLOW numerical code, the one that has been used in this research project is described in the following section.

4.1. THEORETICAL FUNCTIONING OF MODFLOW

MODFLOW is a 3D finite-difference model associated with a modular computer program. The modular structure consists of a main program and a series of highly independent subroutines called "modules". The modules are, in turn, grouped into "packages", each of them dealing with a specific feature of the hydrologic system which is to be simulated. For example, the Well Package simulates the effects of wells, the River Package simulates the effects of rivers and the Drain Package simulates the presence of drains.

The division of the program into modules allows to examine specific hydrologic features of a model independently and to add new modules or packages without modifying the existing ones.

The equation that stands at the base of MODFLOW is the partial-differential equation that describes the three-dimensional movement of groundwater of constant density through porous earth material (McDonald and Harbaugh, 1988):

$$\frac{\partial}{\partial x}\left(K_{xx}\frac{\partial h}{\partial x}\right) + \frac{\partial}{\partial y}\left(K_{yy}\frac{\partial h}{\partial y}\right) + \frac{\partial}{\partial z}\left(K_{zz}\frac{\partial h}{\partial z}\right) + W = S_s \frac{\partial h}{\partial t}$$

Where:

- K_{xx}, K_{yy} and K_{zz} are values of hydraulic conductivity along the x, y and z coordinate axes, which are assumed to be parallel to the major axes of hydraulic conductivity (L/T);
- h is the potentiometric head (L);
- W is a volumetric flux per unit volume representing sources and/or sinks of water, with W< 0 for flow out of groundwater system and W> 0 for flow into the system (T^{-1});
- S_s is the specific storage of the porous material (L^{-1});
- t is time (T)

In general, S_s, K_{xx}, K_{yy} and K_{zz} may be functions of space and h and W may be functions of space and time so that the equation describes ground-water flow under non-equilibrium conditions in a heterogeneous and anisotropic medium.

The equation above, together with specification of flow and/or head conditions at the boundaries of an aquifer system and specification of initial-head conditions, constitutes a mathematical representation of groundwater flow system. A solution of the equation, in an analytical sense, is an algebraic expression giving h(x, y, z, t) such that, when the derivatives of h with respect to space and time are substituted into

the equation, the equation and its initial and boundary conditions are satisfied. Except for very simple systems, analytical solutions are rarely possible so numerical methods must be employed to obtain approximate solutions. The numerical method used by MODFLOW is the finite-difference method in which the continuous system is replaced by a finite set of discrete points in space and time, and the partial derivatives are replaced by terms calculated from the differences in head values at these points. The process leads to systems of simultaneous linear algebraic difference equations and their solution gives values of head at specific points and time.

For this reason, the aquifer system is discretized in a grid of blocks called cells, which location is described in terms of rows, columns and layers and within which there is a point called "node" at which head is calculated. Many schemes for locating nodes in cells could be used; however, MODFLOW uses the block-centred formulation in which the nodes are at the centre of the cells.

The solution of the groundwater flow equation in finite-difference form exploits the application of the continuity equation so the sum of all flows into and out of the cell must be equal to the rate of change in storage within the cell. Under the assumption that the density of ground water is constant, the continuity equation expressing the balance of flow for a cell is:

$$\sum Q_i = SS \, \frac{\Delta h}{\Delta t} \, \Delta V$$

Where:

- Q_i is a flow rate into the cell ($L^3 \, T^{-1}$);
- SS is the specific storage in the finite-difference formulation (L^{-1});
- ΔV is the volume of the cell (L^3); and
- Δh is the change in head over a time interval of length Δt (L).

The term on the right-hand side is equivalent to the volume of water taken into storage over a time interval Δt given a change in head of Δh.

Thanks to the Darcy's law, it's possible to evaluate the volumetric flowrate entering a single cell from each of its adjacent six cells, just knowing values of hydraulic conductivity between the nodes, area of cell faces and distance between nodes.

Such volumetric flowrate is then used as input for the application of the continuity equation, together with changes in storage and eventual external flowrates from outside the aquifer, evaluated with apposite expressions. The time derivative Δh/Δt is approximated using the difference in head at the node, over a time interval that precedes and ends with the time at which flow is evaluated. This one is called a backward-difference approach, in which Δh/Δt is approximated over a time interval that extends backward in time from the time at which the flow terms are calculated.

$$\frac{\Delta h_{i,j,k}}{\Delta t} \cong \frac{h_{i,j,k}^{m} - h_{i,j,k}^{m-1}}{t^m - t^{m-1}}$$

This procedure generates for each cell an equation with seven unknown head values (one for the cell considered and one for each of the six adjacent cells), that cannot be solved independently because it represents a single equation in seven unknowns. However, an equation of this type can be written for each active cell in the grid and, since only one unknown head exists for each cell, it's possible to obtain a system of "n" equations in "n" unknowns that can be solved simultaneously.

MODFLOW utilizes iterative methods to obtain the solution to the system of finite-difference equations. In these methods, the calculation of head values for the end of a given time step is started by arbitrarily assigning or estimate a trial value for the head at each node at the end of that step. A procedure of calculation is then initiated that alters these estimated values, producing a new set of head values that are in closer agreement with the system of equations. These new head values take the place

of the initially assumed heads and the procedure of calculation is repeated, producing a third set of head values. This procedure is repeated successively at each stage, producing a new set of heads that more nearly satisfies the system of equations. Each repetition of the calculation is called an iteration. Ultimately, as the heads approach to values that would exactly satisfy the set of equations, the changes produced by succeeding stages of calculation become very small. Ideally, the iteration should stop when the calculated heads are suitably close to the exact solution but because the actual solution is unknown, an indirect method for specifying when to stop the iteration must be used. The method most commonly employed is to specify that the changes in computed heads, occurring from one iteration level to the next, must be less than a certain quantity, specified by the user and called "closure criterion" or "convergence criterion". After each iteration, absolute values of computed head changes in that iteration are examined for all nodes in the grid. The largest of these absolute head-change values is compared with the closure criterion. If this largest value exceeds the closure criterion, iteration continues while, if this value is less than the closure criterion, iteration is said to have "closed" or "converged," and the process is terminated.

4.2. MODEL SETUP IN STEADY STATE CONDITIONS

The setup of the model can be done following four main steps:

1) Creation of the model and discretization of the model domain: grid and boundary conditions;

2) Assignment of model parameters: time and aquifer properties;

3) Definition of the inputs to the model: stress and flow packages;

4) Evaluation of the model outputs: solvers and results control.

4.2.1. CREATION OF THE MODEL AND DISCRETIZATION OF THE MODEL DOMAIN: GRID AND BOUNDARY CONDITIONS

The mandatory steps for the realization of a groundwater modelling process are: i) define the goals of the model, ii) select a computer code, iii) collect the necessary data, iv) develop a conceptual model of the groundwater system and finally v) define the spatial discretization of the model domain. In a MODFLOW model, an aquifer system is represented by a discretized domain consisting of an array of nodes and associated finite difference blocks, called cells.
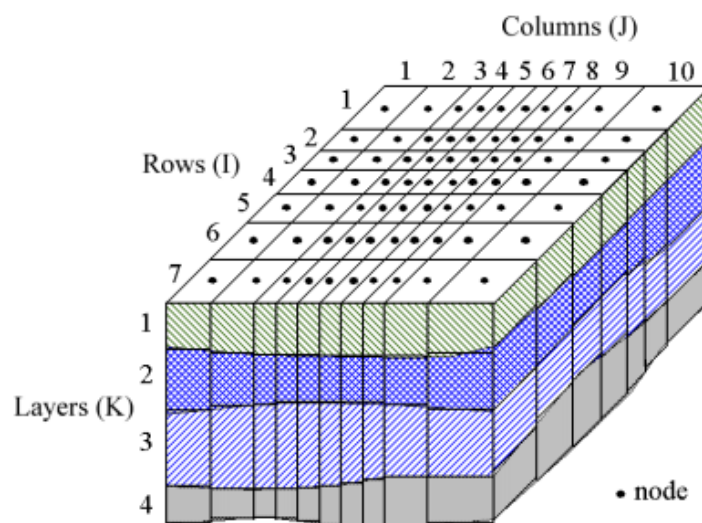

Figure 28-Spatial discretization scheme of an aquifer system

Figure 28 shows the spatial discretization scheme of an aquifer system with a mesh of cells and nodes at which hydraulic heads are calculated. The nodal grid forms the framework of the finite-difference numerical model. Hydrostratigraphic units can be represented by one or more model layers and the layer thickness may vary from cell to cell. Processing Modflow, that is the graphical user interface employed in this study, uses the index notation [Layer, Row, Column] to describe the location of a cell in a 3D array. For example, the cell located in the first layer, 6th row, and 2nd column is denoted by [1, 6, 2]. For 2D arrays instead, the index notation [Row, Column] is used.

For the creation of a new model, it's necessary to select the "Create Model" item on the menu. This action opens the Create Model dialog box (Figure 29) that allows to create a new model. When a model is created within PM, it makes a model data folder in the folder where the PM file is located and all the input and output files of the model are stored in that model data folder.
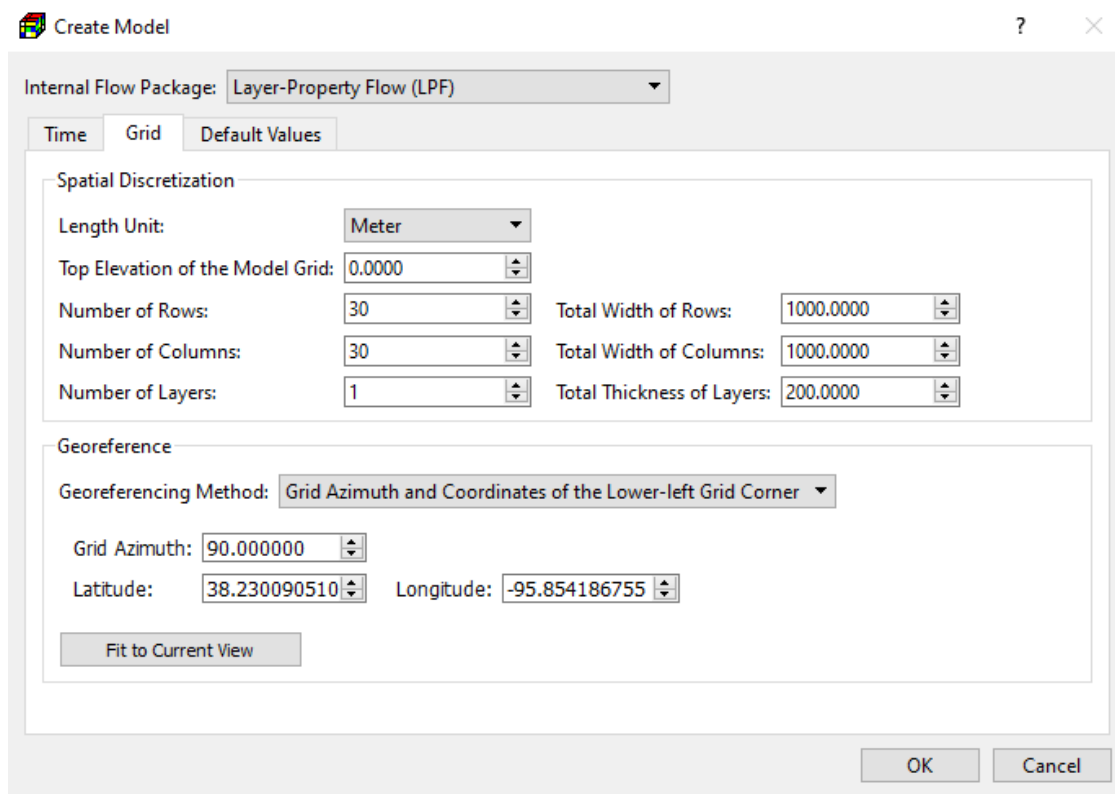

Figure 29-Create model dialog box

The Create model dialog box requires the specification of the Internal Flow Package that will be used to insert all those properties which control groundwater flow between model cells. The three supported Internal Flow Packages are the Layer-Property Flow (LPF), the Block-Centred Flow (BCF) and the Upstream-Weighting (UPW). Specifically, the UPW Package is designed to solve problems involving drying and rewetting non linearities of the unconfined groundwater-flow equation, while BCF and LPF packages, despite they use an identical conceptualization, require different input data.

In addition, the box allows to define temporal discretization parameters, such as Model Start Date/Time, Length of the Simulation, Number of Stress Period and Number of Time Steps; spatial discretization parameters, such as Top Elevation of the Model Grid, Number of Rows, Number of Columns, Number of Layers and the Total Width of Rows and Columns that together allow to define the horizontal model extent.

Finally, the Create Model Dialog box allows to select also the Georeferencing Method that defines how the model grid is associated with a spatial location. Selecting the Longitude/Latitude Coordinates of Grid Corner, the user has to specify the coordinates of the four model grid corners, while selecting Grid Azimuth and Coordinates of the Lower-Left Grid Corner option, it's sufficient to specify the coordinates of the lower-left grid corner and the grid azimuth angle.

After specifying all these parameters and clicking the ok button, the model is created. If the model is created successfully, a model item will be added to the Models group on the Table of Content and the model item will be highlighted in yellow indicating that the new model is set as the active model.

The model domain of the study area is composed by a total on 543120 cells, organized in 584 rows, 310 columns and vertically in 3 layers of different thickness. The width of the model domain along rows is equal to 56500 meters, while the width along columns is equal 150000 meters, so that the area covered by the model grid is equal to 8 474 km^2. The top of the grid represents the local ground surface, ranging from -3,49 to 1642 m a.s.l. and obtained importing the DTM of the Campania region into the software. The bottom of the grid, instead, represents the bottom of unconfined aquifers of the Campania region and it has been obtained interpolating stratigraphic data, taken from reports of borehole analysis contained in the online ISPRA database. It ranges from -83 m below sea level to 144 m above sea level.

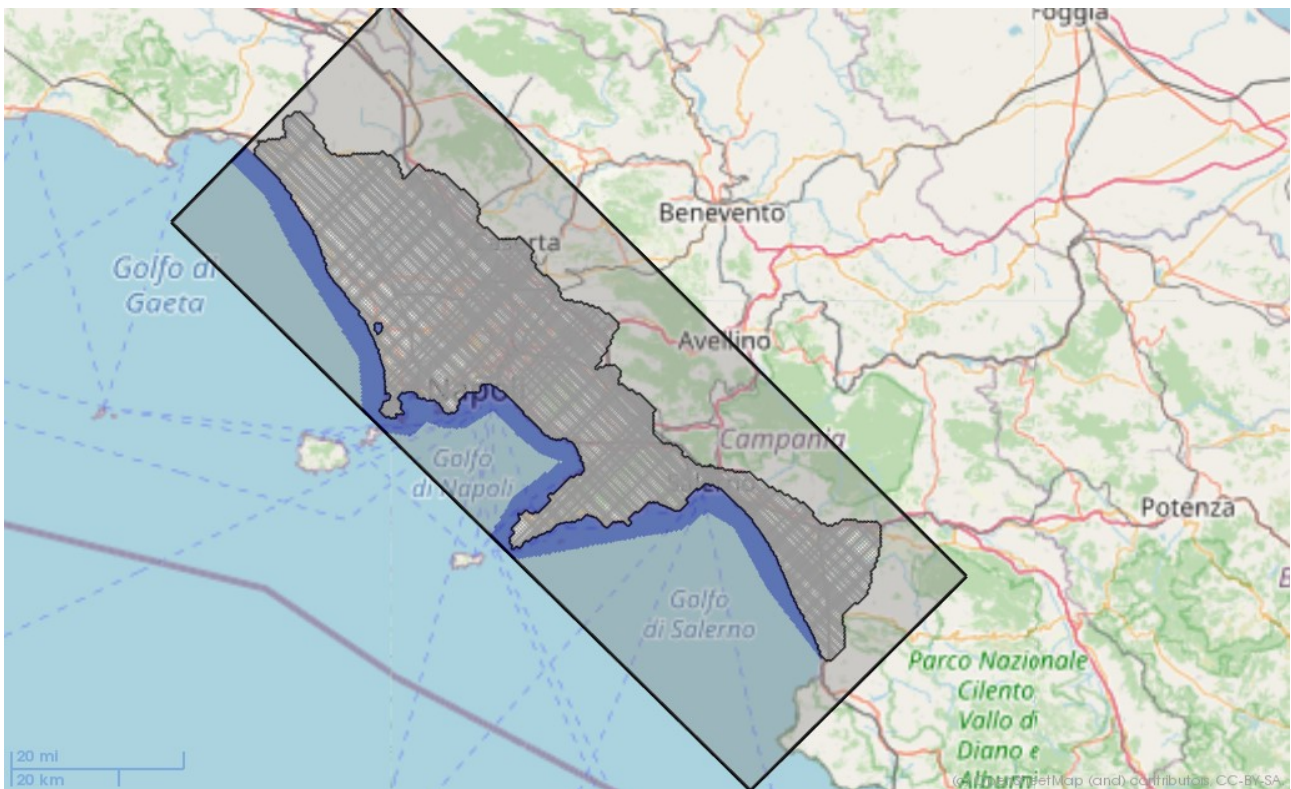Figure 30 shows a representation of the model domain that overlays a base map of the Campania region.

Figure 30- Model grid of the study area

During the discretization of the model domain is also necessary to define the layer properties through the Layer Property dialog box.

Here it's necessary to specify the layer types that affect the numerical formulation of the groundwater flow equation. The available options and required parameters depend on the select internal flow packages. Since UPW Package is the one used in the present study, the supported layer types are confined or convertible.

If the layer type is considered as confined, the required parameters for the simulation are the horizontal hydraulic conductivity (HK), the specific storage (S_s), the vertical hydraulic conductivity (VK) or the vertical anisotropy (VANI). In such case the interblock conductance is calculated based on HK and layer thickness, the storage is calculated based on S_s and layer thickness, while VK or VANI is used for calculating vertical conductance between layers.

If instead the chosen layer type is convertible between confined and unconfined, the required input parameters are the horizontal hydraulic conductivity HK, the specific storage S_s, the specific yield S_y, the vertical hydraulic conductivity VK or the vertical anisotropy VANI. In that case, if the layer is not fully saturated, the storage is calculated based on S_y and the saturated thickness and the interblock conductance is calculated based on HK and the saturated thickness, while if the layer is fully saturated, the storage is calculated based on S_s and the layer thickness and the interblock conductance is calculated based on HK and the layer thickness. VK or VANI is used for calculating vertical conductance between layers.

In addition to the definition of the layer types, the layer properties dialog box requires the specification of the method for the calculation of the interblock transmissivity, the specification of horizontal anisotropy HANI and the indication of the choice between the usage of vertical hydraulic conductivity VK or vertical anisotropy VANI as parameter of the layer. Finally, there is also space for the specification of the ratio of

horizontal transverse dispersivity to the longitudinal dispersivity TRPT and of the ratio of vertical transverse dispersivity to the longitudinal dispersivity TRPV, together with boxes for determining transmissivity values T, vertical leakage values VCONT, confined storage coefficient S and to switch on/off the calculation of storage changes and compaction for specific layers IBS.

In the present study, all the three layers of the model grid are set as convertible between confined and unconfined and the chosen method for the calculation of the interblock transmissivity is the harmonic mean method. The value of horizontal anisotropy HANI is set equal to 1, while the values of TRPT and TRPV are both set equal to 0,10.

Figure 31 shows the representation of the layer property dialog box as set in the project study. The columns for the definition of T, VCONT, S AND IBS are deactivated because such parameters are not supported when UPW Package is used as Internal Flow Package.
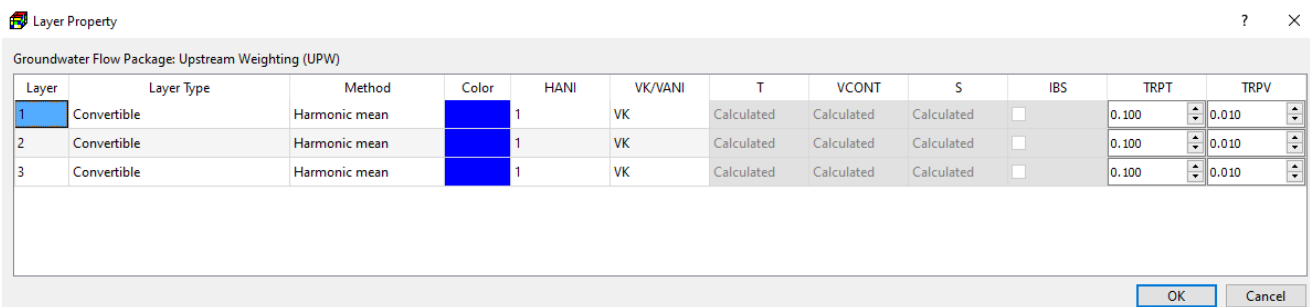

Figure 31- Layer property dialog box

As last step of the discretization of the domain, MODFLOW requires the input of an IBOUND array, which contains a value for each model cell. A positive value in the IBOUND array defines an active cell where the hydraulic head is computed, a negative value defines a constant head cell and the value 0 defines a no-flow cell (i.e., inactive) cell. It is suggested to use 1 for variable-head cells, 0 for no-flow cells and -1 for

constant head cells. For constant head cells, the hydraulic head is hold at the starting value throughout the simulation. A constant head boundary exists when an aquifer is in direct hydraulic contact with a river, a lake, or a reservoir in which the water level is known to be constant. It is important to know that constant head boundaries can provide inexhaustible supply or sink of water. Any outer boundary cell, which is not a constant head cell, is automatically a zero-flux boundary cell. Flux boundary with non-zero fluxes are simulated by assigning appropriate infiltration or pumping wells in the corresponding cell via the well package.

The study area in this project has been delimited by no-flow cells (value 0), while the Tyrrhenian Sea and Patria Lake have been set as constant-head cells (value -1). In addition, in layer 3 the east side border of the study area has been delimited by constant head cells to simulate the recharge form the adjacent carbonate aquifers. All other cells have been instead set as active cells. Figure 32 shows the subdivision of the domain in active, constant-head and no-flow cells. Active cells are represented in white, constant-head cells in blue while no-flow cells are represented in grey.
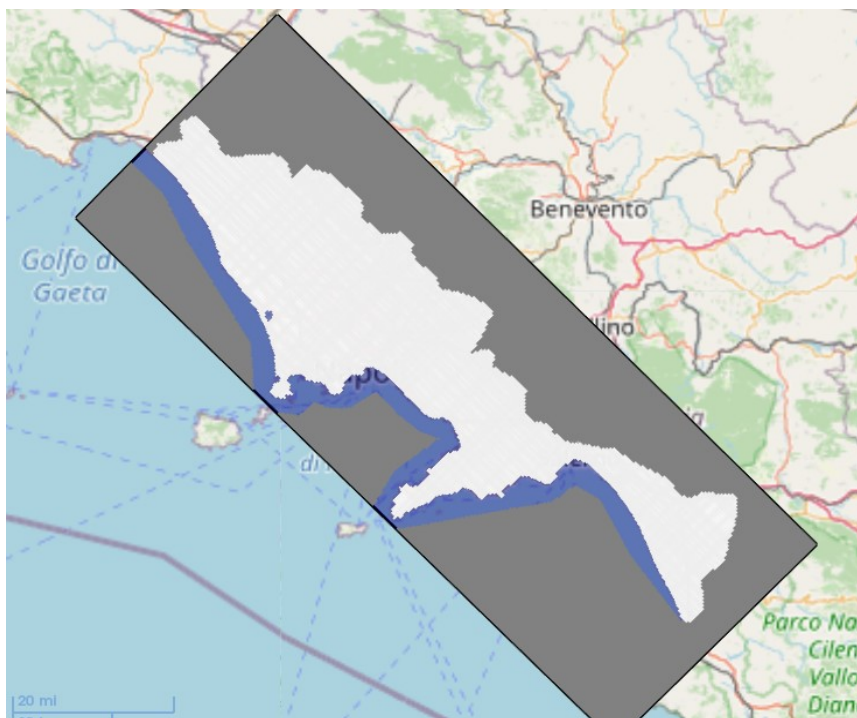

Figure 32- Model domain subdivided in active cells, constant-head cells and no-flow cells

4.2.2. ASSIGNMENT OF MODEL PARAMETERS: TIME AND AQUIFER PROPERTIES

4.2.2.1. TIME

Concerning time, MODFLOW divides the total time length of a simulation into stress periods, which are, in turn, divided into time steps. The temporal discretization scheme can be set in the Time dialog box, in which is necessary to define the number of stress periods, the length of stress periods PERLEN, expressed in the unit selected by the Time Unit dropdown box, the number of time steps within a stress period and the time step multiplier TSMULT, defined as the ratio of length of each time step to that of the preceding time step.

In addition, there is a box to check or uncheck depending if the stress period is considered as steady state or transient and finally is necessary to indicate the starting date/time and the end date/time of each stress period.

In this stage of the project, only a single stress period has been considered in order to calibrate the model in steady state condition, using as reference a piezometry of the Campania region recorded in the year 2000 and exploiting the functionalities of PEST for parameter estimation.

Figure 33 shows the PM Time dialog box in which is described the assigned stress period, the length of the stress period, the number of time steps, the time step multiplier and the end date of the stress period that has been used in the model. The columns related to the parameters DT0, MXSTRN, TTSMULT and TTSMAX are not considered and left as default since such parameters describe features about transport steps, not used in this project.
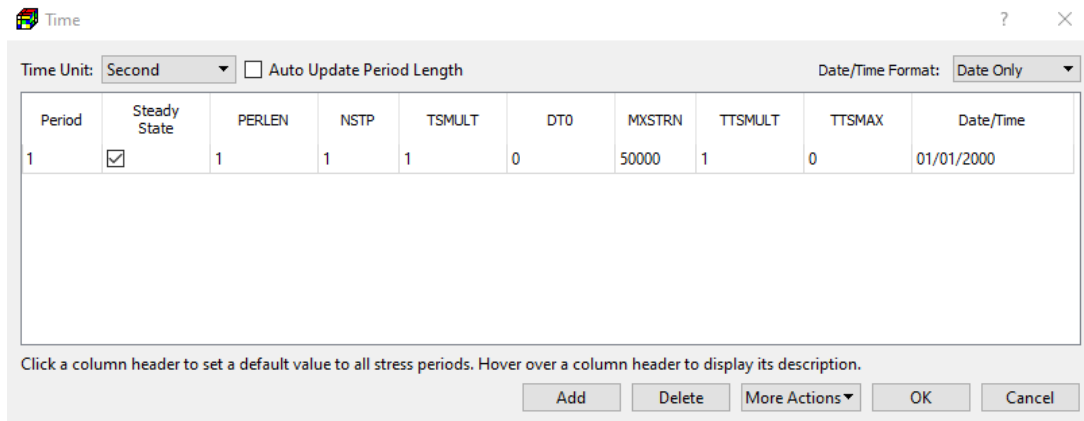
Figure 33-Processing Modflow Time dialog box

4.2.2.2.   STARTING HYDRAULIC HEAD

MODFLOW requires a starting hydraulic head value for each model cell at the beginning of a flow simulation. Starting heads at constant head cells are used as prescribed head values and remain constant throughout the flow simulation. For steady-state flow simulations, the starting heads are used as initial values for the iterative equation solvers and should be set as close as possible to the final head solution. Furthermore, the starting head of a constant head cell must be higher than the elevation of the cell bottom, otherwise the constant head cell went dry and the simulation is aborted. In a transient flow simulation instead, the starting heads provide a reference elevation for the solution and it's recommended to use heads generated by a steady-state model as the initial head for a transient model.

For the steady state simulation of the present project the values of starting head have been imported in the model from a shapefile with isopiezometric lines of the Campania region. The values of starting head in the constant-head cell in the Tyrrhenian Sea have been set to 0 m and, in order to ensure that no cell become dry, all constant head cells at the eastern border of the domain have been inspected manually to check that the imported value of starting head was higher than the elevation of the cell bottom.

4.2.2.3. HORIZONTAL HYDRAULIC CONDUCTIVITY (HK)

The values of horizontal hydraulic conductivity assigned to the model have been obtained using the hydraulic conductivity values estimated during the preliminary activities, and using a digital geological map of the Campania region.

The estimation performed in the preliminary phase, which procedure is described in the chapter 3.3 of the present thesis, has produced a value of horizontal hydraulic conductivity for each of the 91 boreholes that have been analysed. Knowing the location of the boreholes and using the digital geological map, it has been possible to cluster such boreholes in function of the geological formation in which they have been taken. Then, the values of hydraulic conductivity, corresponding to boreholes in the same cluster, have been averaged in order to obtain an average value of hydraulic conductivity for each geological formation in the study area. Such average values have been assigned to the model, exploiting the polygon input method. In this way, the model domain has been subdivided in polygons, which extension corresponds to the extension of the different geological formations reported in the geological map, and the average values of hydraulic conductivity have been assigned to such polygons and as consequence to all the cells contained inside each polygon. Figure 34 shows the distribution of the average values of horizontal hydraulic conductivity over the study area and from that is possible to notice that this parameter is very heterogenous in the model domain, ranging from 1×10^{-6} in the coastal part of the Volturno plain, where clay layers are present, to values of $6,6 \times 10^{-4}$ in the Vesuvio area, where highly fractured volcanic rock are present. The distribution is identical for layer 1 and layer 2 of the model domain, while it is slightly different in the third layer, in which the clay layer in the Volturno plain is no more present and is replaced with by a sand layer with higher conductivity.
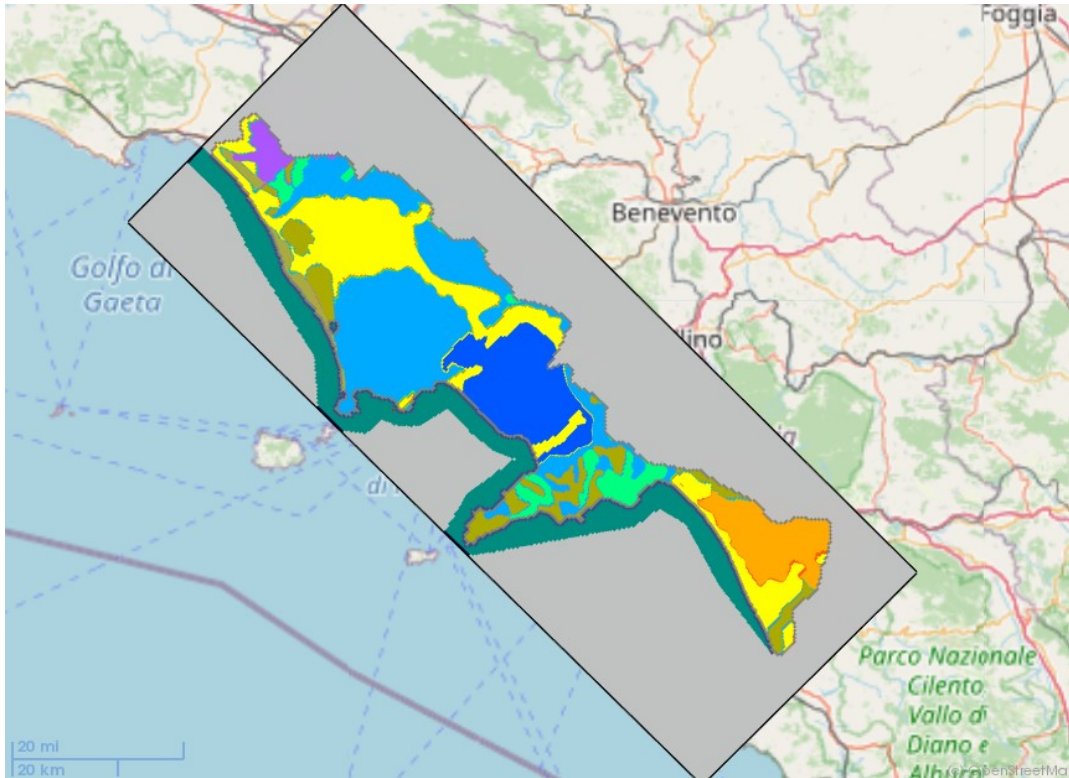
Figure 34-Distribution of horizontal hydraulic conductivity values in the model domain
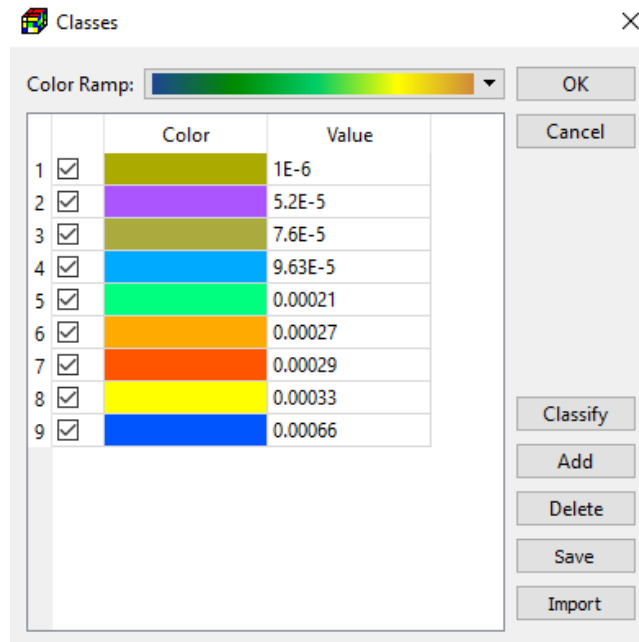

Figure 35- Legend that shows the relation between values of horizontal hydraulic conductivity and displayed colours

Figure 36-Matrix of horizontal hydraulic conductivity in the model domain

4.2.2.4.   VERTICAL HYDRAULIC CONDUCTIVITY (VK)

In the present study, the value of vertical hydraulic conductivity in each cell of the model domain was set equal to the value of horizontal hydraulic conductivity assigned to that cell. In order to do that the 3D matrix of horizontal hydraulic conductivity values has been exported and subsequently imported in the model as 3D matrix of vertical hydraulic conductivity values.

4.2.3. DEFINITION OF THE INPUTS TO THE MODEL: STRESS AND FLOW PACKAGES

A package of MODFLOW is the part of the program that deals with a single aspect of simulation. For example, the Well Package simulates the effect of wells or the River Package simulates the effect of rivers.

The MODFLOW packages that have been used in the present study are the Evapotranspiration package (EVT), the Recharge package (RCH), the River package (RIV) and the Well package (WEL). A description of these packages is reported in the following sections.

4.2.3.1. EVAPOTRANSPIRATION (EVT)

The Evapotranspiration (EVT) Package simulates the effects of plant transpiration and direct evaporation by removing water from the saturated groundwater regime.

The evapotranspiration rate is calculated for a cell in each vertical column of model cells by:

- $R_{et} = EVTR$ $if\ h > SURF$
- $R_{et} = EVTR \cdot \frac{h-(SURF-EXDP)}{EXDP}$ $if\ (SURF - EXDP) \leq h \leq SURF$
- $R_{et} = 0$ $if\ h < SURF - EXDP$

where:

- R_{et} (LT^{-1}) is the rate of loss per unit surface area of water table due to evapotranspiration;
- h (L) is the calculated hydraulic head in the cell from which the evapotranspiration occurs;
- EVTR (LT^{-1}) is the maximum possible value of R_{et} or potential evapotranspiration rate;

- SURF (L) is the ET surface elevation;

- EXDP (L) is the cut-off or extinction depth.

The evapotranspiration flow rate Q_{et} (L^3T^{-1}) drawn from the model cell is:

$$Q_{et} = R_{et} \; x \; Area_c$$

where $Area_c$ is the area of the model cell.

The parameters for the functioning of EVT package have to be assigned through the Evapotranspiration Package dialog box. Here is necessary to specify the potential evapotranspiration rate EVTR, the elevation of the evapotranspiration surface SURF and the evapotranspiration extinction depth EXDP.

In addition, it's also necessary to specify, for each vertical column, the cells where Q_{et} is drawn from. They can be only the cells in the top grid layer, or the cells contained the layers specified by the user through the layer indicator or the highest-variable head cells in each vertical column.

In the present study, for the simulation in steady state condition, a uniform value of potential evapotranspiration rate has been assumed for the entire domain. The assigned value, taken from literature, is equal to 2×10^{-8} m/s, as visible in the figure 37. In addition, it has been established that the evapotranspiration flow rate has to be calculated only for cells in the top grid layer and that the extinction depth, below which no evapotranspiration take place, is equal 2 m for the entire domain.

Figure 37- Matrix of values of potential evapotranspiration rate

4.2.3.2. RECHARGE (RCH)

The Recharge (RCH) Package is designed to simulate distributed recharge to the ground-water system. With this package, a value of recharge flux, called RECH (LT^{-1}) is assigned to a cell in each vertical column of the model cells, not allowing recharge to occur simultaneously at multiple depths in the same vertical column. The recharge rate to the groundwater system Q_{rch} (L^3T^{-1}) is calculated by:

$$Q_{rch} = RECH \; x \; Area_c$$

where RECH (LT^{-1}) is the recharge flux at the cell, and $Area_c$ is the area of the cell.

The parameters required for the functioning of the Recharge package are specified in the Recharge package dialog box. Here is necessary to specify the recharge flux RECH (L/T^{-1}) and if the recharge is applied only to the top layer, or it is applied with a vertical

distribution in more than one layer or it is applied to the highest variable-head cell in each vertical column.

In the steady state simulation of the present study the values of recharge have been kept constant for the entire simulation. A recharge flux of 3 x 10^{-9} m/s has been applied for most part of the domain, while a recharge flux equal to 6 x 10^{-9} m/s has been applied in the areas of Monte Massico and Monti Lattari in order to simulate the higher recharge connected with the presence of carbonate aquifers. Furthermore, a recharge flux of 7 x 10^{-9} has been assigned to the area of Phlegrean Fields and a flux of 5 x 10^{-9} has been assigned to the Vesuvio zone where values of recharge are generally high.

4.2.3.3.   RIVER (RIV)

The purpose of the River (RIV) Package is to simulate the effects of flow between surface-water features and groundwater systems. In fact, rivers and streams can bring water to or drain water from a groundwater system, depending on the head gradient between the river and the ground-water regime. In MODFLOW a river is implemented dividing it into reaches so that each reach is completely contained in a single model cell. In alternative, multiple reaches can be assigned to a model cell.

For each reach, the flowrate between the reach and the model cell is calculated as:

$$Q_{riv} = C_{riv} \cdot (h_{riv} - h) \qquad if \; h > B_{riv}$$

$$Q_{riv} = C_{riv} \cdot (h_{riv} - B_{riv}) \qquad if \; h < B_{riv}$$

where:

- Q_{riv} (L^{3}T^{-1}) is the flow rate between the reach and the model cell;
- h (L) is the calculated hydraulic head in the cell containing the reach;
- h_{riv} (L) is the head in the reach;

- B_{riv} (L) is the elevation of the riverbed bottom of the reach;
- C_{riv} (L^2T^{-1}) is the riverbed conductance of the reach.

In the present study, in order to include the rivers that cross the simulated area, the Processing Modflow Polyline input method has been used. With this method has been necessary to draw in the model domain polylines that simulate the actual pathway of the river and then to assign river parameters to the vertices of such polylines. The assigned river parameters are the riverbed conductance per unit length C_{rivl} (LT^{-1}), that depends on the material and characteristics of the riverbed and the immediate environment, the river stage h_{riv} (L) and the elevation of the riverbed bottom B_{riv} (L). Thickness of riverbed sediments, river water density and concentration parameters, even if they are included in the River Package dialog box, have not to be specified since they are only required for SEAWAT simulations, not performed in the present study.

Such parameters have been assigned to the most upstream vertex and to the most downstream vertex of the river polylines and such vertex data have then been applied to the model cells by means of the MODFLOW linear interpolation in which the distances along the polyline between a cell and those two vertices are used as weights for linear interpolation. Furthermore, the interpolated cell value C_{rivl} is multiplied with the length of the river within the cell to obtain the riverbed conductance C_{riv}.

Such procedure has been applied to simulate, from North to South, Garigliano, Savone, Agnena, Volturno, Regi Lagni, Sarno, Reginna Majo, Picentino, Tusciano, Sele and Calore rivers.

River bed conductance per unit length of each inserted river has been evaluated using the equation:

$$C = \frac{K \, x \, W}{D}$$

in which K (L/T) is the hydraulic conductivity of the riverbed sediments within the cell, W (L) is the width of the river within the cell and D (L) is the thickness of the riverbed sediment. D has been assumed equal to 1, W has been estimated using actual images from Google Earth and K has been retrieved from the value of horizontal hydraulic conductivity assigned to the cell.

Riverbed stage has been assumed close to the assigned starting head value and kept constant for the entire simulation, while the elevation of the bottom of the river bed has been assumed few meters lower than the river stage in the cells.

4.2.3.4.   WELL (WEL)

The Well (WEL) Package is designed to simulate features, such as wells, that withdraw water from or add water to the aquifer at a constant rate during a stress period, where the rate is independent of both the cell area and the head in the cell.

The wells that have been considered in this research project are those that have been analysed from the online ISPRA database. In fact, the 91 borehole reports analysed in chapter 3.3. of the present thesis, contain, together with stratigraphic information, also information on the applied pumping rates.

With the purpose of assigning such wells to the model, a Well file has been created in Excel and imported into the model. The created Well file consists in a list of wells, for which has been specified the name, the coordinates and the depth of the screens, together with the corresponding pumping rate.

Since the specified wells penetrate more than one model layer, the total pumping rate has not been distributed over the penetrated layers, but it has been assigned to the lowest cell of the well, belonging to the third model layer.

4.2.4. EVALUATION OF THE MODEL OUTPUTS: SOLVERS AND RESULTS CONTROL

The last steps of the model setup in steady state condition consist in the selection of the solver that have to be used to solve the system of finite-difference equations and in the control of the output results obtained at the end of simulation.

4.2.4.1. SOLVER

To calculate hydraulic heads, MODFLOW prepares one finite difference equation for each cell, expressing the relationship between the head at a node and the heads at each of the six adjacent nodes at the end of each time step. Because each equation may involve up to seven unknown values of head, and because the set of unknown head values changes from one equation to the next through the grid, the equations for the entire grid must be solved simultaneously at each time step. The system of simultaneous finite difference linear equations can be expressed in matrix notation:

$$A \cdot x = b$$

where A is a coefficient matrix assembled by MODFLOW using user-specified model data; b is a vector of defined flows, terms associated with head-dependent boundary conditions and storage terms at individual cells; x is a vector of hydraulic heads at individual cells. During a MODFLOW run, the vector x is solved with one of the supported solvers.

The solver that has been used in this model is the Newton Solver NWT.

4.3. MODEL CALIBRATION

In the calibration phase, it has been necessary to add Observation Points to the model. The observation points, and observation values referred to the observation points, have been defined using the Observation Tool of Processing Modflow 11. This tool allows to import observation points from an Excel file, called Observation File, that is generally composed by two or more sheets, depending on the number of observed parameters to add to the model. In the first sheet are contained information about the name of the observation points, the labels that will be displayed in the model, the layer to which the observation points belong and the geographic coordinates of the observation points, in terms of latitude and longitude. The following sheets are specific for the single observation parameter to add and in particular the second sheet contains information about observed heads. Here is reported, for each observation point, name, observed head value and the observation time, expressed in simulation time from the beginning of the simulation or in a calendar date/time format.

In this research project, in order to calibrate the model using observed values of heads, a piezometry of the Campania region for the year 2000 has been employed. Such piezometry was originally composed by 451 points and, for each of these points, was reported the geographical coordinates and the groundwater level above sea level. Since the used piezometry was referred to the entire Campania region, so with extent larger than the extent of the study area, some of these points fell into regions outside the model domain. Such points have been removed from the list and an observation file has been produced in order to import such points into the model. Figure 38 shows the distribution of the imported observation points, relative to the recorded piezometry of the year 2000 over the model domain.

Once the observation points have been uploaded into the model, the model simulation has been run and a head value for each cell of the model has been calculated.
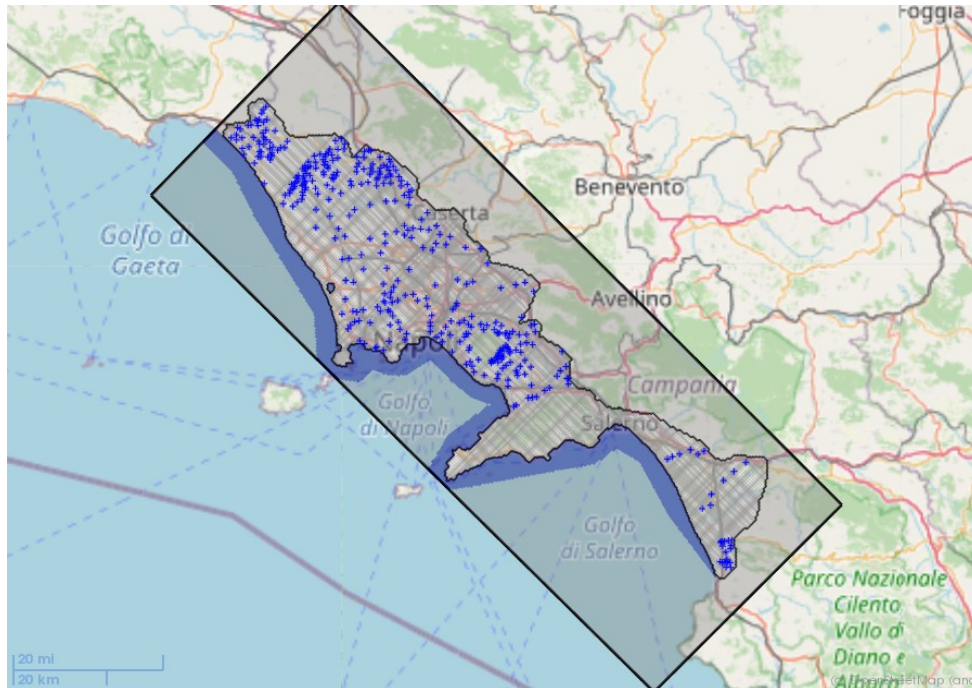
Figure 38-Distribution of observation points over the model domain

Calibration is the process that allows to adjust the input parameters in order to obtain a good fit between the heads calculated by the model and the observed field data, in this case the piezometry of the year 2000. In the present study the process of calibration has been performed exploiting the functionalities of PEST, that is a supported numerical code for parameter estimation. Since the most uncertain input parameters are the values of horizontal hydraulic conductivity, obtained as results of an estimation process, those values have been set as estimable parameters through PEST and a parameter number has been univocally assigned to them. During a parameter estimation process, PEST searches optimum parameter values for which the sum of squared deviations between model-calculated and observed values at the observation points is reduced to a minimum. After the process of calibration, the

simulation has been run again and the newly calculated head values have been compared with the observed head values.

Such comparison has been performed using the Processing Modflow Scatter Chart for Head. The chart displays a scatter diagram using the simulated and observed data. The x-axis represents the observed values and the y-axis represents the calculated values. A linear least squares regression line can be displayed for each observation point if it has more than one data point. The regression line attempts to model the relationship between calculated and observed values by fitting the linear equation: $y = m \cdot x + b$, where m is the slope of the line and b is the intercept of the line with the y-axis. Scatter diagrams are often used to present the goodness of fit of the observed data and the calculated data. If there is an exact agreement between measurement and simulation, all points lie on a 45° line with both the slope m and the coefficient of determination r^2 equal to 1.

Figure 39 shows the obtained scatter diagram, exported in Excel, in which the blue points represent pairs of calculated and observed values of heads. The resulting coefficient of determination r^2 is equal to 0,9429. Given the regional scale of the model, the result is considered acceptable.
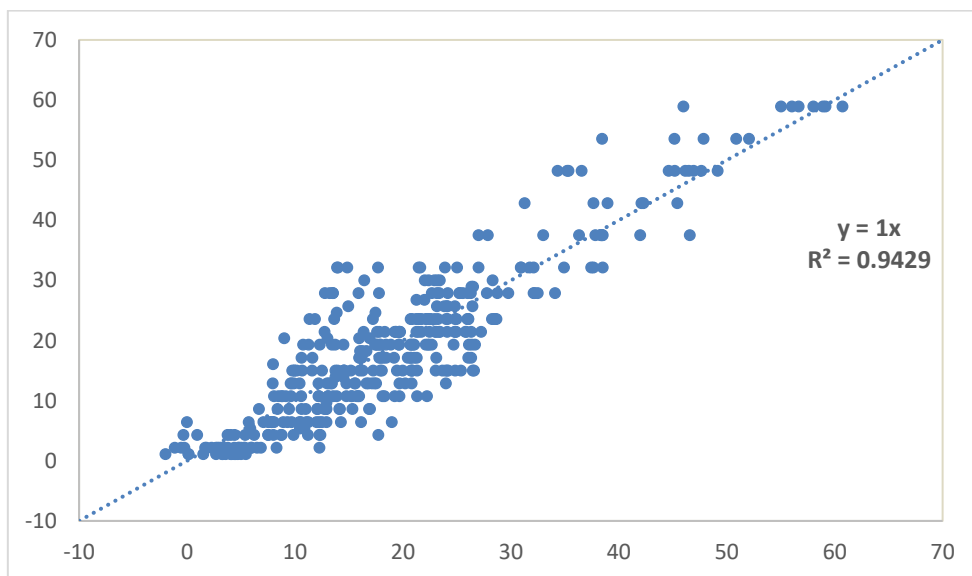
Figure 39- Scatter chart obtained at the end of calibration process

4.4. MODEL SETUP IN TRANSIENT CONDITIONS

The calibrated model generated at the end of the steady state simulation has been used as starting point to setup the model in transient conditions. The transient simulation has been adopted in this study in order to investigate changes in the groundwater system associated with temporal variation of evapotranspiration and recharge patterns, recorded for the period 2000-2015.

The procedure to setup the model in transient condition is nearly the same as the one to setup the steady state model, but anyway it requires some modifications, described in the following sections.

4.4.1. TEMPORAL DISCRETIZATION

The first important modification concerns the temporal discretization of the model domain that passes from a single stress period to multiple stress periods associated with different input parameters.

The temporal discretization scheme used in the model has been made of 64 stress periods of seasonal length, each of them subdivided in 3 time steps of equal length, representative of single months in the considered time span.

Figure 40 shows the PM Time dialog box in which are visible the length of individual stress periods, the number of time steps in each stress period, the time step multiplier and the end date of each stress period that have been used in the model. The columns related to the parameters DT0, MXSTRN, TTSMULT and TTSMAX have been not considered and left as default since such parameters describe features about transport steps, not used in this project.

Period	Steady State	PERLEN	NSTP	TSMULT	DT0	MXSTRN	TTSMULT	TTSMAX	Date/Time
1	☐	7862400	3	1	0	50000	1	0	04/01/2000
2	☐	7862400	3	1	0	50000	1	0	07/01/2000
3	☐	7948800	3	1	0	50000	1	0	10/01/2000
4	☐	7948800	3	1	0	50000	1	0	01/01/2001
5	☐	7776000	3	1	0	50000	1	0	04/01/2001
6	☐	7862400	3	1	0	50000	1	0	07/01/2001
7	☐	7948800	3	1	0	50000	1	0	10/01/2001
8	☐	7948800	3	1	0	50000	1	0	01/01/2002
9	☐	7776000	3	1	0	50000	1	0	04/01/2002
10	☐	7862400	3	1	0	50000	1	0	07/01/2002
11	☐	7948800	3	1	0	50000	1	0	10/01/2002
12	☐	7948800	3	1	0	50000	1	0	01/01/2003
13	☐	7776000	3	1	0	50000	1	0	04/01/2003
14	☐	7862400	3	1	0	50000	1	0	07/01/2003
15	☐	7948800	3	1	0	50000	1	0	10/01/2003
16	☐	7948800	3	1	0	50000	1	0	01/01/2004
17	☐	7862400	3	1	0	50000	1	0	04/01/2004
18	☐	7862400	3	1	0	50000	1	0	07/01/2004
19	☐	7948800	3	1	0	50000	1	0	10/01/2004
20	☐	7948800	3	1	0	50000	1	0	01/01/2005
21	☐	7776000	3	1	0	50000	1	0	04/01/2005
22	☐	7862400	3	1	0	50000	1	0	07/01/2005

Figure 40- Processing Modflow Time dialog box indicating the adopted temporal discretization scheme in transient simulation

4.4.2. STARTING HYDRAULIC HEAD

Another modification respect to the steady state model is about the starting hydraulic head parameter.

As recommended by the software developer, the starting hydraulic head for the transient simulation has been set equal to the head values calculated at the end of the steady state simulation. This operation has been done exporting calculated head values from the model in steady state and importing the same values as starting hydraulic head for the transient simulation.

4.4.3. SPECIFIC STORAGE (S_S)

During the initial steady state simulation, the temporal variation has not been considered by the model and so it was not necessary to assign such parameter. In the transient simulation instead, the Specific Storage parameter S_s has become relevant because MODFLOW requires a storage term, given by the dimensionless Storage Coefficient S. The Storage Coefficient is directly calculated by MODFLOW multiplying the Specific Storage by the layer thickness. Specific storage is defined as the volume fraction of water that a unit column of aquifer releases from storage under a unit decline in hydraulic head. The specific storage is a function of the compressibility of the water and the elastic property of the soil matrix and ranges in value from 3.3×10^{-6} m^{-1} in rocks to 2.0×10^{-2} m^{-1} in plastic clay.

In this project Specific Storage parameter has been initially set equal to 0,0001 m^{-1} for the entire domain but later it has been modified in function of the type of geologic material, using literature values reported by Batu (1998) and shown in Figure 41. Anyway, this modification has not brought significant effects in the calculation of the final water budget with the budget components that have been resulted only slightly affected. For this reason, the original choice to assign a Specific Storage equal to 0,0001 m^{-1} for the entire domain has been confirmed.

Material	S_s (ft^{-1})
Plastic clay	7.8×10^{-4} to 6.2×10^{-3}
Stiff clay	3.9×10^{-4} to 7.8×10^{-4}
Medium hard clay	2.8×10^{-4} to 3.9×10^{-4}
Loose sand	1.5×10^{-4} to 3.1×10^{-4}
Dense sand	3.9×10^{-5} to 6.2×10^{-5}
Dense sandy gravel	1.5×10^{-5} to 3.1×10^{-5}
Rock, fissured	1×10^{-6} to 2.1×10^{-5}
Rock, sound	$< 1 \times 10^{-6}$

Figure 41-Values of specific storage for different geologic material according to Batu (1998)

4.4.4. SPECIFIC YIELD (S$_y$)

Even the Specific Yield parameter was not required by MODFLOW for steady state simulation, while it has become relevant for transient simulation.

Specific yield is defined as the volume of water that an unconfined aquifer releases from storage per unit surface area of aquifer per unit decline in the water table.

In a similar way to Specific Storage, Specific Yield parameter has been originally assigned equal to 0,20 to all the cells of model domain and subsequently modified in function of the type of geologic material, using as reference literature values. Even in this case the modification has not induced significant differences in terms of water budget and so the original assumption has been considered valid. Figure 42 shows representative values of specific yield for various geological materials published by Morris and Johnson (1967).

Material	Specific Yield (%)
Gravel, coarse	21
Gravel, medium	24
Gravel, fine	28
Sand, coarse	30
Sand, medium	32
Sand, fine	33
Silt	20
Clay	6
Sandstone, fine grained	21
Sandstone, medium grained	27
Limestone	14
Dune sand	38
Loess	18
Peat	44
Schist	26
Siltstone	12
Till, predominantly silt	6
Till, predominantly sand	16
Till, predominantly gravel	16
Tuff	21

Figure 42- Values of specific yield for different geologic material according to Morris and Johnson (1967)

4.4.5. EVAPOTRANSPIRATION (EVT)

In the transient simulation, the Evapotranspiration Package has not been assumed as constant for the entire simulation but it has been considered as variable in time, assigning different values to different stress periods.

The data of potential evapotranspiration rate, assigned to each stress period, have been derived from satellite data recorded by MODIS (Moderate Resolution Imaging Spectroradiometer) instrument on board of Terra and Aqua NASA satellites.

A grid of values of evapotranspiration has been obtain for each season starting from the year 2000 until the year 2015.

Such seasonal values have then been converted into m/s to match the units of the model and Comma Separated Value Files, indicating the coordinates of the grid points and the corresponding evapotranspiration values, have been produced for each stress period of seasonal length. The CSV files have been imported to the corresponding stress periods and finally the parameter of potential evapotranspiration rate, required by the Evapotranspiration Package, has been assigned to each cell of the model domain using the linear interpolation.

Such temporal variation has been considered only for the potential evapotranspiration rate parameter and not for the other parameters of the Evapotranspiration Package, such as extinction depth parameter that has been kept constant and equal to 2 m from ground level.

4.4.6. RECHARGE (RCH)

Similarly to the Evapotranspiration Package, also the Recharge Package has been considered as variable in time, assigning different values to different stress periods.

The data about recharge rate, assigned to the different stress periods, have been retrieved, this time, from the global numerical hydrologic model published by de Graaf et al. (2017).

The available dataset was composed by values of recharge rate, spatially distributed over a grid of 6144 points covering the Campania region and reported with seasonal frequency from the year 2000 to the year 2015.

Such seasonal values have then been converted into m/s to match the units of the model and Comma Separated Value Files, indicating the coordinates of the grid points and the corresponding recharge rate values, have been produced for each stress period of seasonal length. The CSV files have been imported to the corresponding stress periods and finally the recharge flux parameter, required by the Recharge Package, has been assigned to each cell of the model domain using the linear interpolation.

4.5. MODEL VALIDATION

After the specification of the above-mentioned parameters, the phase of model setup has been concluded running the transient simulation. MODFLOW has been able to solve the system of differential equation for the entire temporal domain, calculating head values at the end of each time step.

In order to validate the model, the calculated values have to be compared with a dataset of observed values. For that purpose, in the present study, the dataset that has been used is a piezometry of the Campania region, recorded in March 2013 and derived from a global groundwater depth dataset (Fan et al., 2013) interpolated with the DTM. It is discretized in 201 points of known coordinates, each of them associated with a value of groundwater level. Using the same procedure employed during the model calibration phase, such points have been reported into and Excel Observation File paying attention to match the correct simulation time and then imported as observation points into the model. Figure 43 shows the distribution of the newly imported observation point over the model domain.
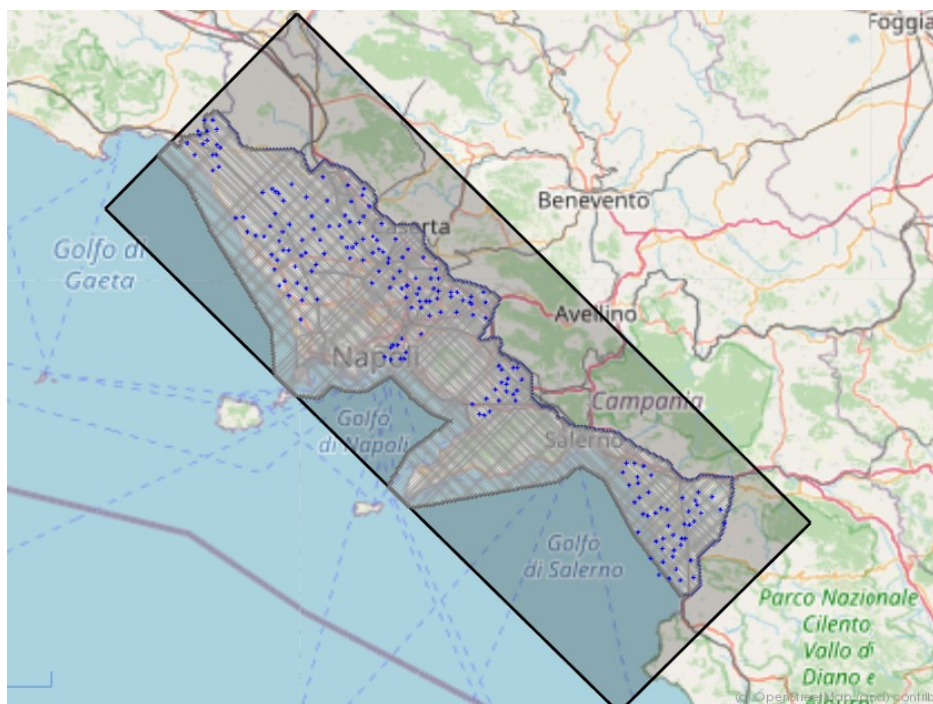
Figure 43- Distribution of observation points over the model domain

The comparison of calculated and observed head values in correspondence of the observation points, has been performed exploiting the Scatter Chart of Processing Modflow. The results of the comparison have been exported to an Excel file and the match between the calculated and observed value has been inspected analysing the obtained scatter diagram.

Figure 44 shows the scatter diagram of the validation process. The resulting coefficient of determination r^2 has resulted equal to 0,92. This value shows the goodness of the results considering also the regional scale of the model.
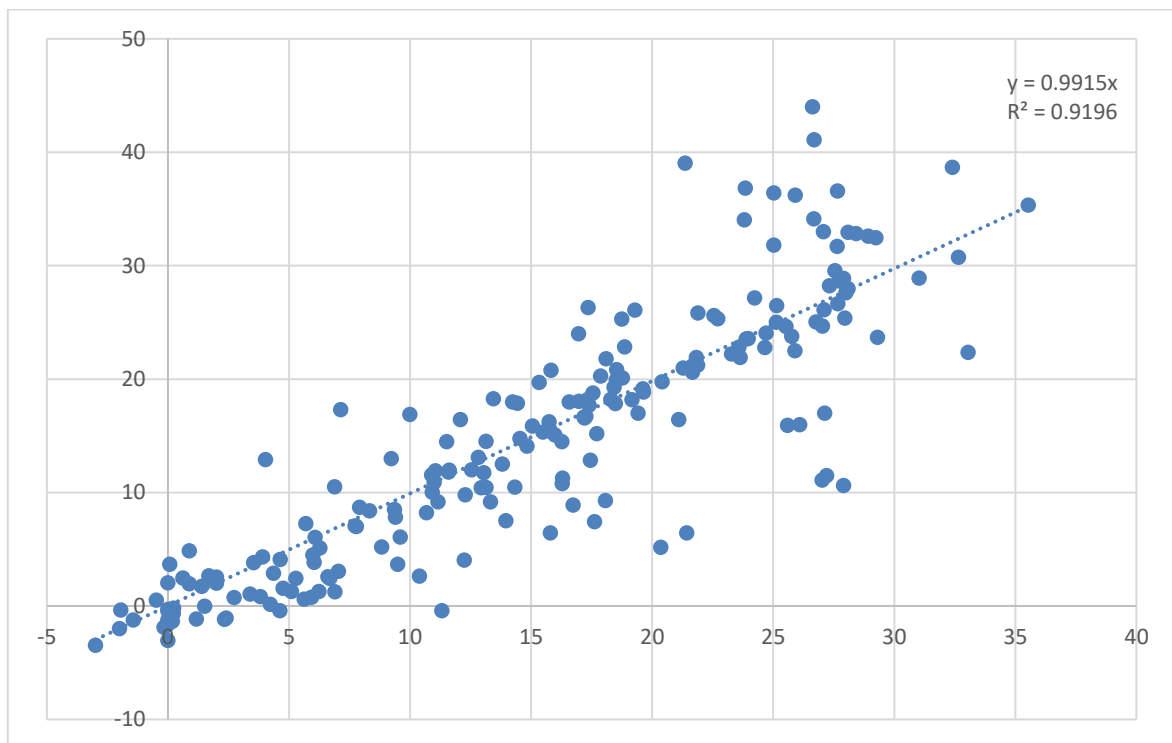
Figure 44- Scatter diagram of the validation process

5. RESULTS AND DISCUSSION

The produced calibrated model simulates the behaviour of the studied aquifer system in the period 2000-2015, considering the temporal variation of evapotranspiration and recharge patterns.

The model simulated by MODFLOW is representative of the actual situation in the unconfined coastal aquifers of the Campania region, since it has been built to get head results as close as possible to the observed data. This has been proved in the model validation phase, described in the section 4.5. of the present thesis.

The results generated by the model are illustrated in the figures below. Figures 45, 46, 47 show the piezometries, respectively of the first, second and third layer, that have been calculated by MODFLOW at the end of the simulation, corresponding to the stress period 64 (Autumn 2015). Similar results have been obtained for each stress period considered in the time span.

The areas between isolines have been filled with colours, which meaning is described in the attached legend. The areas in red are instead representative of dry cells, that are present in the first two layers, while they disappear in layer 3 where all the cells are wet by groundwater.

From the obtained piezometry is possible to deduce that the northern part of the domain is characterized by a high hydraulic gradient, in correspondence of the Roccamonfina volcano, where the head contour lines are very close to each other. This structure generates also a groundwater flow with radial patterns that bring groundwater both to the Garigliano and Volturno plains.

In the Volturno plain instead the potentiometric surface is very low, reaching values of 15 m as maximum in the inland areas. In some zones near the coast, the potentiometric surface is found also below ground level.

Another radial pattern of groundwater flow is encountered near the Phlegraean Fields but associated with a smaller hydraulic gradient than the Roccamorfina's one.

South, in the Sele plain, the calculated piezometry is more linear inducing a groundwater flow from East to West, recharged by the surrounding carbonate aquifers.
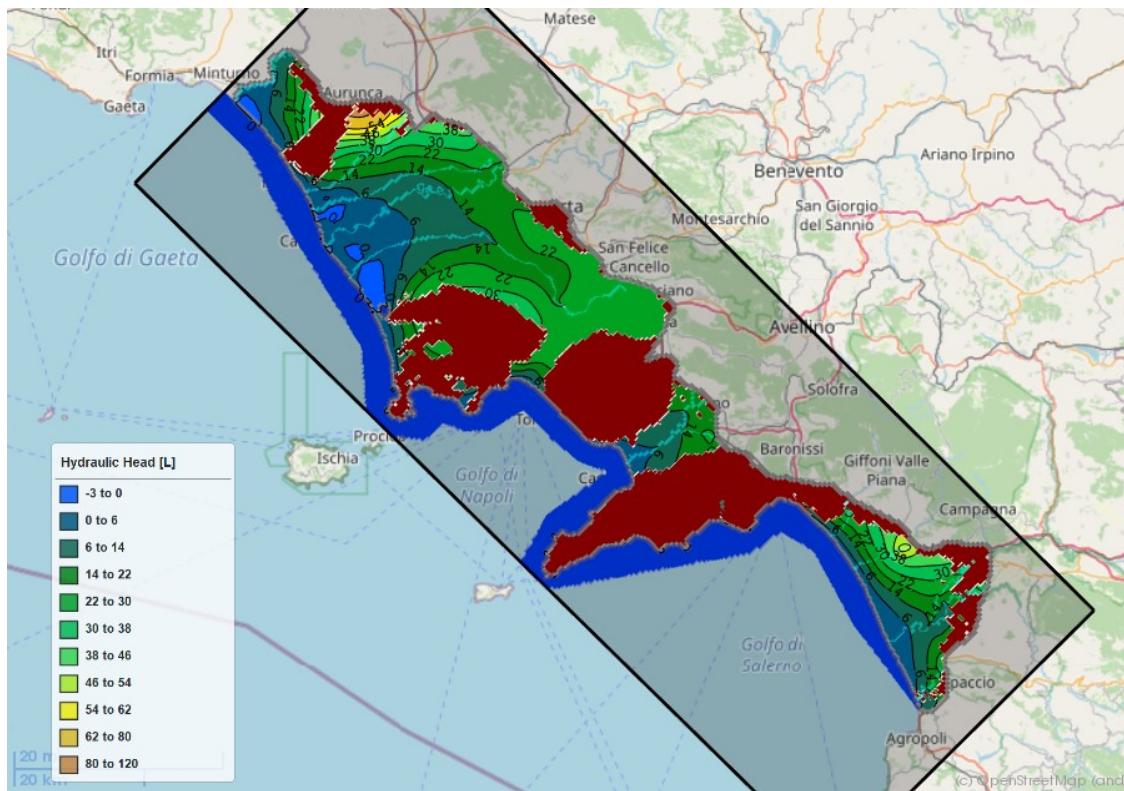
Figure 45- Calculated piezometry for layer 1 in Autumn 2015
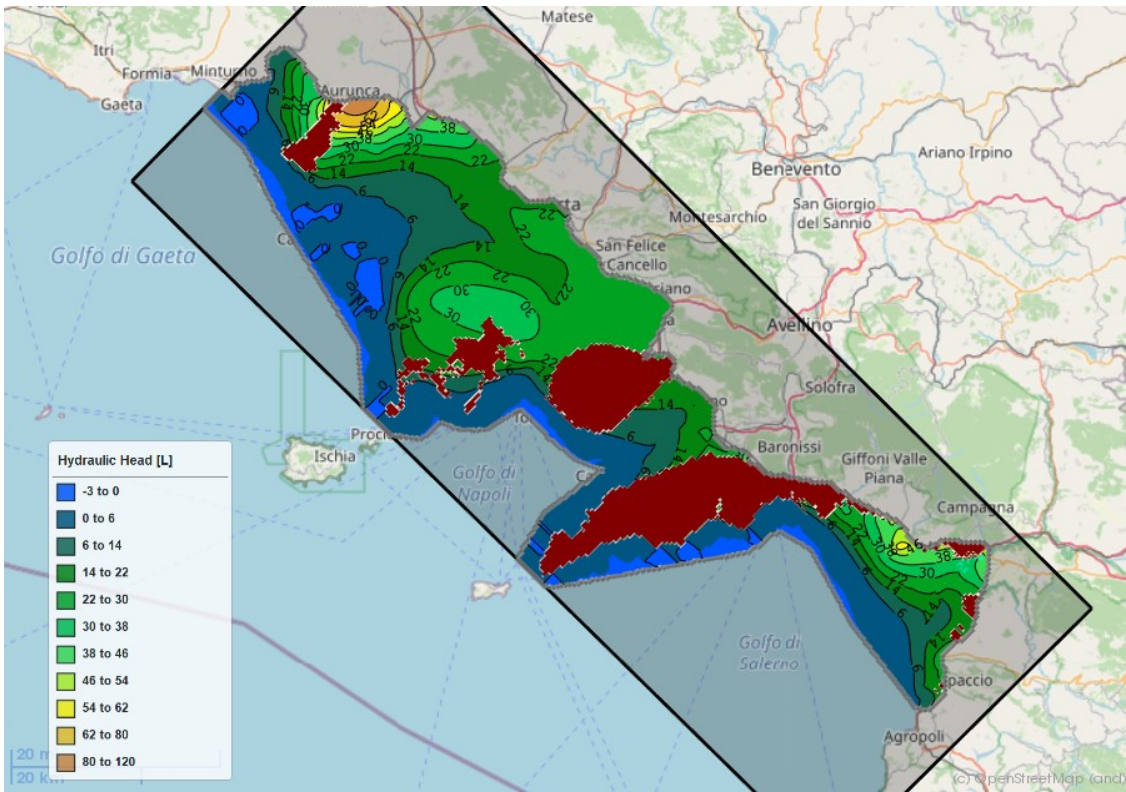
Figure 46- Calculated piezometry for layer 2 in Autumn 2015
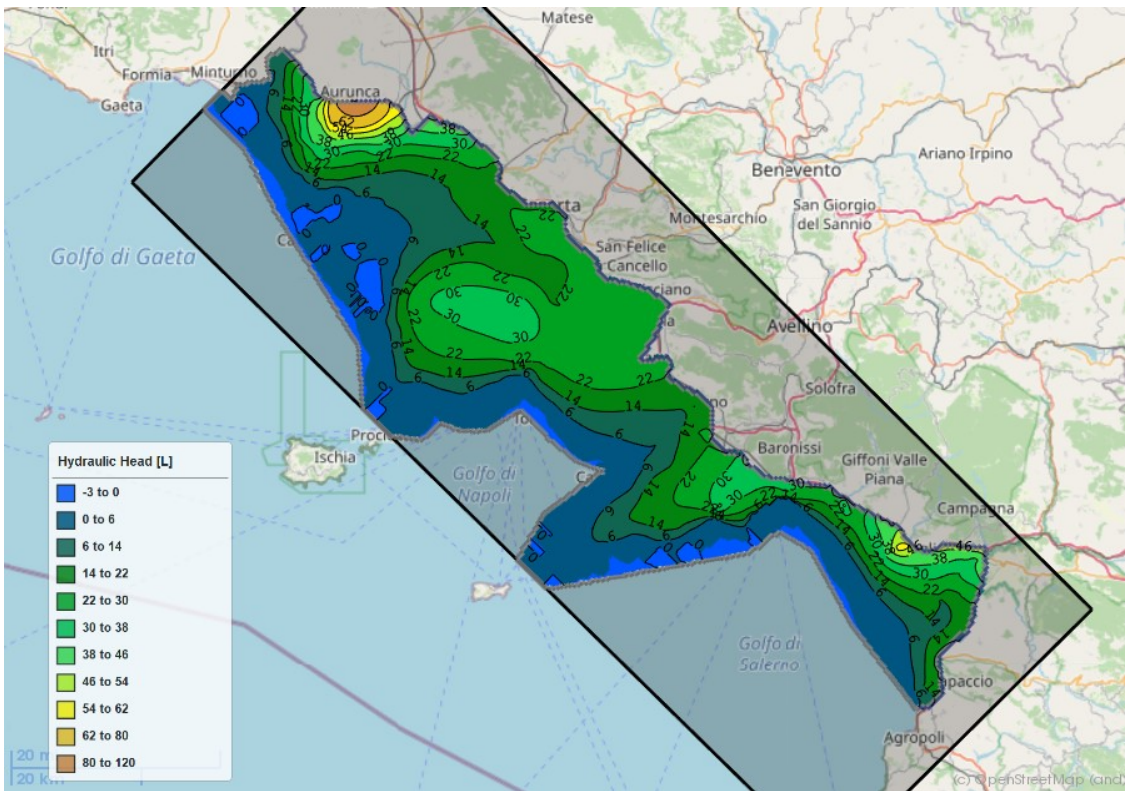
Figure 47- Calculated piezometry for layer 3 in Autumn 2015

Figure 48 instead, shows a 3-dimensional representation of the obtained piezometry, obtained importing the heads calculated by MODFLOW in the Model Viewer software.
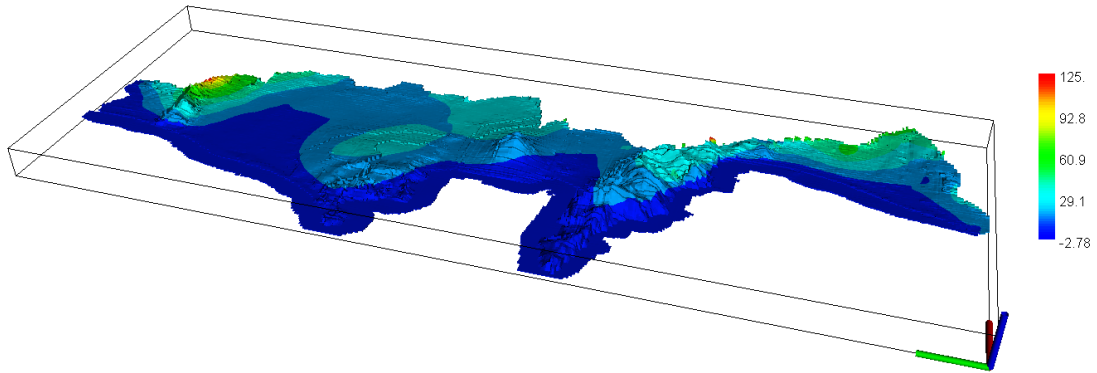
Time = 1.13e+008 s (15-1)

Figure 48- 3D representation of the calculated piezometry in the unconfined aquifers of the Campania region

Another interesting output of the model is the temporal trend of the potentiometric surface, evaluated in correspondence of observation points, that can be analysed for the entire simulation time.

Figures 49-53 shows examples of different trends of potentiometric surface calculated by the model in correspondence of different observation points. Each trend is characterized by a more or less pronounced oscillation, related to the behaviour of the groundwater system in the different seasons.
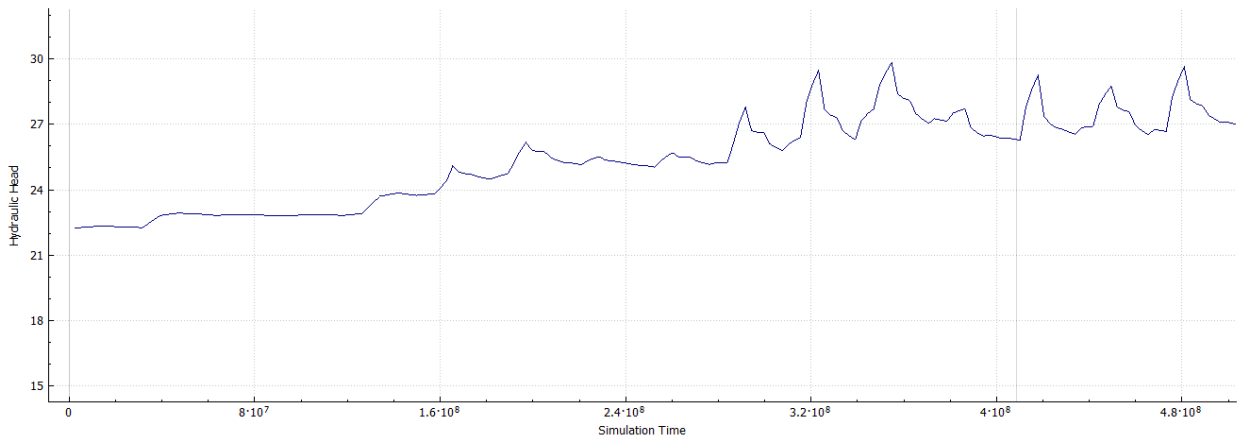
Figure 49-Trend of potentiometric surface calculated in the Volturno plain
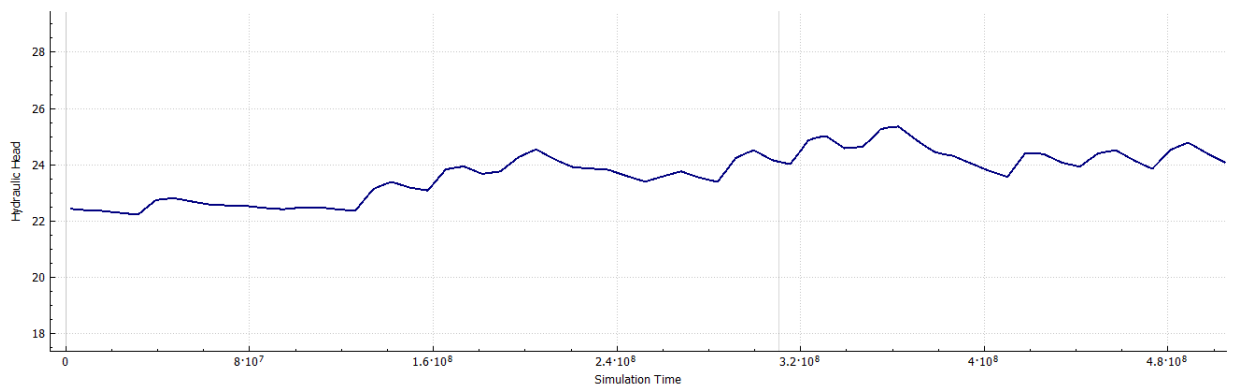
Figure 50-Trend of potentiometric surface calculated in the area of Napoli
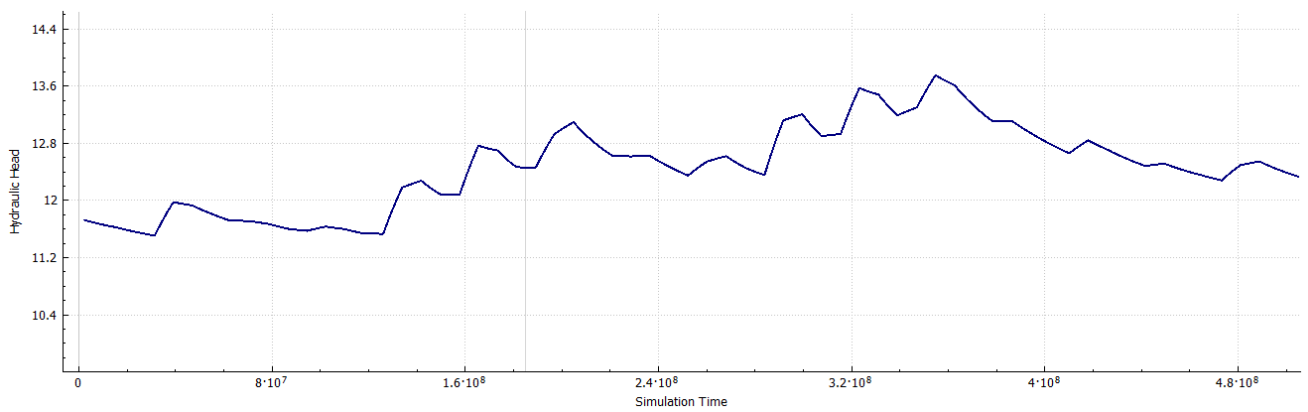
Figure 51-Trend of potentiometric surface calculated in the Sarno area
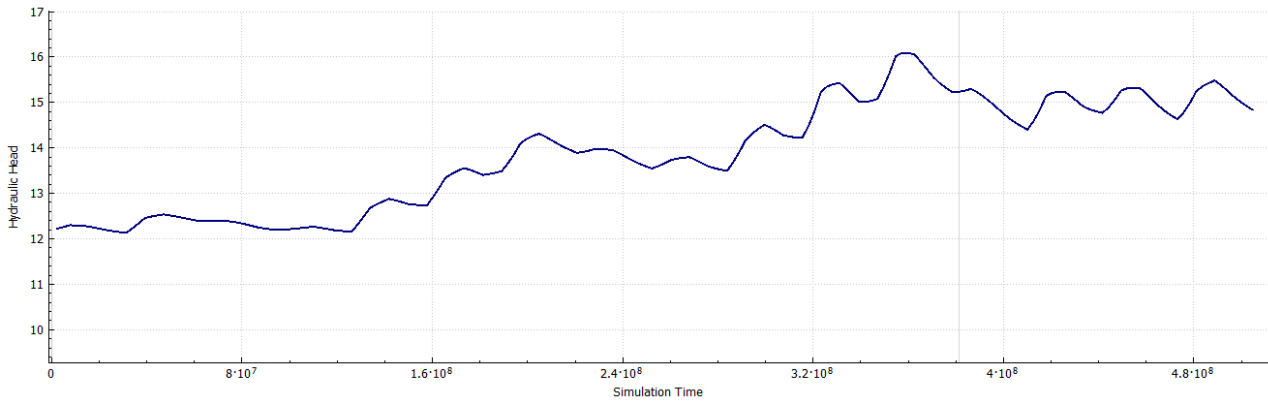
Figure 52-Trend of potentiometric surface calculated in the Garigliano plain
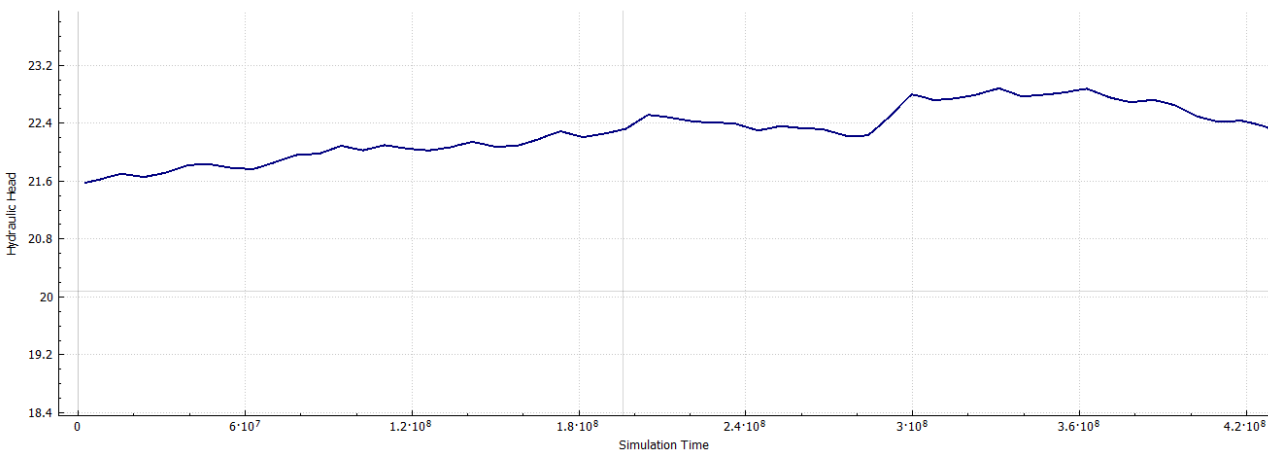
Figure 53- Trend of potentiometric surface calculated in the Sele river plain

In addition, MODFLOW gives the possibility to calculate water budgets at the end of each stress period. In this way is possible to evaluate the fluxes associated to the single components of the water budget, that can be useful for a better management of the territory. In particular, is possible to evaluate inputs to and outputs from the model domain at the end of each time step. Such values, expressed as cumulative volume of water or corresponding rates, are subdivided in storage, constant head, wells, river leakage, evapotranspiration and recharge components.

As example, the water budgets calculated for different seasons of the year 2015 are reported in the figures below.

Figure 54 represents the water budget calculated at the end of winter season of 2015. Being winter, the largest input to the aquifer system is attributed to the recharge with a rate of 51,9 m³/s, followed by the leakage from river and inputs from constant head (so the surrounding carbonate aquifers), with rates equal to 10,2 m³/s and 6,1 m³/s, respectively.

Very small inputs come from storage, while null inputs are attributed to wells and evapotranspiration.

The largest output flux is instead constituted by storage, with a rate of 33,5 m³/s, followed by discharge in river (14,9 m³/s) and submarine groundwater discharge in the constant head cells of Tyrrhenian Sea (12,9 m³/s). A flux of 6,5 m³/s is removed by the evapotranspiration component while 0,4 m³/s are removed from the domain through wells.

```
VOLUMETRIC BUDGET FOR ENTIRE MODEL AT END OF TIME STEP    1, STRESS PERIOD  61
-----------------------------------------------------------------------------

    CUMULATIVE VOLUMES      L**3        RATES FOR THIS TIME STEP      L**3/T
    ------------------                  ------------------------

          IN:                                IN:
          ---                                ---
          STORAGE      =    2640011264.0000        STORAGE      =        4.4844E-02
    CONSTANT HEAD      =    3030288640.0000   CONSTANT HEAD      =        6.1161
          WELLS      =             0.0000          WELLS      =        0.0000
    RIVER LEAKAGE      =    5734379520.0000   RIVER LEAKAGE      =       10.2682
             ET      =             0.0000             ET      =        0.0000
       RECHARGE      =    8838105088.0000       RECHARGE      =       51.9097

         TOTAL IN = 20242784256.0000              TOTAL IN =       68.3389

          OUT:                               OUT:
          ----                               ----
          STORAGE      =    3576332032.0000        STORAGE      =       33.5396
    CONSTANT HEAD      =    5601699328.0000   CONSTANT HEAD      =       12.9773
          WELLS      =     192719280.0000          WELLS      =        0.4056
    RIVER LEAKAGE      =    5676387328.0000   RIVER LEAKAGE      =       14.9081
             ET      =    5183211520.0000             ET      =        6.5445
       RECHARGE      =       3330594.2500       RECHARGE      =        0.0000

        TOTAL OUT = 20233678848.0000             TOTAL OUT =       68.3751

        IN - OUT =       9105408.0000             IN - OUT =       -3.6179E-02

 PERCENT DISCREPANCY =           0.04      PERCENT DISCREPANCY =          -0.05
```

Figure 54- Volumetric water budget calculated in Winter 2015

Volumetric water budget for Spring 2015 (Figure 55) is slightly different respect to the winter one. The inputs as recharge are much lower (26,2 m^3/s) while the influent flow from storage becomes relevant with a rate of 5,4 m^3/s. The inputs from river and surrounding constant head cells are instead more or less the same (11,07 m^3/s and 6,1 m^3/s respectively).

Concerning the outputs, it's possible to see a large increment of the evapotranspiration component, that reaches the highest value in spring (17,2 m^3/s). Other important effluent fluxes are those directed to sea and river, both equal to 13,2 m^3/s. The effluent as storage is instead much lower than the winter case (4,6 m^3/s).

```
VOLUMETRIC BUDGET FOR ENTIRE MODEL AT END OF TIME STEP    1, STRESS PERIOD  62
-----------------------------------------------------------------------------

   CUMULATIVE VOLUMES      L**3        RATES FOR THIS TIME STEP      L**3/T
   ------------------                  ------------------------

       IN:                                IN:
       ---                                ---
          STORAGE   =    2654372352.0000         STORAGE   =           5.4259
    CONSTANT HEAD   =    3077415936.0000   CONSTANT HEAD   =           6.1384
            WELLS   =             0.0000           WELLS   =           0.0000
    RIVER LEAKAGE   =    5814609920.0000   RIVER LEAKAGE   =          11.0757
               ET   =             0.0000              ET   =           0.0000
         RECHARGE   =    9175904256.0000        RECHARGE   =          26.2135

         TOTAL IN = 20722302976.0000              TOTAL IN =          48.8534

       OUT:                               OUT:
       ----                               ----
          STORAGE   =    3740567552.0000         STORAGE   =           4.6063
    CONSTANT HEAD   =    5708040192.0000   CONSTANT HEAD   =          13.2692
            WELLS   =     195884704.0000           WELLS   =           0.4056
    RIVER LEAKAGE   =    5799963136.0000   RIVER LEAKAGE   =          13.2944
               ET   =    5265270784.0000              ET   =          17.2287
         RECHARGE   =       3330594.2500        RECHARGE   =           0.0000

        TOTAL OUT = 20713056256.0000             TOTAL OUT =          48.8042

         IN - OUT =       9246720.0000             IN - OUT =       4.9229E-02

  PERCENT DISCREPANCY =           0.04     PERCENT DISCREPANCY =           0.10
```

Figure 55-Volumetric water budget calculated in Spring 2015

In the summer season the volumetric water budget (Figure 56) is characterized by a very low recharge (4,4 m³/s), but is still relevant the contribution of stored groundwater (15,7 m³/s). The input from river is slightly increased (13 m³/s) while the input from constant-head cells remains at same rate (6,43 m³/s).

The largest outflows are connected to evapotranspiration (15,7 m³/s), that remain relevant even in summer and to the discharge into sea and rivers.

```
VOLUMETRIC BUDGET FOR ENTIRE MODEL AT END OF TIME STEP    1, STRESS PERIOD  63
----------------------------------------------------------------------------

   CUMULATIVE VOLUMES      L**3        RATES FOR THIS TIME STEP      L**3/T
   -----------------                   ------------------------

       IN:                                 IN:
       ---                                 ---
         STORAGE    =   2712566784.0000        STORAGE    =          15.7288
   CONSTANT HEAD    =   3126704128.0000   CONSTANT HEAD   =           6.4388
           WELLS    =            0.0000          WELLS    =           0.0000
   RIVER LEAKAGE    =   5909699584.0000   RIVER LEAKAGE   =          13.0264
              ET    =            0.0000             ET    =           0.0000
        RECHARGE    =   9325036544.0000       RECHARGE    =           4.4279

         TOTAL IN = 21074006016.0000          TOTAL IN =           39.6219

       OUT:                                OUT:
       ----                                ----
         STORAGE    =   3761767168.0000        STORAGE    =        5.4980E-03
   CONSTANT HEAD    =   5809061376.0000   CONSTANT HEAD   =          12.1071
           WELLS    =    199085184.0000          WELLS    =           0.4056
   RIVER LEAKAGE    =   5895884800.0000   RIVER LEAKAGE   =          11.2870
              ET    =   5395347456.0000             ET    =          15.7434
        RECHARGE    =      3335408.5000       RECHARGE    =        1.8169E-03

        TOTAL OUT = 21064480768.0000         TOTAL OUT =           39.5503

        IN - OUT =      9525248.0000          IN - OUT =         7.1587E-02

   PERCENT DISCREPANCY =         0.05    PERCENT DISCREPANCY =          0.18
```

Figure 56-Volumetric water budget calculated in Summer 2015

The autumn situation is similar to the summer case (Figure 57), with small recharge contribution (4,09 m³/s) but with smaller storage (9,96 m³/s). River leakage and constant-head cells inputs are nearly the same as before.

As output, it is possible to notice a smaller evapotranspiration rate (8,6 m³/s) balance with a slightly larger storage contribution (1,03 m³/s).

```
VOLUMETRIC BUDGET FOR ENTIRE MODEL AT END OF TIME STEP    1, STRESS PERIOD  64
------------------------------------------------------------------------------

   CUMULATIVE VOLUMES      L**3         RATES FOR THIS TIME STEP      L**3/T
   ------------------                   ------------------------

        IN:                                  IN:
        ---                                  ---
          STORAGE    =   2811265024.0000          STORAGE    =           9.9615
    CONSTANT HEAD    =   3178682880.0000     CONSTANT HEAD    =           6.5316
            WELLS    =            0.0000             WELLS    =           0.0000
    RIVER LEAKAGE    =   6013479936.0000     RIVER LEAKAGE    =          12.2484
               ET    =            0.0000                ET    =           0.0000
         RECHARGE    =   9359357952.0000          RECHARGE    =           4.0976

           TOTAL IN =  21362786304.0000            TOTAL IN =          32.8391

        OUT:                                 OUT:
        ----                                 ----
          STORAGE    =   3764512768.0000          STORAGE    =           1.0326
    CONSTANT HEAD    =   5901694976.0000     CONSTANT HEAD    =          11.5538
            WELLS    =    202309056.0000             WELLS    =           0.4056
    RIVER LEAKAGE    =   5983068160.0000     RIVER LEAKAGE    =          11.2530
               ET    =   5498163712.0000                ET    =           8.6234
         RECHARGE    =      3345037.0000          RECHARGE    =           0.0000

          TOTAL OUT =  21353093120.0000           TOTAL OUT =          32.8683

          IN - OUT =      9693184.0000            IN - OUT =       -2.9133E-02

  PERCENT DISCREPANCY =          0.05    PERCENT DISCREPANCY =          -0.09
```

Figure 57-Volumetric water budget calculated in Autumn 2015

The MODFLOW results in terms of water budget have been exported to Excel, in order to investigate the variation in time of the single water budget components. Figure 58 shows the variation with time of the influent recharge flux, calculated at different time steps along the simulated period. Here is visible the typical oscillating trend of recharge flux along the year but looking to the trendline it's possible to notice that the trend is generally increasing, described by the linear equation reported in the top-right corner of the figure with an approximate increase of 0,5 m^3/y, that is consistent with the field observation of MIPAAF database. Figure 59 and figure 60 show the trends of influent flux from river leakage and influent flux from constant head cells, both characterized by a decreasing trend in time.
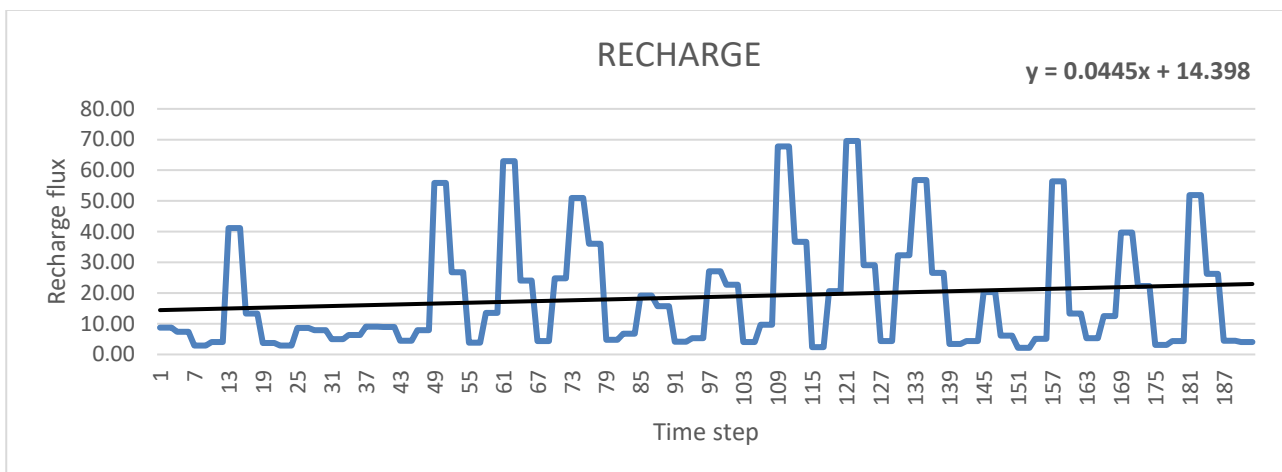

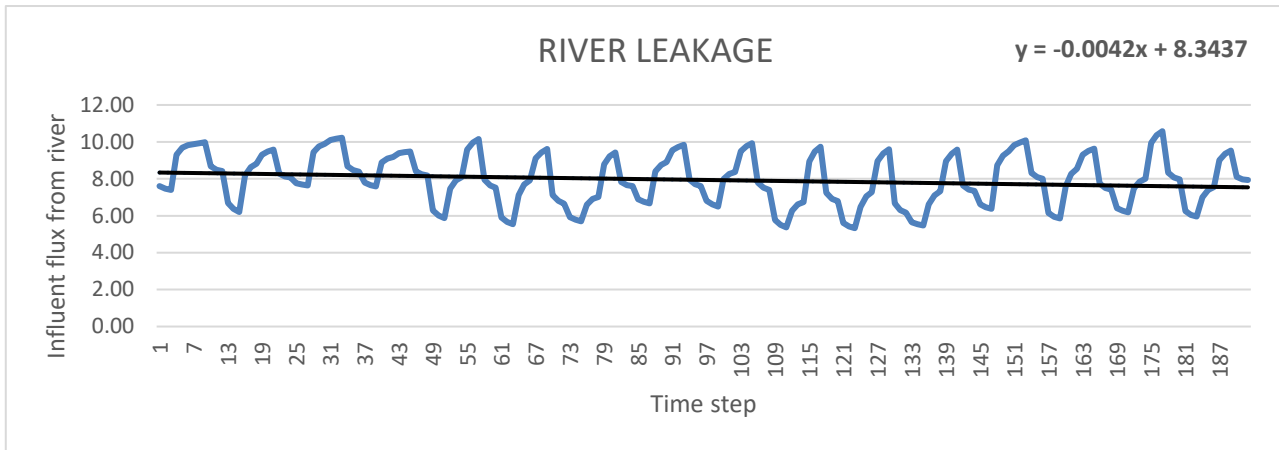*Figure 58-Trend of calculated recharge flux at different time steps*

Figure 59- Trend of calculated influent flux from the rivers at different time steps
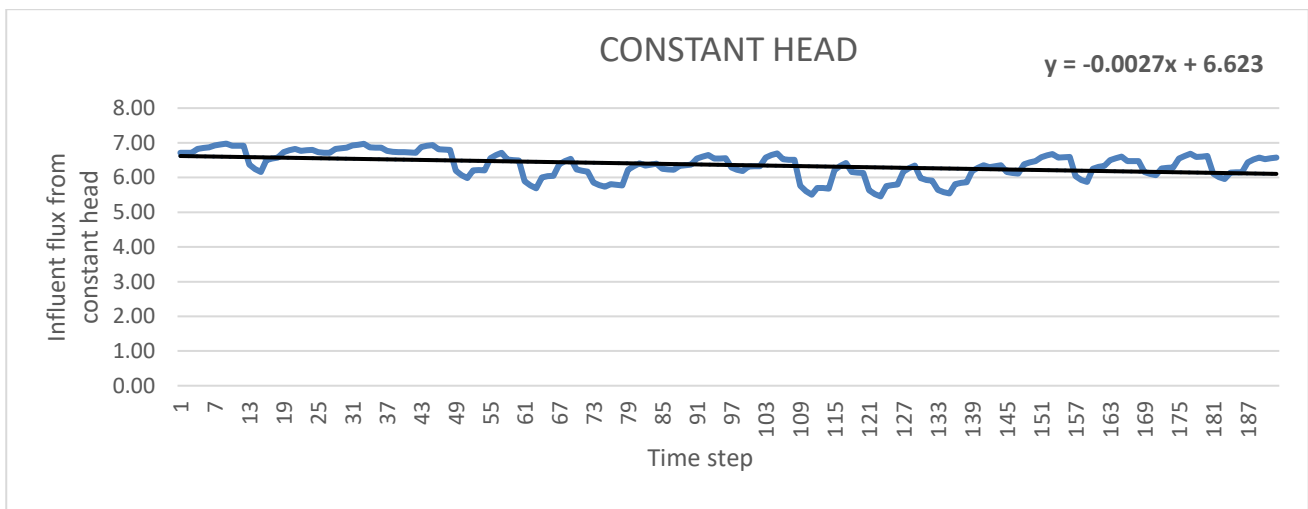

Figure 60-Trend of calculated influent flux from constant head at different time steps

Figure 61 instead describes the trend of evapotranspiration flux from the groundwater system. This graph is particularly important to understand that the evapotranspiration rate is strongly increased along the simulated period, as proved by the slope of the calculated trendline with an average increase of 0,25 m^3/y.

Similarly, also the flux discharged in constant-head cells, representing Tyrrhenian Sea, is increased in the time span, as shown by figure 62.

These two latter groundwater fluxes are extremely challenging to be quantified, and usually are not well understood at the regional scale. For this reason, it is extremely important to implement such large-scale numerical flow model.
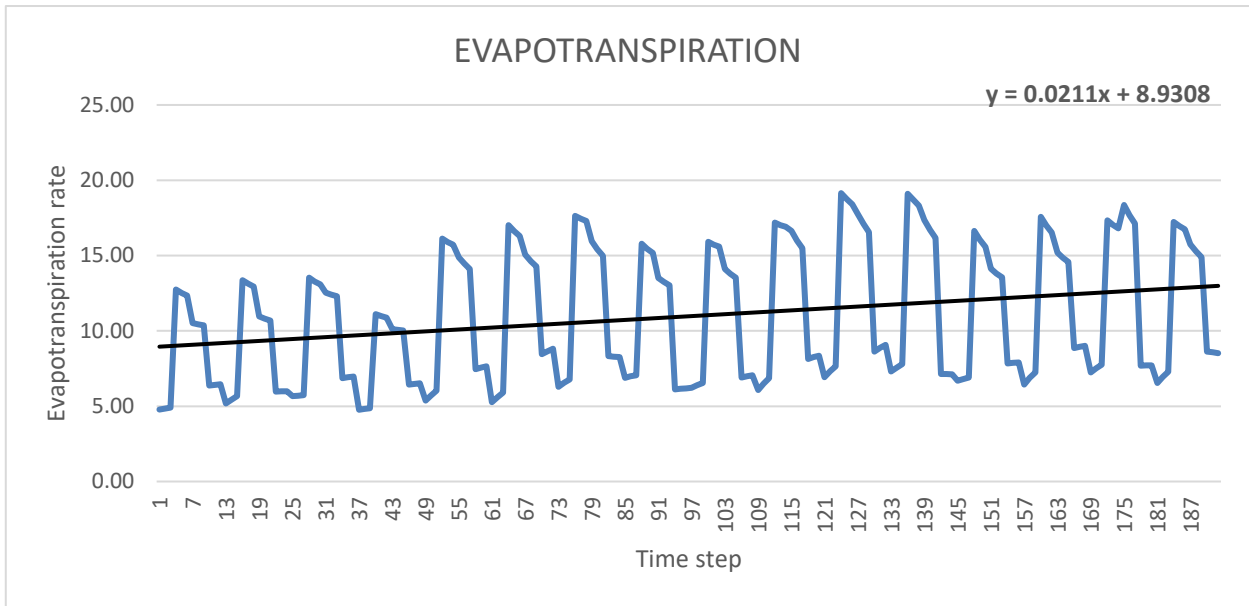
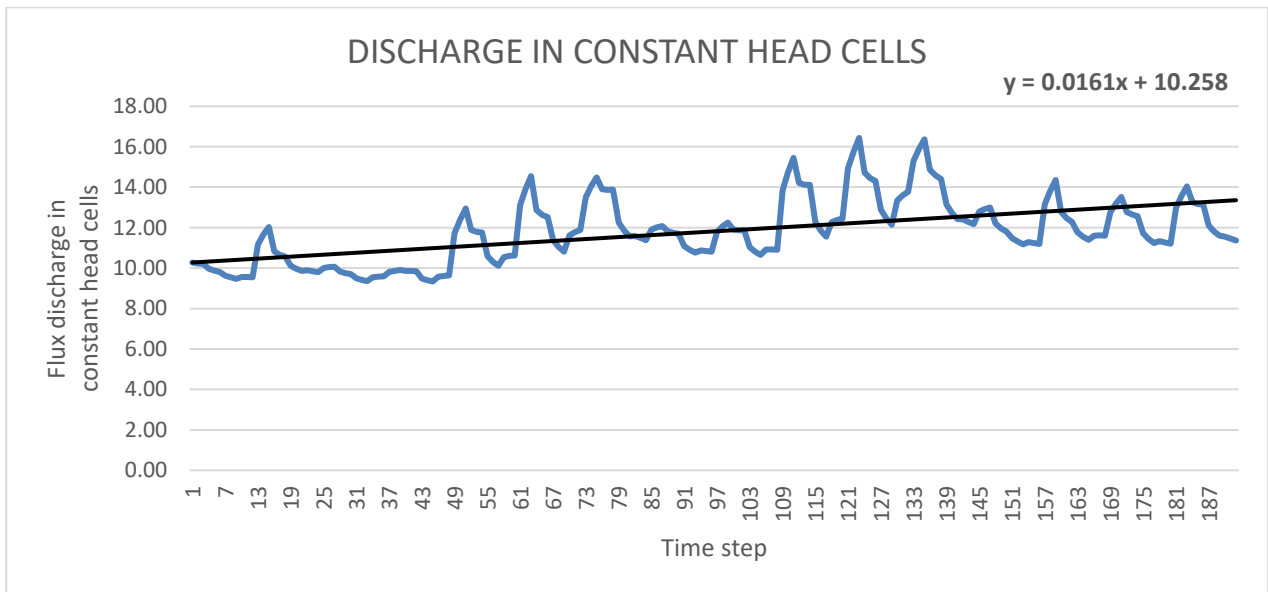*Figure 61- Trend of calculated evapotranspiration rate at different time steps*

Figure 62- Trend of calculated flux discharged in constant head cells at different time steps

6. CONCLUSION

This study has contributed to expand the hydrogeological knowledge of the unconfined alluvial aquifers of the Campania region with the development of a numerical model that well simulate the local groundwater system.

As demonstrated by the work of this thesis about the period 2000-2015, such numerical model has proved to be particularly useful to analyse the temporal and spatial variations of the groundwater flow system related to the changes in patterns of recharge and evapotranspiration components.

In fact, the use of a calibrated and validated groundwater flow model allows to obtain accurate calculations of the volumetric groundwater budget, also pointing the attention on single water budget components.

In addition, the estimation of the fluxes toward the sea or the estimation of the fraction of total evapotranspiration that is taken directly from groundwater resources are possible only with physically based models such the one here employed.

These aspects are very important for the understanding of the relations between all the various compartments of the hydrological cycle, the knowledge of which is a crucial point for an optimal management of the territory.

The present study is based on some assumptions and it can be further expanded by future studies in order to have an even more detailed understanding of the aquifer's behaviour. For example, is possible to consider the hydrometric level in the rivers as variable in time and not constant throughout the entire simulation, as assumed in the present study, or it is possible to consider different extinction depths of evapotranspiration in relation to different land covers and soil texture (Shah et al., 2007).

7. BIBLIOGRAPHY

Allocca, V., Manna, F., De Vita, P. (2014). Estimating annual groundwater recharge coefficient for karst aquifers of the southern Apennines (Italy). Hydrology and Earth System Science, Volume 18, Pages 803-817.

Allocca, V., Coda, S., De Vita, P., Di Rienzo, B., Ferrara, L., Giarra, A., Mangoni, O., Stellato, L., Trifuoggi, M., Arienzo, M. (2018). Hydrogeological and hydrogeochemical study of a volcanic-sedimentary coastal aquifer in the archaeological site of Cumae (Phlegraean Fields, southern Italy). Journal of Geochemical Exploration, 185, 105-115.

AppEEARS Team (2020). Application for extracting and exploring analysis ready samples (AppEEARS). Ver. 2.40. NASA EOSDIS Land Processes Distributed Active Archive Center (LP DAAC), USGS/Earth Resources Observation and Science (EROS) Center, Sioux Falls, South Dakota, USA. Accessed May 3, 2020. https://lpdaacsvc.cr.usgs.gov/appeears

Arnell, N. (1999). Climate change and global water resources. Global Environmental Change, Volume 9, Supplement 1, Pages S31-S49.

Batu, V. (1998). *Aquifer Hydraulics: A Comprehensive Guide to Hydrogeologic Data Analysis*, John Wiley & Sons, New York, 727p.

Brancaccio, L., Cinque, A., Romano, P., Rosskopf, C., Russo, F., Santangelo, N., Santo, A. (1991). Geomorphology and neotectonic evolution of a sector of the Tyrrhenian flank of the southern Apennines (Region of Naples, Italy). Zeitschrift fur Geomorphologie, Supplementary Issue 82, Pages 47-58.

Busico, G., Buffardi, C., Ntona, M. M., Vigliotti, M., Colombani, N., Mastrocicco, M., Ruberti, D. (2021). Actual and Forecasted Vulnerability Assessment to Seawater Intrusion via GALDIT-SUSI in the Volturno River Mouth (Italy). Remote Sensing, 13(18), 3632.

Busico, G., Ntona, M. M., Carvalho, S. C. P., Patrikaki, O., Voudouris, K., Kazakis, N. (2021). Simulating future groundwater recharge in coastal and inland catchments. Water Resources Management, 35(11), 3617-3632.

Chiang, E. (2020). Processing Modflow Version 11.0.1: A graphical user interface for MODFLOW, GSFLOW, MODPATH, MT3D, PEST, SEAWAT, and ZoneBudget. Simcore Software. https://www.simcore.com/wp/processing-modflow-11/

Colombani, N., Osti, A., Volta, G., Mastrocicco, M. (2016). Impact of Climate Change on Salinization of Coastal Water Resources. Water Resource Management, Volume 30, Pages 2483-2496.

Corniello, A., Ducci, D. (2014). Hydrogeochemical characterization of the main aquifer of the "Litorale Domizio-Agro Aversano NIPS" (Campania – southern Italy). Journal of Geochemical Exploration 137, Pages 1-10.

Cramer, W., Guiot, J., Fader, M., Garrabou, J., Gattuso, J.-P., Iglesias, A., Lange, M.A., Lionello, P., Llasat, M.C., Paz, S., Penuelas, J., Snoussi, M., Toreti, A., Tsimplis, M.N., Xoplaki, E. (2018). Climate change and interconnected risk to suistainable development in the Mediterranean. Nuture Climate Change, Volume 8, Pages 972-980.

de Graaf, I. E., van Beek, R. L., Gleeson, T., Moosdorf, N., Schmitz, O., Sutanudjaja, E. H., & Bierkens, M. F. (2017). A global-scale two-layer transient groundwater model: Development and application to groundwater depletion. Advances in water Resources, 102, 53-67.

De Vita, P., Allocca, V., Celico, F., Fabbroncino, S., Cesaria, M., Monacelli, G., Musilli, I., Piscopo, V., Scalise, A.R., Summa, G., Tranfaglia, G., Celico, P. (2018). Hydrogeology of continental southern Italy. Journal of Maps, 14:2, Pages 230-241.

Ducci, D., Travaglia, G. (2008). Effects of climate change on groundwater resources in Campania (southern Italy). Geological Society London Special Pubblications 288, Pages 25-31.

Erturk, A., Ekdal, A., Gurel, M., Karakaya, N., Guzel, C., Gonenc, E. (2014). Evaluating the impact of climate change on groundwater resources in a small Mediterranean watershed. Science of the Total Environment 499, Pages 437- 447.

Famiglietti, J. S. (2014). The global groundwater crisis. Nature Climate Change, 4(11), 945-948.

Fan, Y., Li, H., Miguez-Macho, G. (2013). Global patterns of groundwater table depth. Science, 339(6122), 940-943.

Gomarasca, M.A. (2009). BASICS OF GEOMATICS. Springer.

Lancia, M., Petitta, M., Zheng, C., Saroli, M. (2020). Hydrogeological insight and modelling for sustainable use of a stressed carbonate aquifer in the Mediterranean area: From passive withdrawals to active management. Journal of Hydrology: Regional Studies 32.

Harbaugh, A.W. (2005). MODFLOW-2005, The U.S. Geological Survey modular ground-water model—the Ground-Water Flow Process. U.S. Geological Survey Techniques and Methods 6- A16.

Mastrocicco, M., Gervasio, M.P., Busico, G., Colombani, N. (2021). Natural and anthropogenic factors driving groundwater resources salinization for agricultural use in the Campania plains (Southern Italy). Science of the Total Environment 758.

Mastrocicco, M., Busico, G., Colombani, N., Vigliotti, M., Ruberti, D. (2019). Modelling actual and future seawater intrusion in the variconi coastal wetland (italy) due to climate and landscape changes.

Matano, F., Sacchi, M., Vigliotti, M., Ruberti, D. (2018). Subsidence Trends of Volturno River Coastal Plain (Northern Campania, Southern Italy) Inferred by SAR Interferometry Data. Geoscience, 8, 8.

Mc Donald, J.M., Harbaugh, A.W. (1988). MODFLOW, a modular 3D finite difference ground-water flow model. U.S. Geological Survey Open File Report, 83-875, 586.

Morris, D.A., Johnson, A.I. (1967). Summary of hydrologic and physical properties of rock and soil materials as analyzed by the Hydrologic Laboratory of the U.S. Geological Survey, U.S. Geological Survey Water-Supply Paper 1839-D, 42p.

Mu, Q., Zhao, M., & Running, S. W. (2011). Improvements to a MODIS global terrestrial evapotranspiration algorithm. Remote sensing of environment, 115(8), 1781-1800.

Oude Essink, G.H.P., van Baaren, E.S., de Louw P.G.B. (2010). Effects of climate change on coastal groundwater systems: A modelling study in the Netherlands. Water Resource Research, Volume 46, Issue 10.

Pappone, G., Alberico, I., Amato, V., Aucelli, P.P.C., Di Paola, G. (2011). Recent evolution and present-day conditions of the Campanian Coastal plains (South Italy): the case history of Sele River Coastal plain. WIT Transactions on Ecology and the Environment, Volume 149, Pages 15-27.

Priyantha Ranjan, S., Kazama, S., Sawamoto, M. (2006). Effects of climate and land use changes on groundwater resources in coastal aquifers. Journal of Environmental Management, Volume 80, Pages 25-35.

Running, S., Mu, Q., Zhao, M., Moreno, A. (2019) MOD16A2GF MODIS/Terra Net Evapotranspiration Gap-Filled 8-Day L4 Global 500 m SIN Grid V006. NASA EOSDIS Land Processes DAAC. https://doi.org/10.5067/MODIS/MOD16A2GF.006

Ruberti, D., Vagliotti, M. (2017). Land use and landscape pattern changes driven by land reclamation in a coastal area: the case of Volturno delta plain, Campania region, southern Italy. Environmental Earth Science 76, 694.

Shah, N., Nachabe, M., Ross, M. (2007). Extinction depth and evapotranspiration from ground water under selected land covers. Groundwater, 45(3), 329-338.

Stellato, L., Coda, S., Arienzo, M., De Vita, P., Di Rienzo, B., D'Onofrio, A., Ferrara, L., Marzaioli, F., Trifuoggi, M., Allocca, V. (2020). Natural and Anthropogenic Groundwater Contamination in a Coastal Volcanic-Sedimentary Aquifer: The Case of the Archaeological Site of Cumae (Phlegraean Fields, Southern Italy). Water, 12(12), 3463.

Sutanudjaja, E. H., van Beek, R., Wanders, N., Wada, Y., Bosmans, J. H. C., Drost, N., van der Ent, R. J., de Graaf, I. E. M., Hoch, J. M., de Jong, K., Karssenberg, D., López López, P., Peßenteiner, S., Schmitz, O., Straatsma, M. W., Vannametee, E., Wisser, D., and Bierkens, M. F. P. (2018). PCR-GLOBWB 2: a 5 arcmin global hydrological and water resources model, Geosci. Model Dev., 11, 2429–2453, https://doi.org/10.5194/gmd-11-2429-2018.

Tufano, R., Allocca,V., Coda, S., Cusano, D., Fusco, F., Nicodemo, F., Pizzolante, A., De Vita, P. (2020). Groundwater vulnerability of the principal aquifers of the Campania region (southern Italy). Journal of Maps, Volume 16, Number 2, Pages 565-576.

Wada, Y., Van Beek, L. P., Van Kempen, C. M., Reckman, J. W., Vasak, S., & Bierkens, M. F. (2010). Global depletion of groundwater resources. Geophysical research letters, 37(20).

7.2. WEB REFERENCES

http://www.eea.europa.eu/help/glossary/eea-glossary/digital-terrain-model

https://www2.jpl.nasa.gov/srtm/instrumentinterfmore.html

http://sgi2.isprambiente.it/viewersgi2/

https://earth.google.com/web/

https://www.mareografico.it/

https://modis.gsfc.nasa.gov/

http://www.aqtesolv.com/aquifer-tests/aquifer_properties.htm